簡介地震學新進開發技術及其在自然災害監測與防災應用

黃柏壽

中央研究院 地球科學所

2018/05/28_NCREE

報告大綱:

- 地動旋轉量(Rotation)的觀測與應用
- 地震源與波傳的數值模擬
- 高頻GPS的地動觀測及其應用
- 簡介DAS觀測原理及其應用

地動旋轉量的觀測與應用

Accelerometer, the hart of the broad band seismometer and the accelerometer

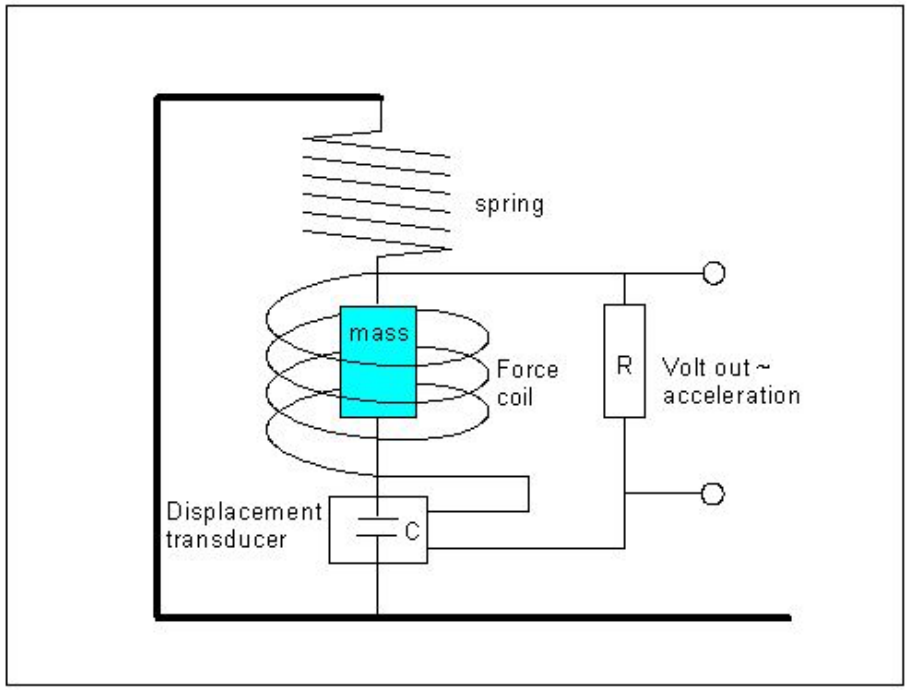

Simplified principle behind Force Balanced Accelerometer. The displacement transducer normally uses a capacitor *C*, whose capacitance varies with the displacement of the mass. A current, proportional to the displacement transducer output, will force the mass to remain stationary relative to the frame.

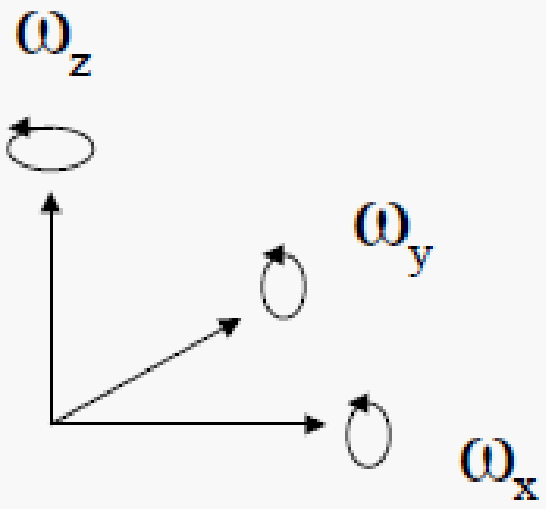

Rotation rate

Rotation sensor

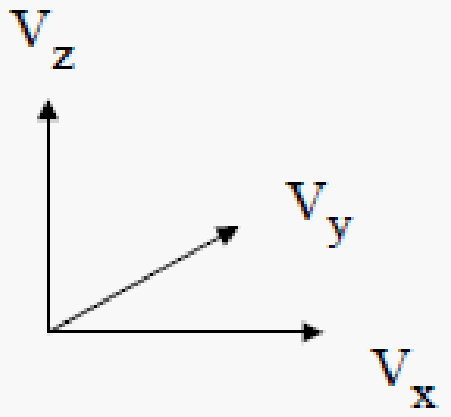

Ground velocity

Seismometer

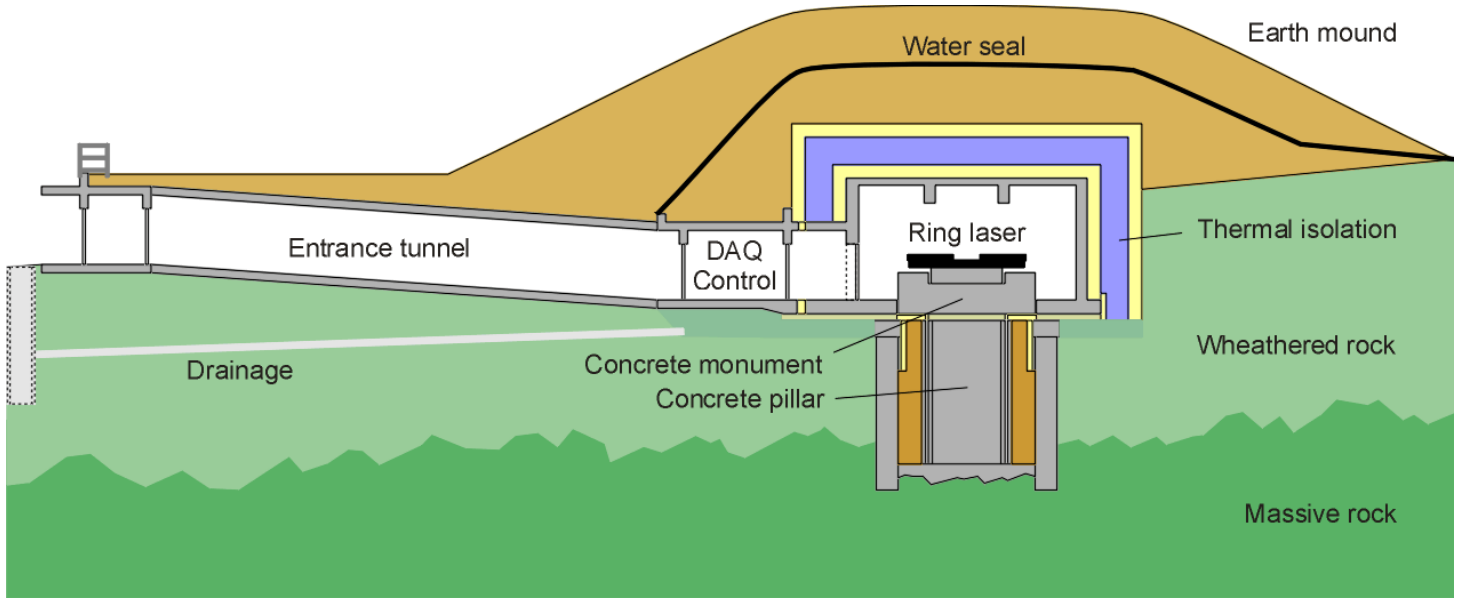

Single Component Rotation (Wz)

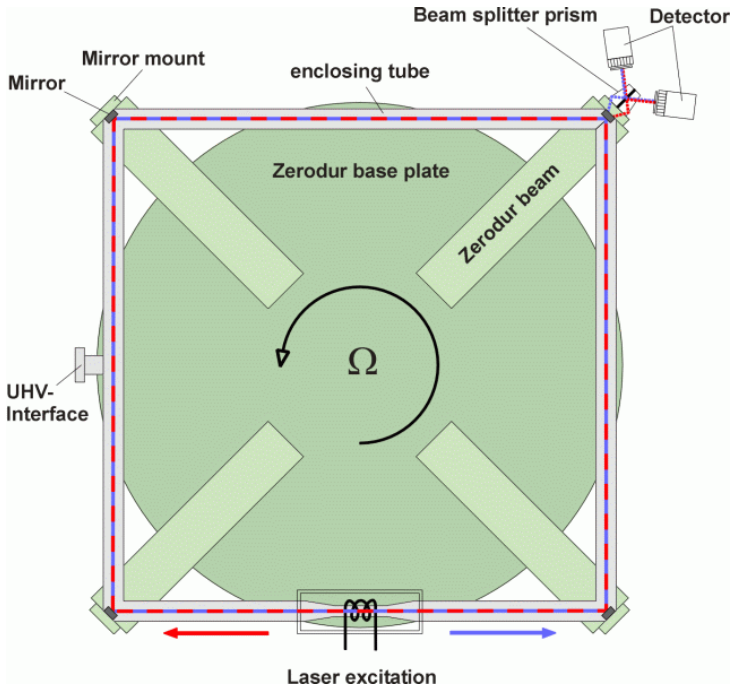

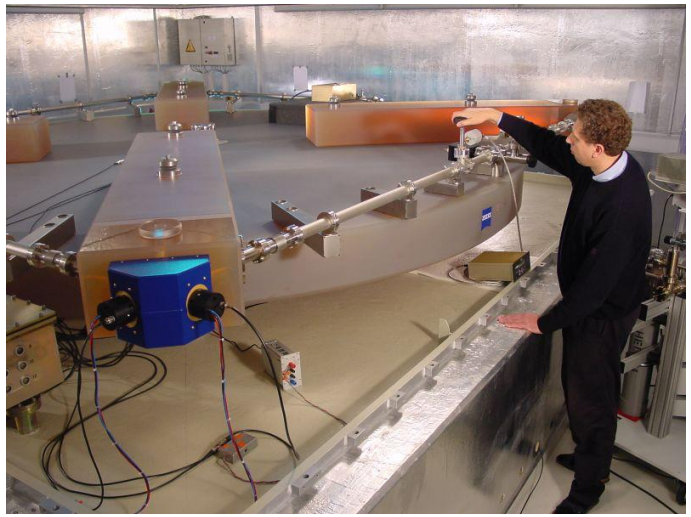

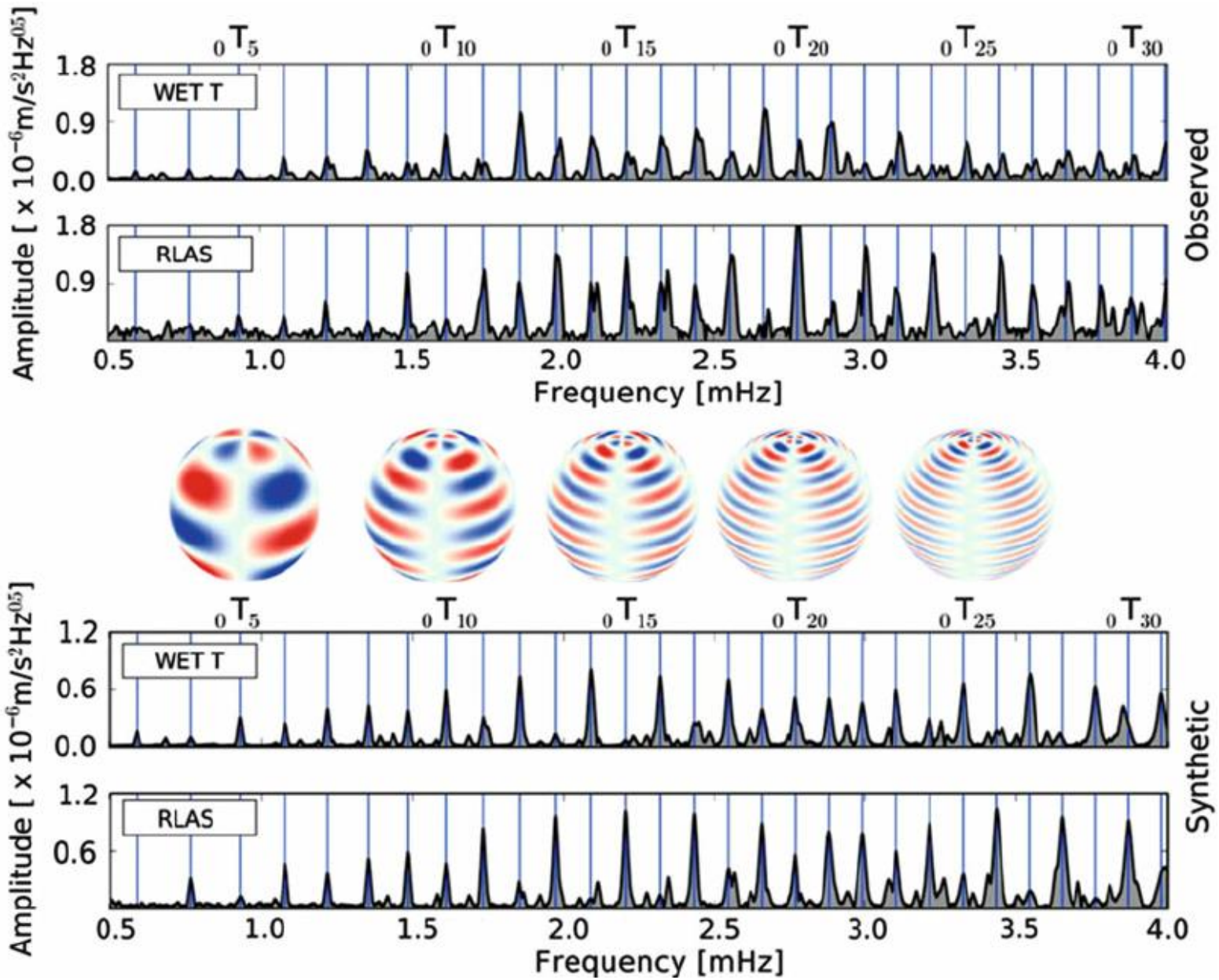
$_0T_5$
$_0T_{10}$
$_0T_{15}$
$_0T_{20}$
$_0T_{25}$
$_0T_{30}$
WET T
RLAS
Observed
Amplitude [x 10^{-6}m/s^{2}Hz^{05}]
1.8
0.9
0.0
0.5
1.0
1.5
2.0
2.5
3.0
3.5
4.0
Frequency [mHz]
1.2
0.6
Synthetic

Observation of rotational deformations after earthquake

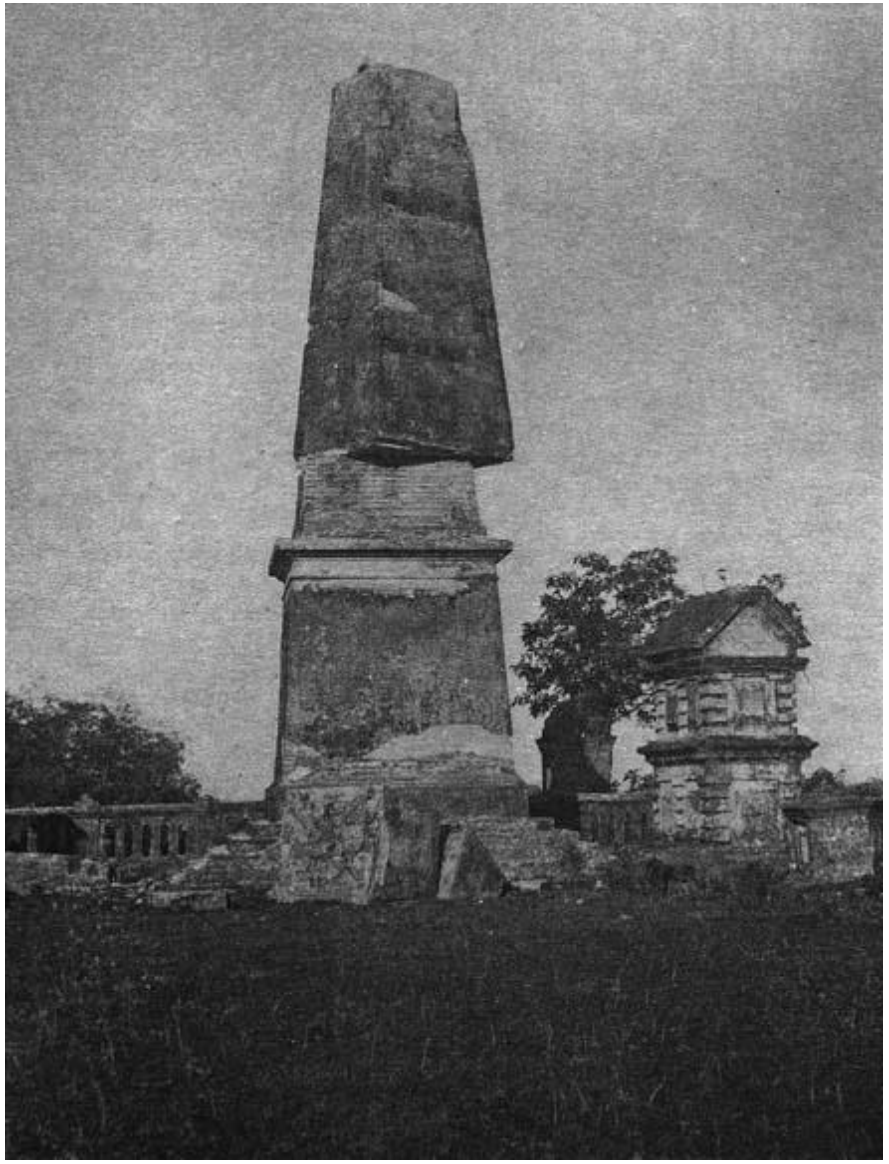

the Great Shillong Earthquake in 1897, India

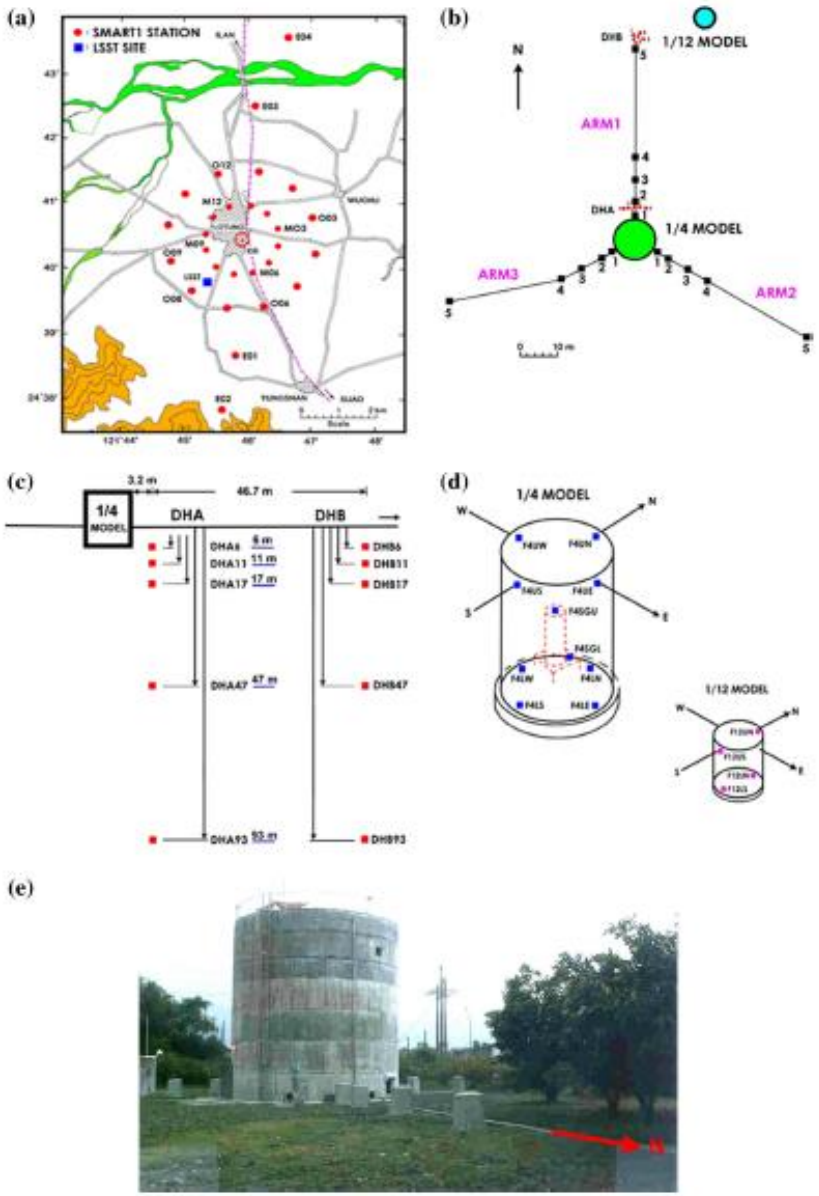

Array-derived rotations

$$\begin{pmatrix}\omega_x\\ \omega_y\\ \omega_z\end{pmatrix} = \frac{1}{2}\nabla\times\underline{\mathbf{v}} = \frac{1}{2}\begin{pmatrix}\partial_y v_z - \partial_z v_y\\ \partial_z v_x - \partial_x v_z\\ \partial_x v_y - \partial_y v_x\end{pmatrix}$$

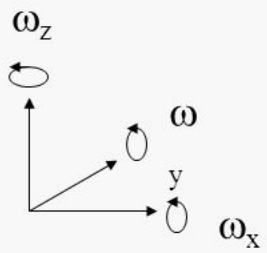

Rotation rate

Rotation sensor

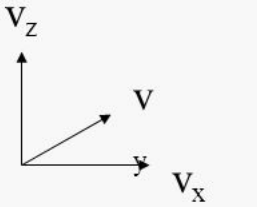

Ground velocity

Seismometer

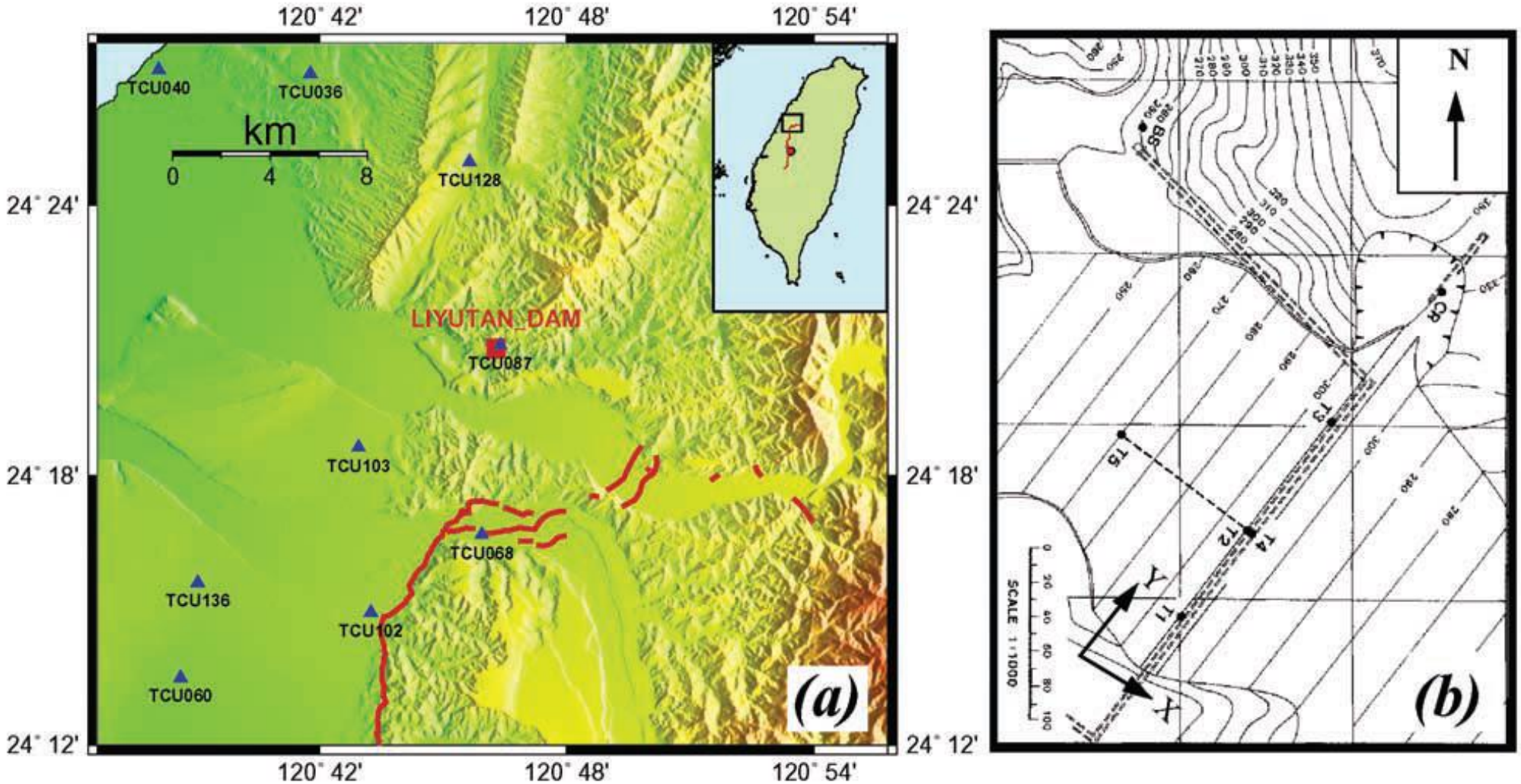

Huang, 2003 (GRL)

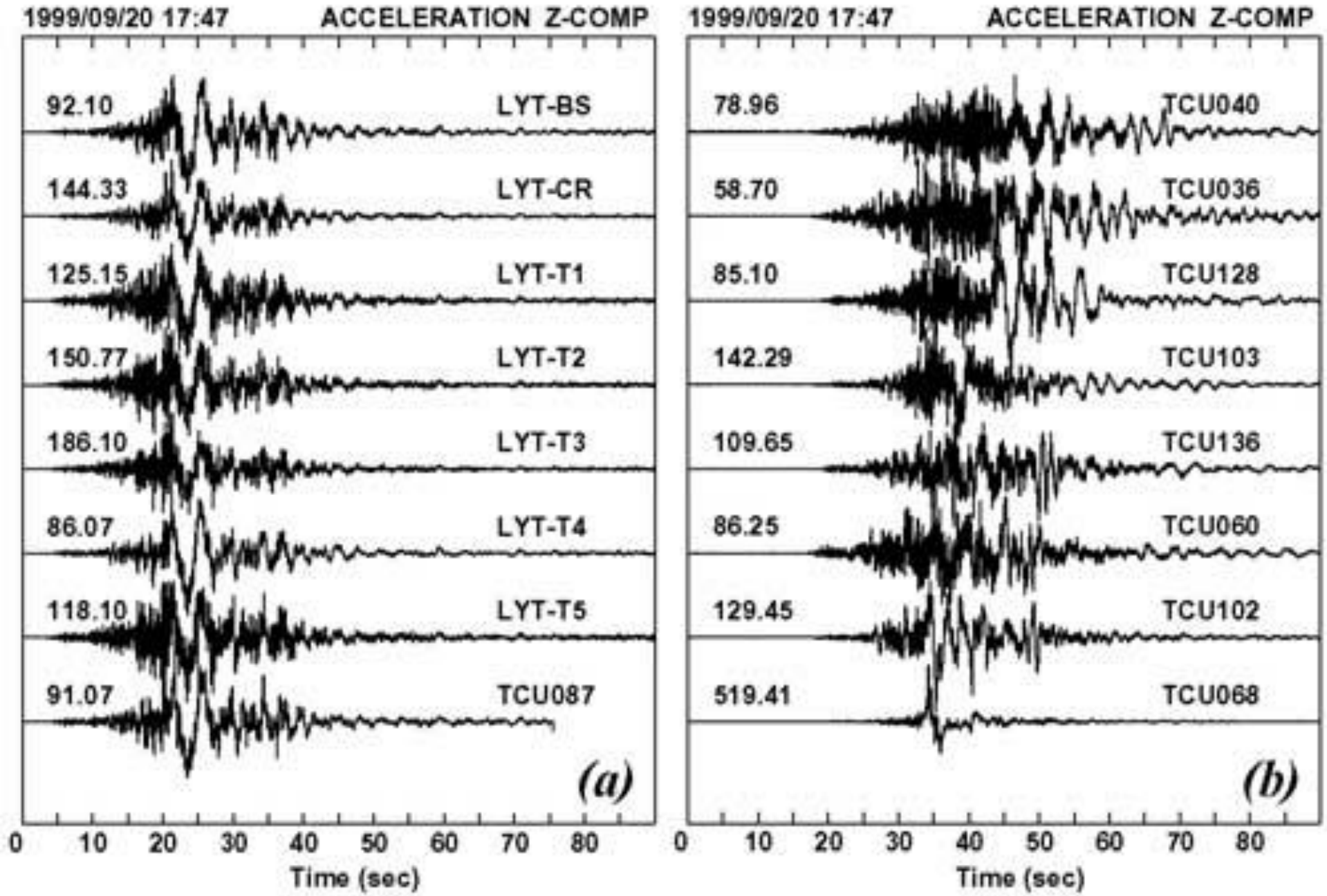
1999/09/20 17:47
ACCELERATION Z-COMP
92.10
LYT-BS
144.33
LYT-CR
125.15
LYT-T1
150.77
LYT-T2
186.10
LYT-T3
86.07
LYT-T4
118.10
LYT-T5
91.07
TCU087
(a)
0 10 20 30 40 50 60 70 80
Time (sec)
1999/09/20 17:47
ACCELERATION Z-COMP
78.96
TCU040
58.70
TCU036
85.10
TCU128
142.29
TCU103
109.65
TCU136
86.25
TCU060
129.45
TCU102
519.41
TCU068
(b)
0 10 20 30 40 50 60 70 80
Time (sec)

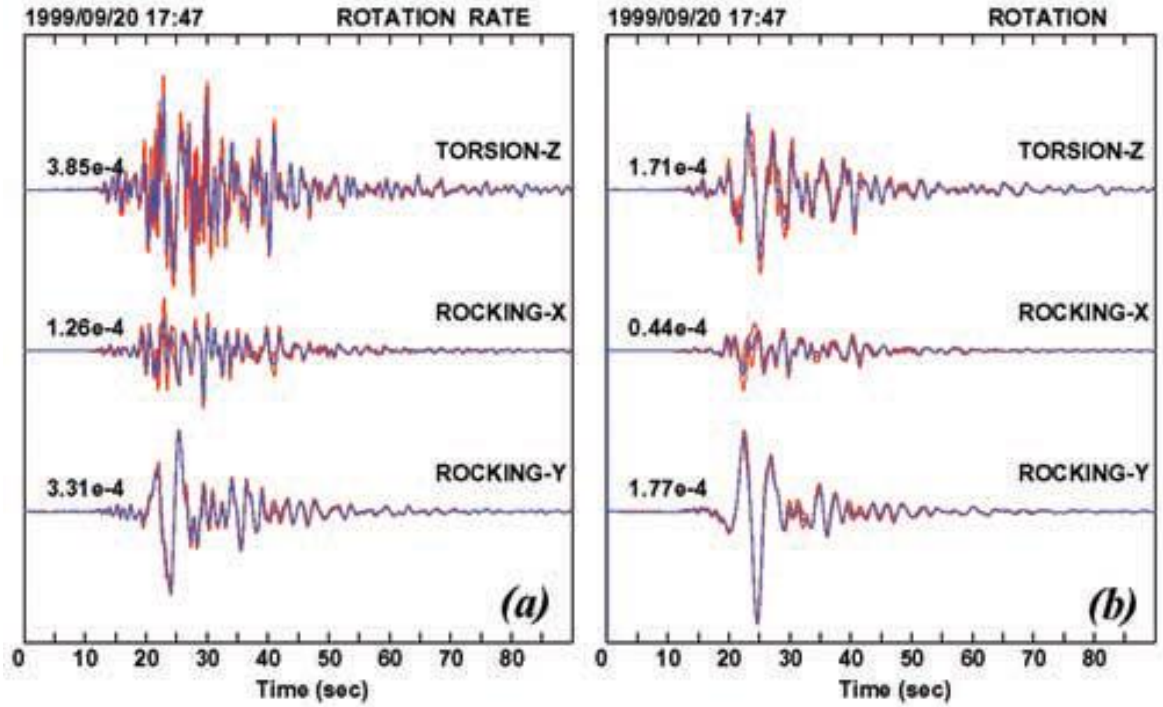
1999/09/20 17:47
ROTATION RATE
TORSION-Z
3.85e-4
ROCKING-X
1.26e-4
ROCKING-Y
3.31e-4
(a)
0 10 20 30 40 50 60 70 80
Time (sec)
1999/09/20 17:47
ROTATION
TORSION-Z
1.71e-4
ROCKING-X
0.44e-4
ROCKING-Y
1.77e-4
(b)
0 10 20 30 40 50 60 70 80
Time (sec)

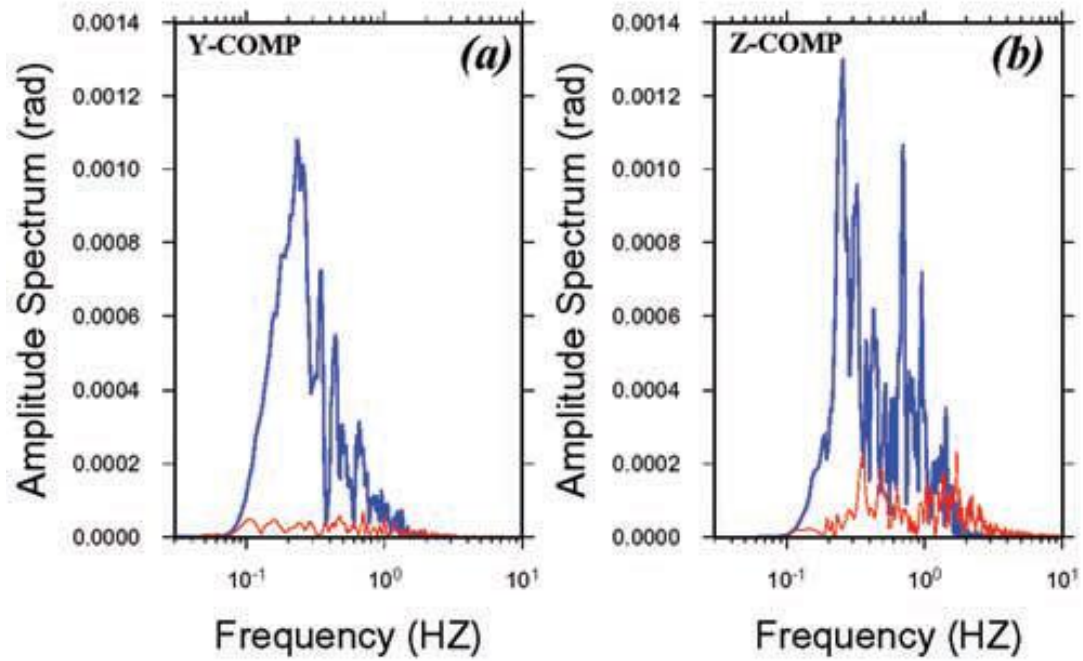
Y-COMP
(a)
Amplitude Spectrum (rad)
0.0014
0.0012
0.0010
0.0008
0.0006
0.0004
0.0002
0.0000
10^{-1}
10^{0}
10^{1}
Frequency (HZ)
Z-COMP
(b)
Amplitude Spectrum (rad)
0.0014
0.0012
0.0010
0.0008
0.0006
0.0004
0.0002
0.0000
10^{-1}
10^{0}
10^{1}
Frequency (HZ)

Portable rotational ground motion sensors for local earthquake

a)

b)

c)

d)

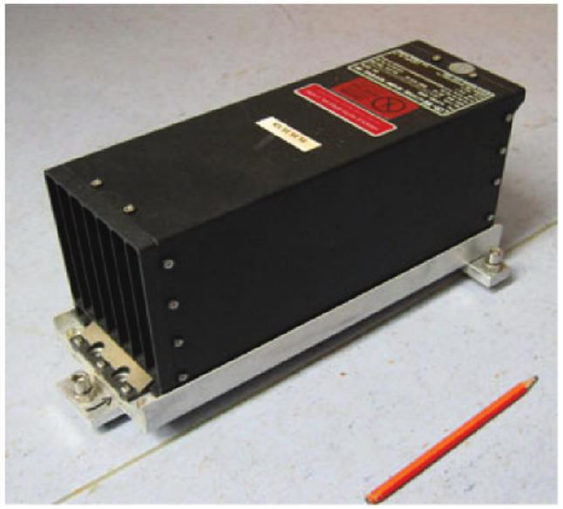

製造原理: **Sagnac effect**

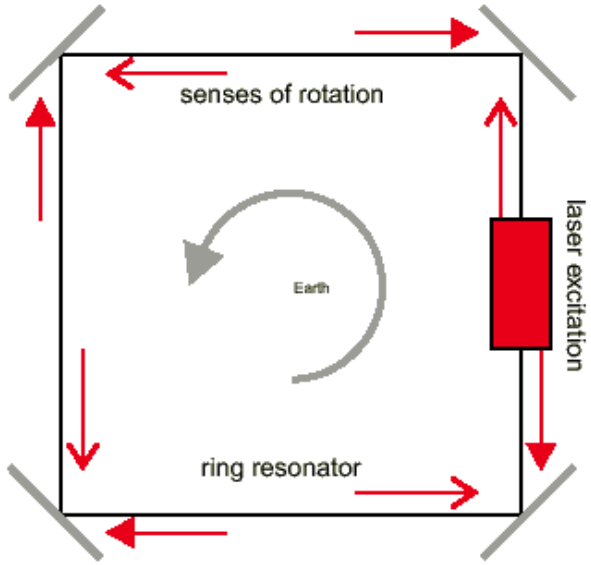

$$\Delta\nu_{Sagnac} = \frac{4\mathbf{A}\cdot\Omega}{\lambda P}$$

討論：地震學上應用(六分量地動觀測)

- 地下構造推求
- 地震定位
- 地震波入射方位尋角
- 震源破裂過程

討論：地震工程

- Rotational motions (地震）→ Torsional motions （工程）
- The lateral and torsional modes are coupled if the structure is asymmetric, that is center of stiness differ from centers of floor mass
- Rotational motion was responsible for the splitting of peaks in their resonance frequencies (Ghayamghamian, M.R. & Matosaka, M., 2003)
- the local rotational motion may appear to be due to wave propagation in heterogeneous soil layers at the site
- The effects of torsional response and or coupling of motions may remarkably change the site amplification characteristics at the site

www.sciencemag.org/news/2017/04/buried-lasers-will-sense-earths-spin-and-quakes-doing-twist

Ring of truth

Buried near Munich, Germany, is Rotational Motions in Seismology (ROMY), a giant ring laser. It will sense the rotation of Earth and tiny wobbles of its spin axis—helping calibrate GPS satellites. It also will detect twisting motions from earthquakes, which researchers have typically ignored.

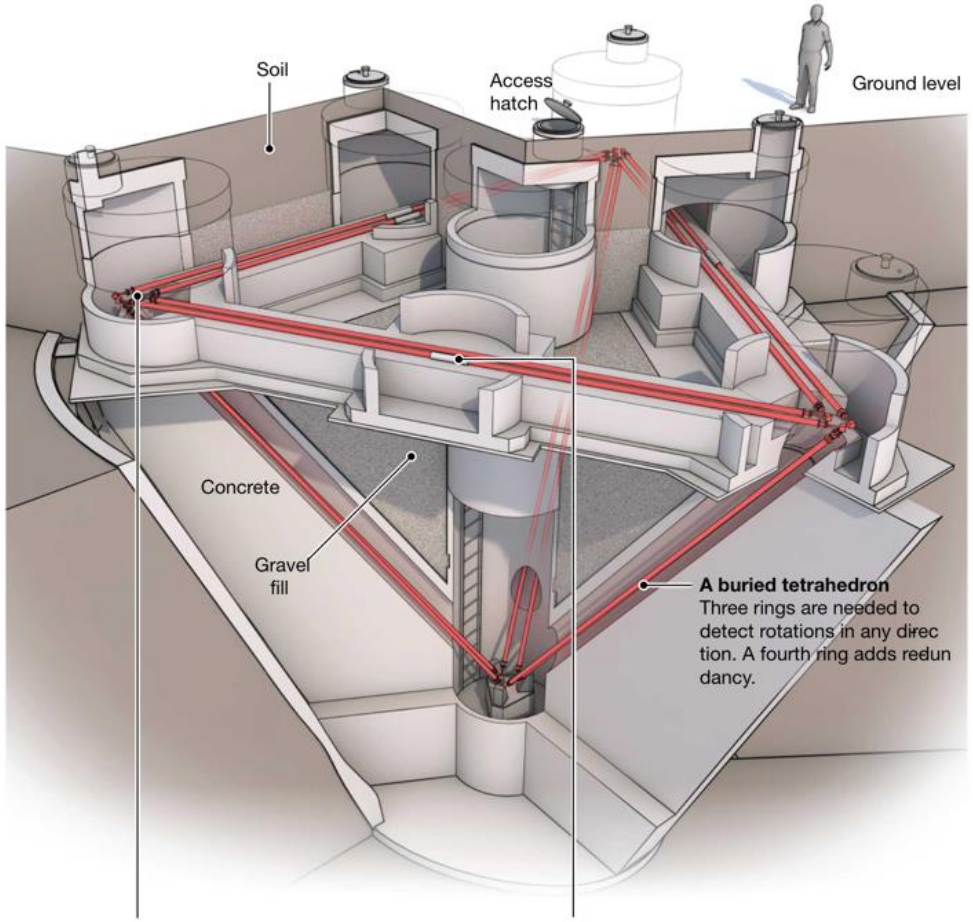

Nanao Array (南澳)

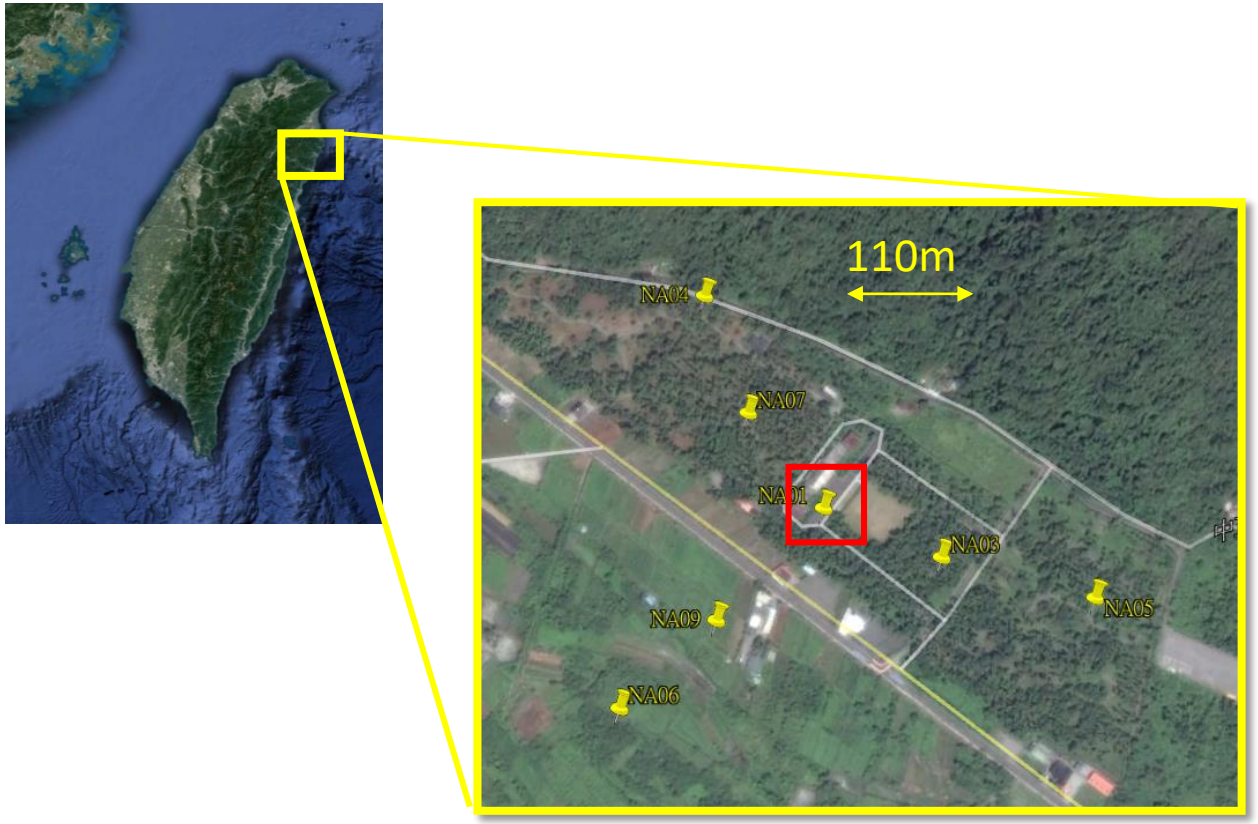

Nanao array is organized by
Wu-Cheng Chi (since 2011)

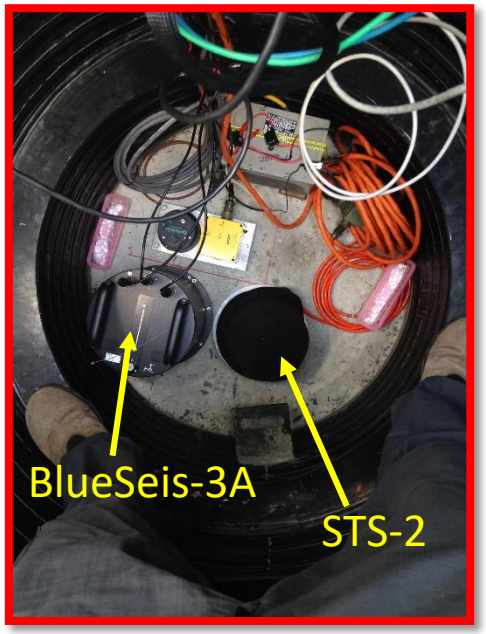

You are welcome
to request data.

動態應變量的觀測與應用

Strain Deformation

Strain Deformation

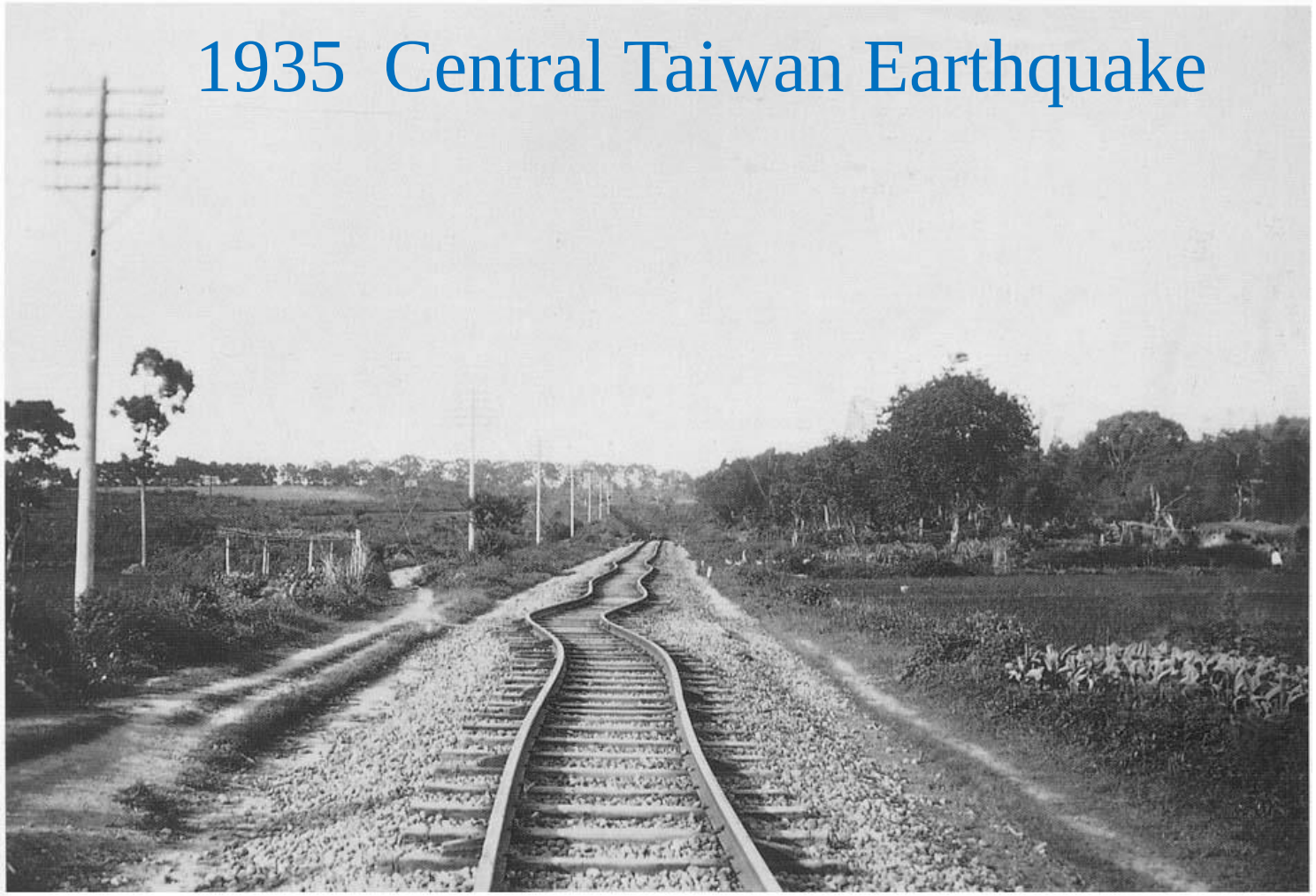

提供人／陳桂田先生

后里站北方第八號隧道南出口山線鐵路彎曲，這乃是「雁行斷層」呈東北—西南走向而產生的彎曲。

1999 Chi-Chi Taiwan Earthquake

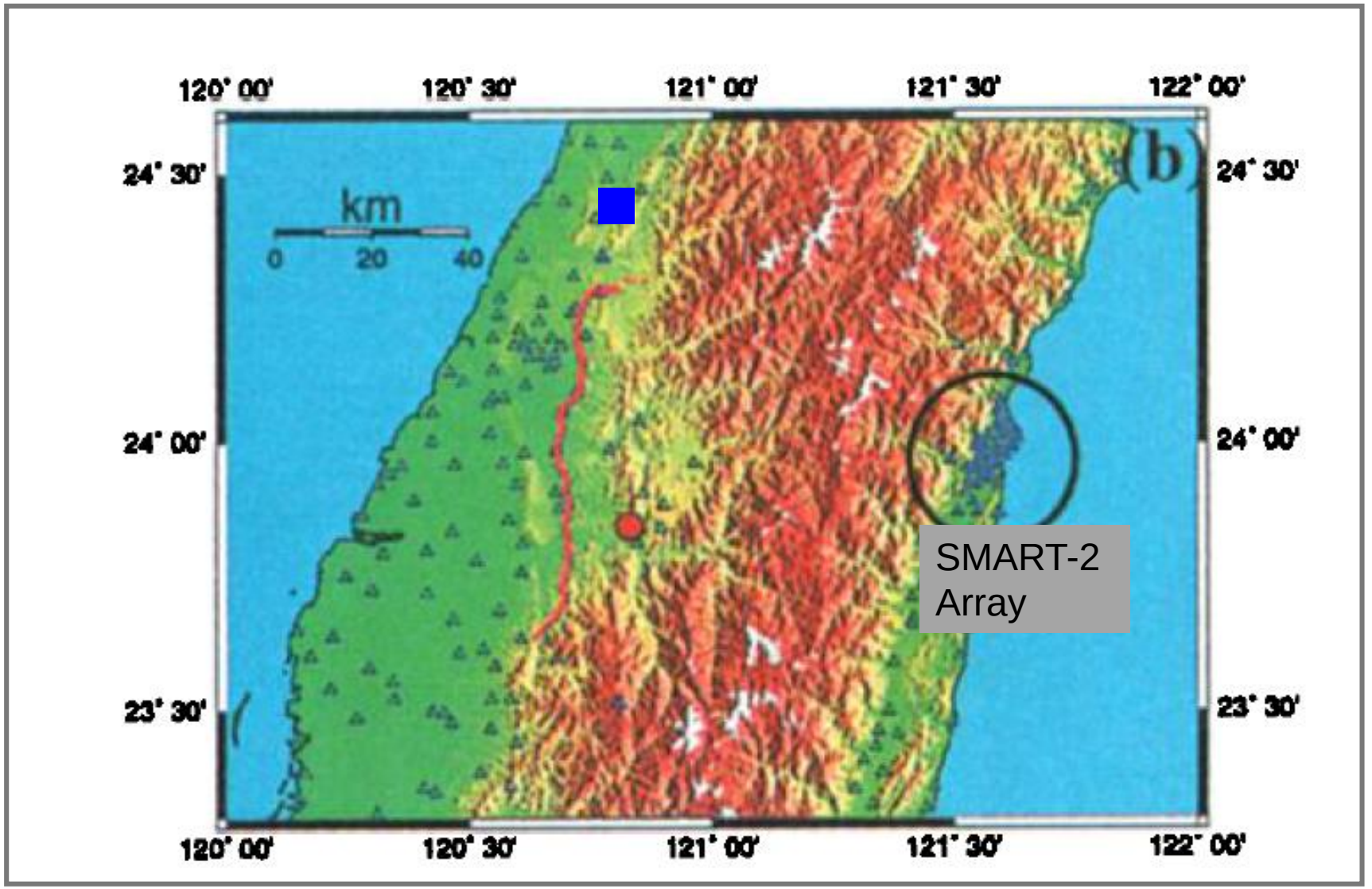

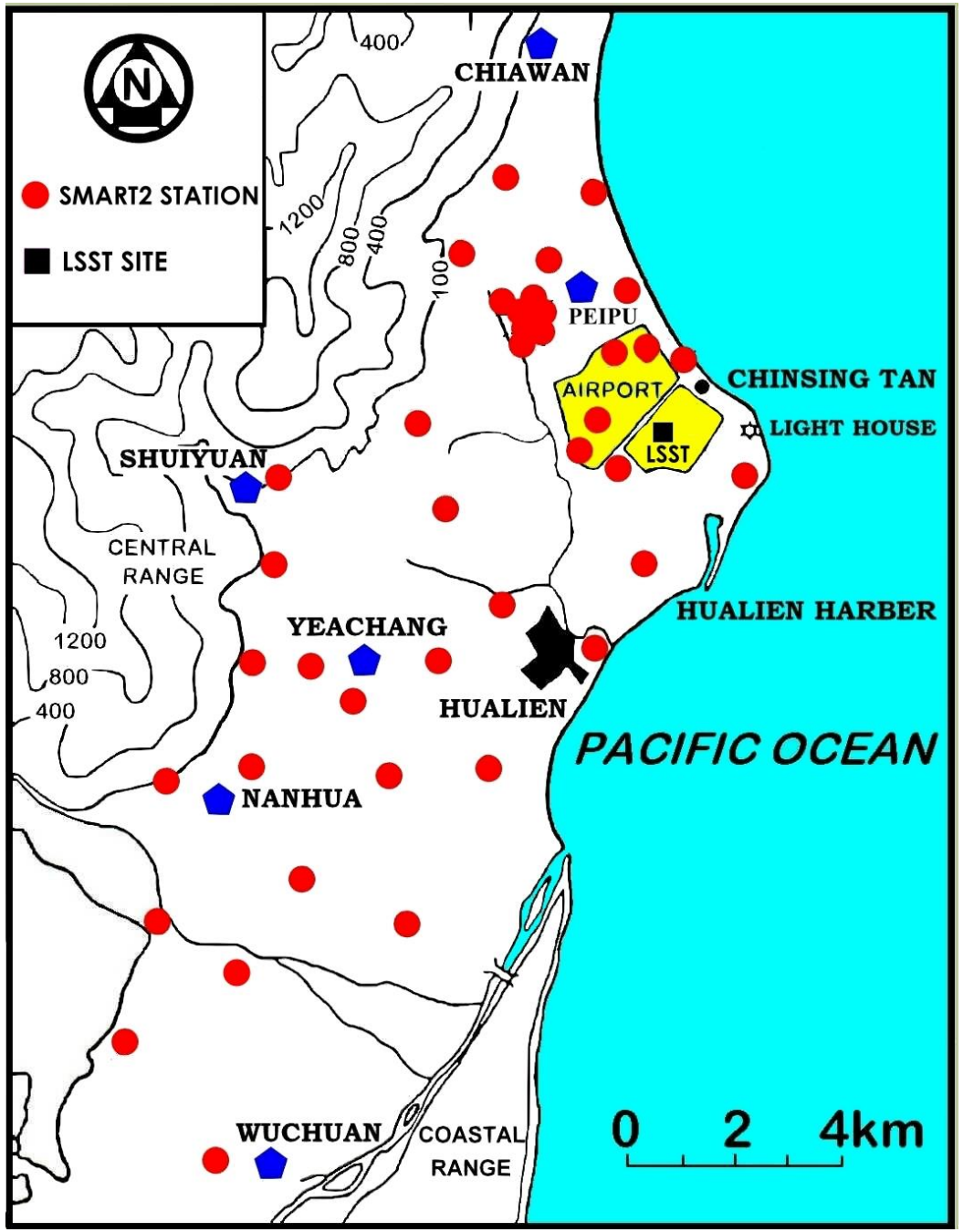
N
SMART2 STATION
LSST SITE
400
1200
800
400
100
CHIAWAN
PEIPU
AIRPORT
LSST
CHINSING TAN
LIGHT HOUSE
SHUIYUAN
CENTRAL
RANGE
1200
800
400
YEACHANG
HUALIEN HARBER
HUALIEN
PACIFIC OCEAN
NANHUA
WUCHUAN
COASTAL
RANGE
0 2 4km

Hualien Large Scale Seismic Test (HLSST)

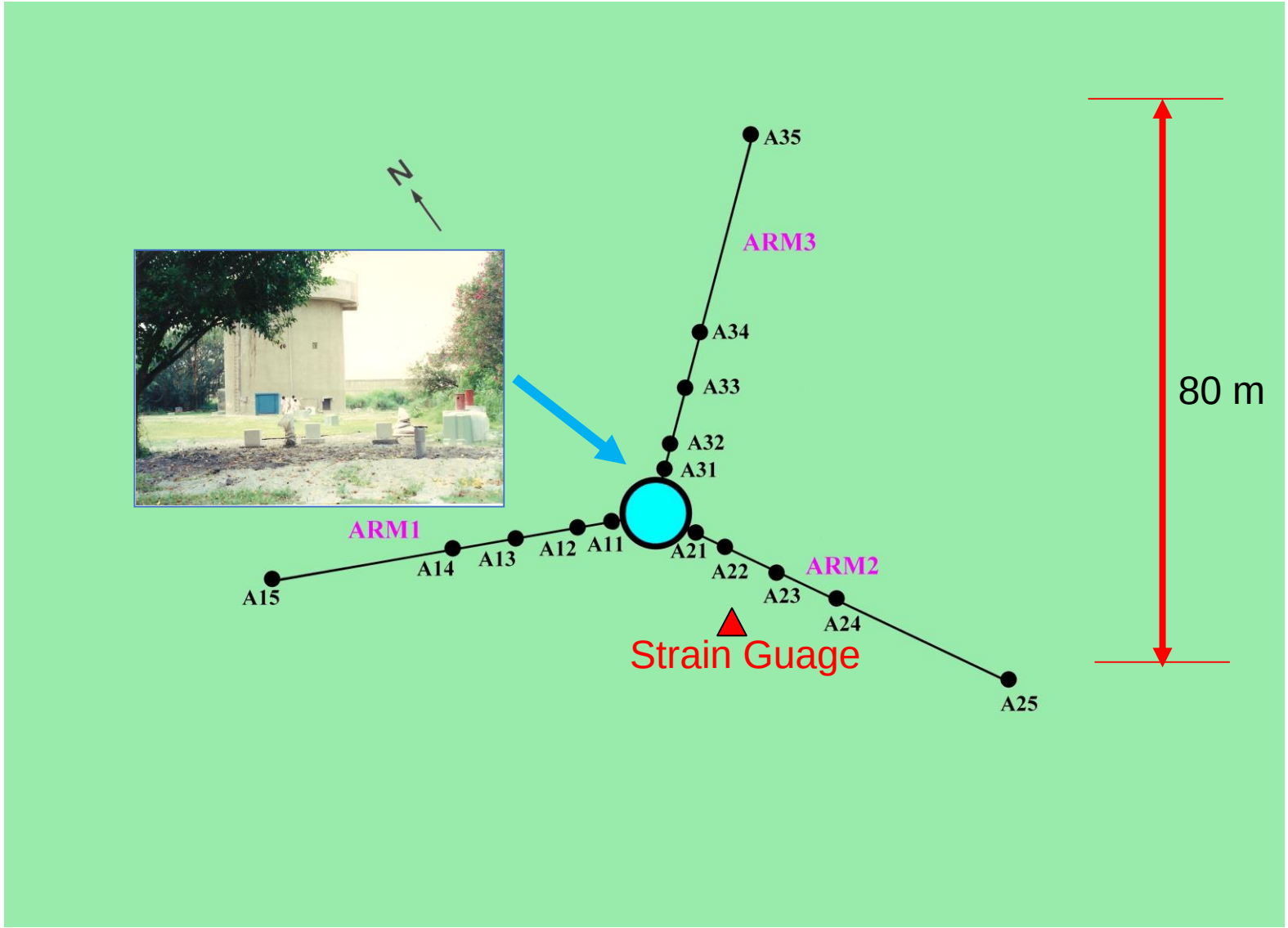

Array recorded translation ground motions (Vertical component)

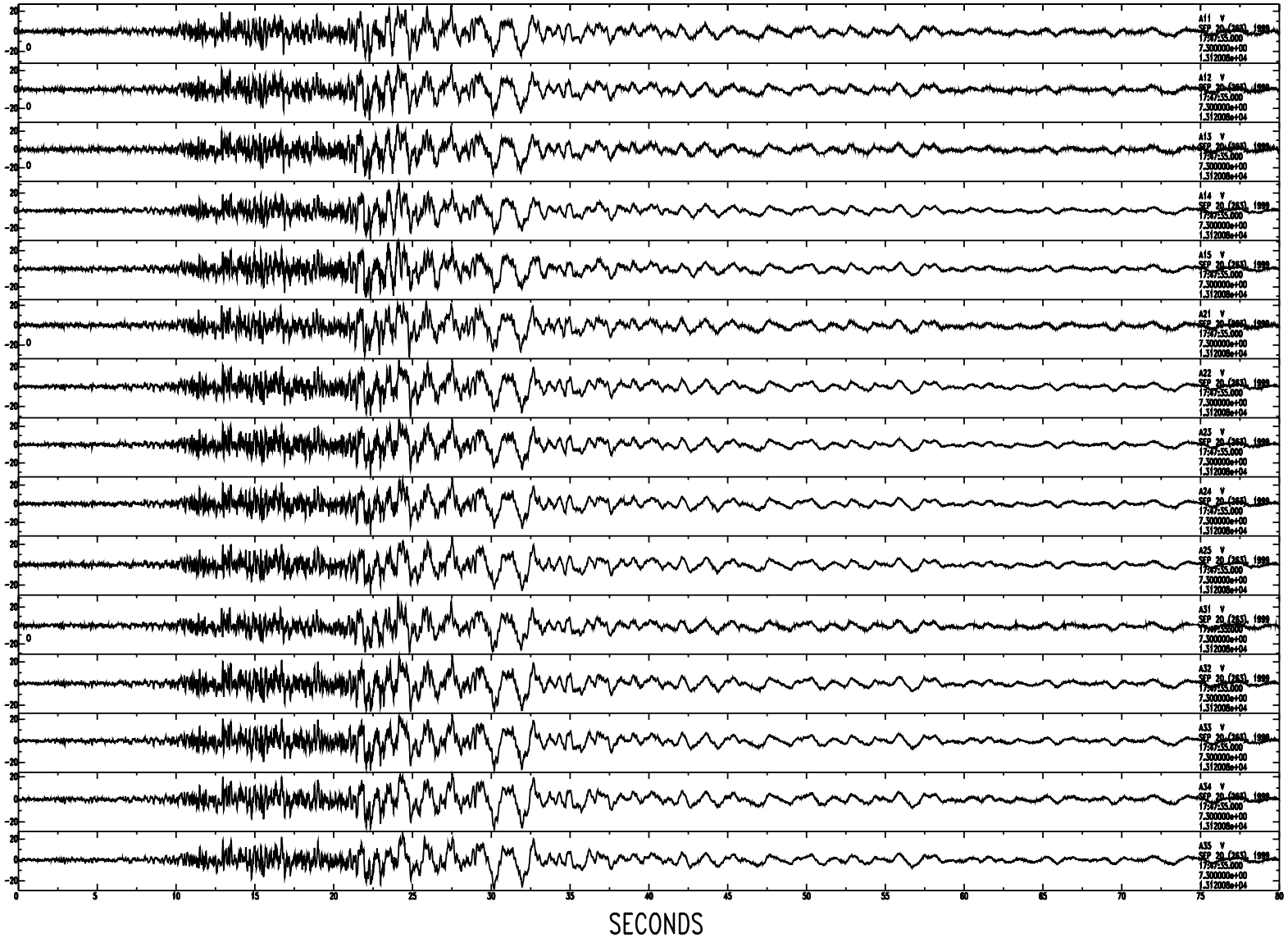

Array recorded translation ground motions (EW component)

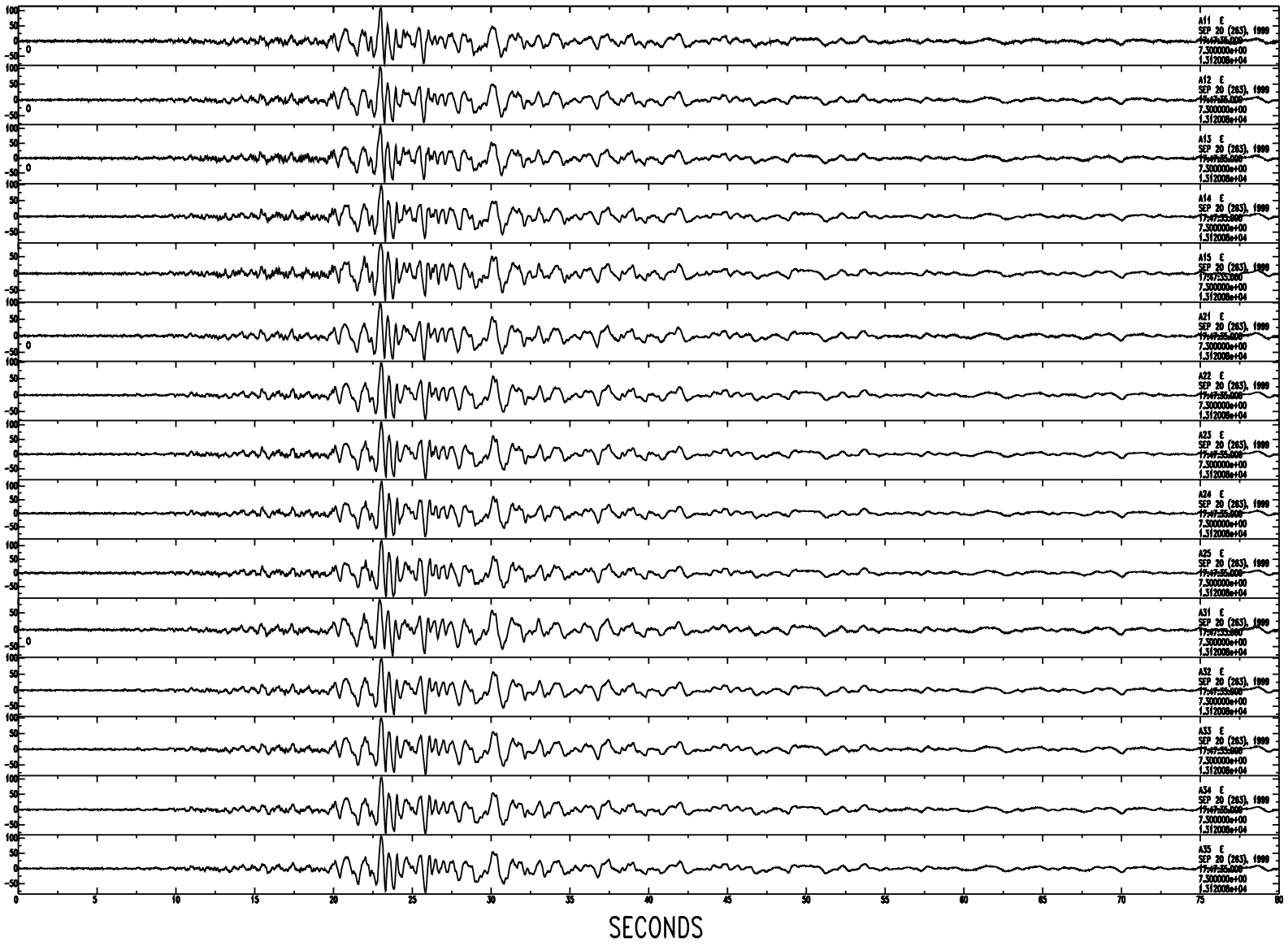

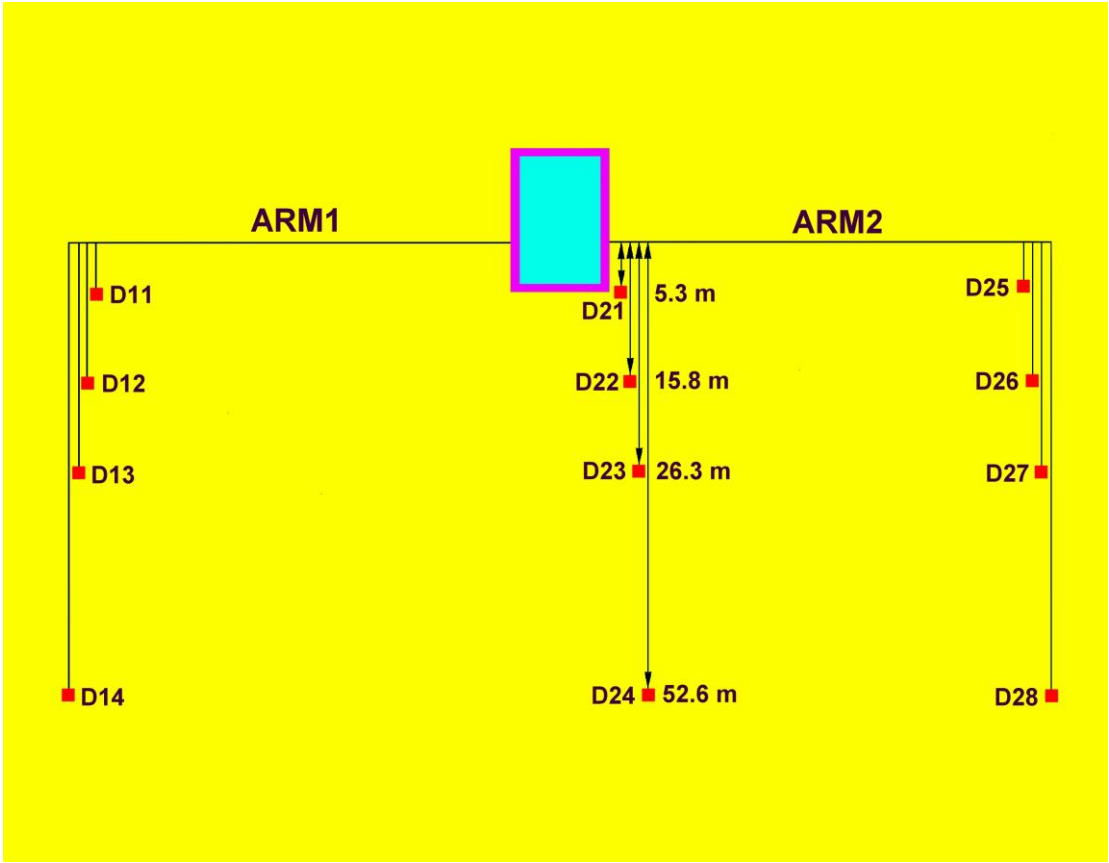
ARM1
ARM2
D11
D12
D13
D14
D21
5.3 m
D22
15.8 m
D23
26.3 m
D24
52.6 m
D25
D26
D27
D28

Dynamic Strains and rotations (aftershock)

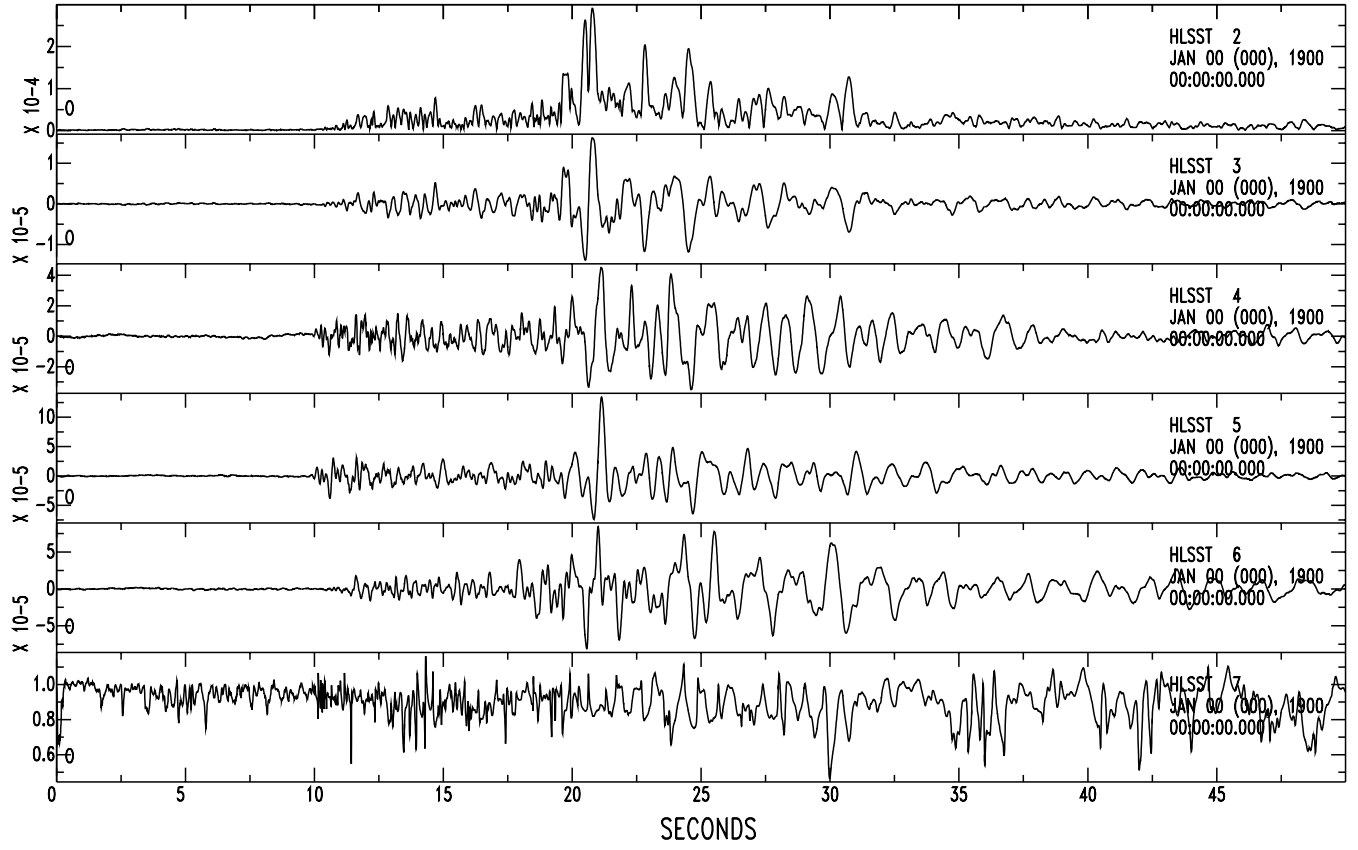

Previous Rupture process reports of the Chi-Chi EQ

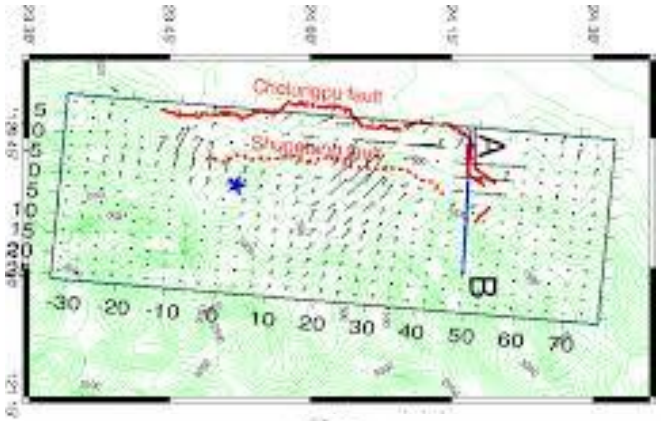

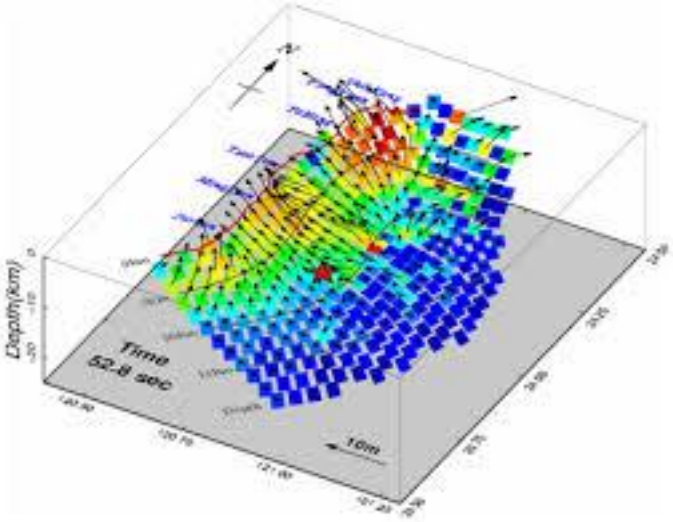

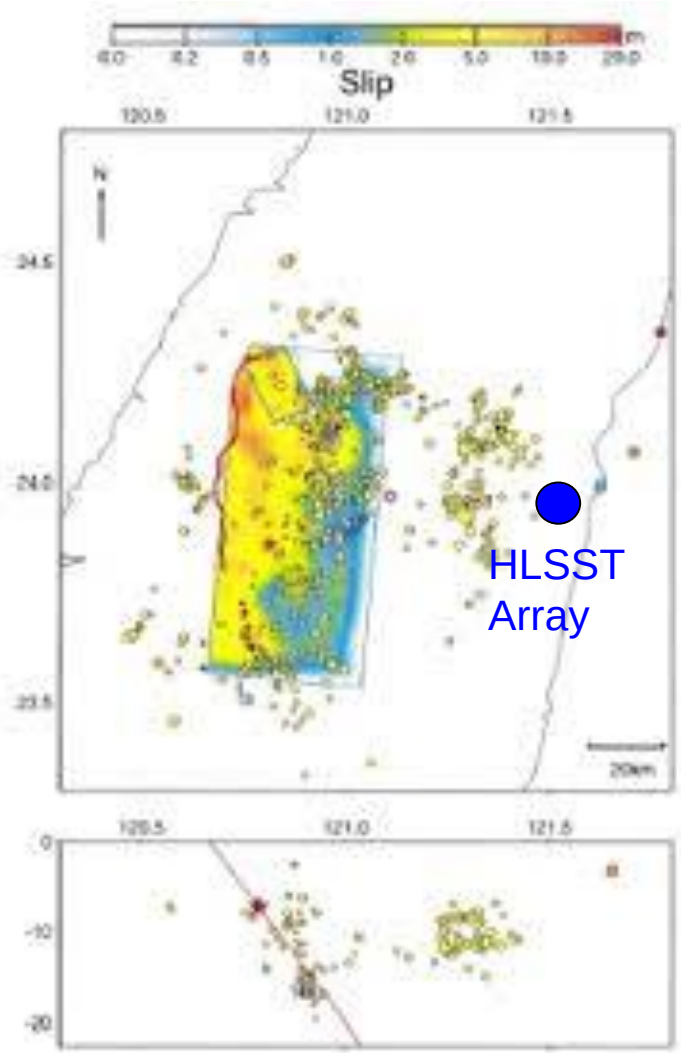

地震源與波傳的數值模擬

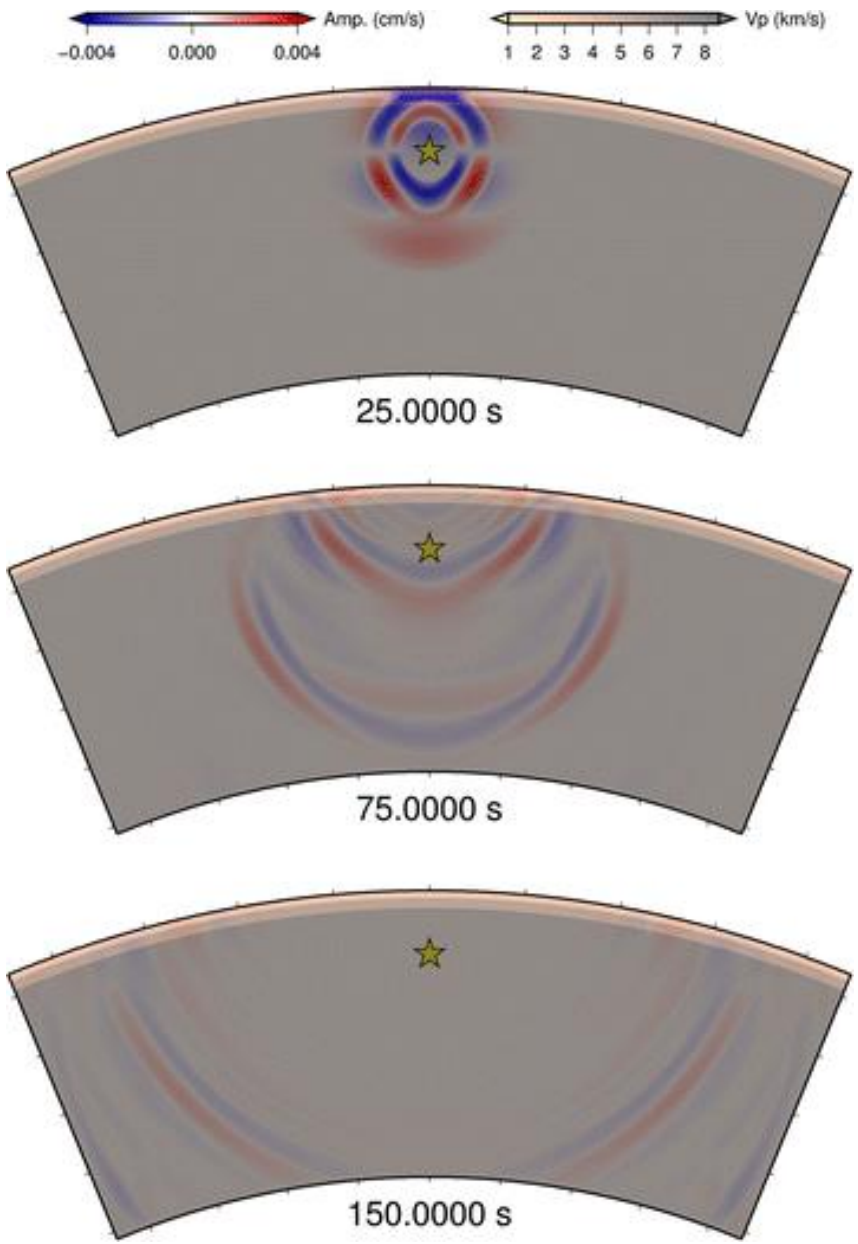
Amp. (cm/s)
−0.004
0.000
0.004
Vp (km/s)
1 2 3 4 5 6 7 8
25.0000 s
75.0000 s
150.0000 s

解析解 vs 數值解

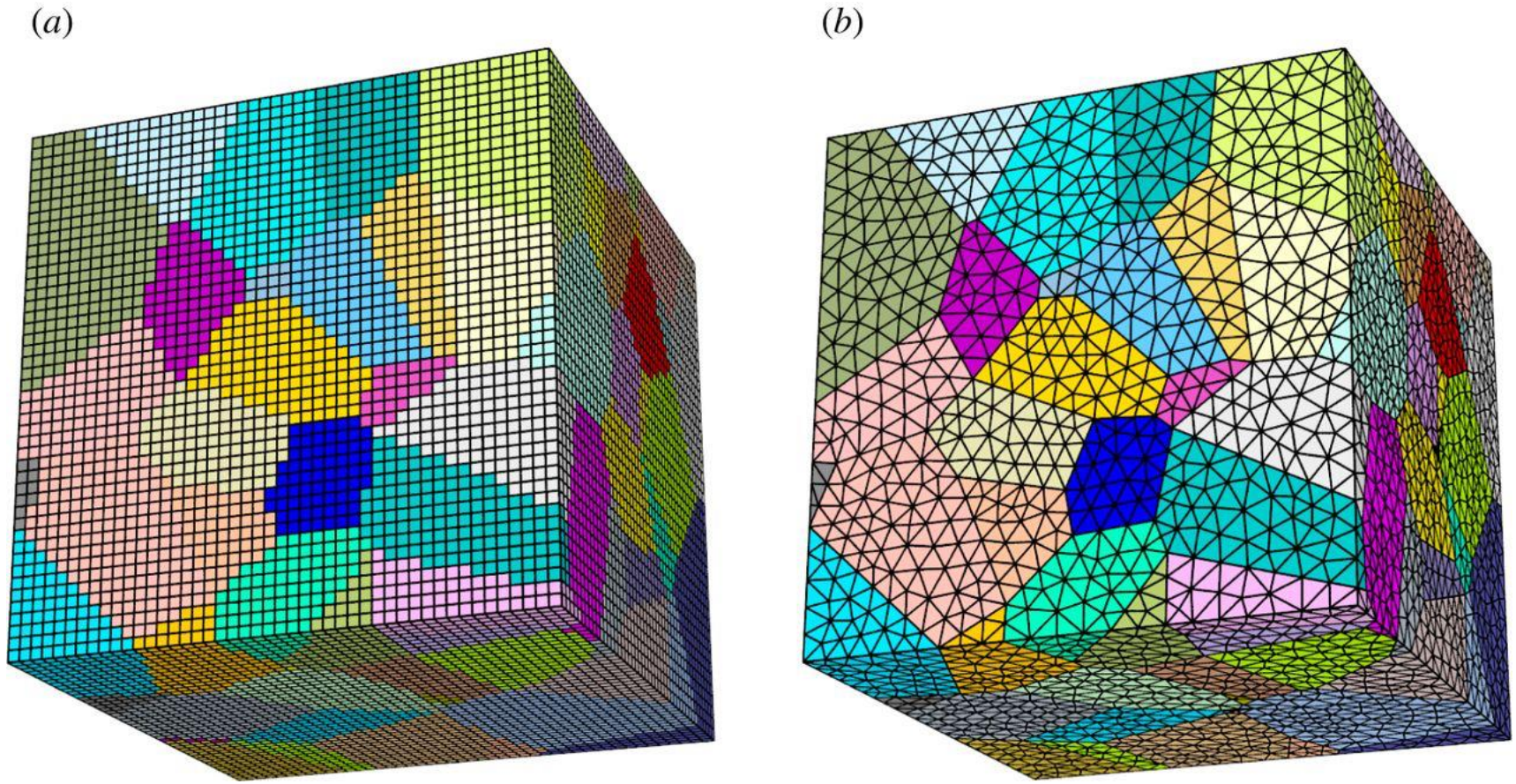
(a)
(b)

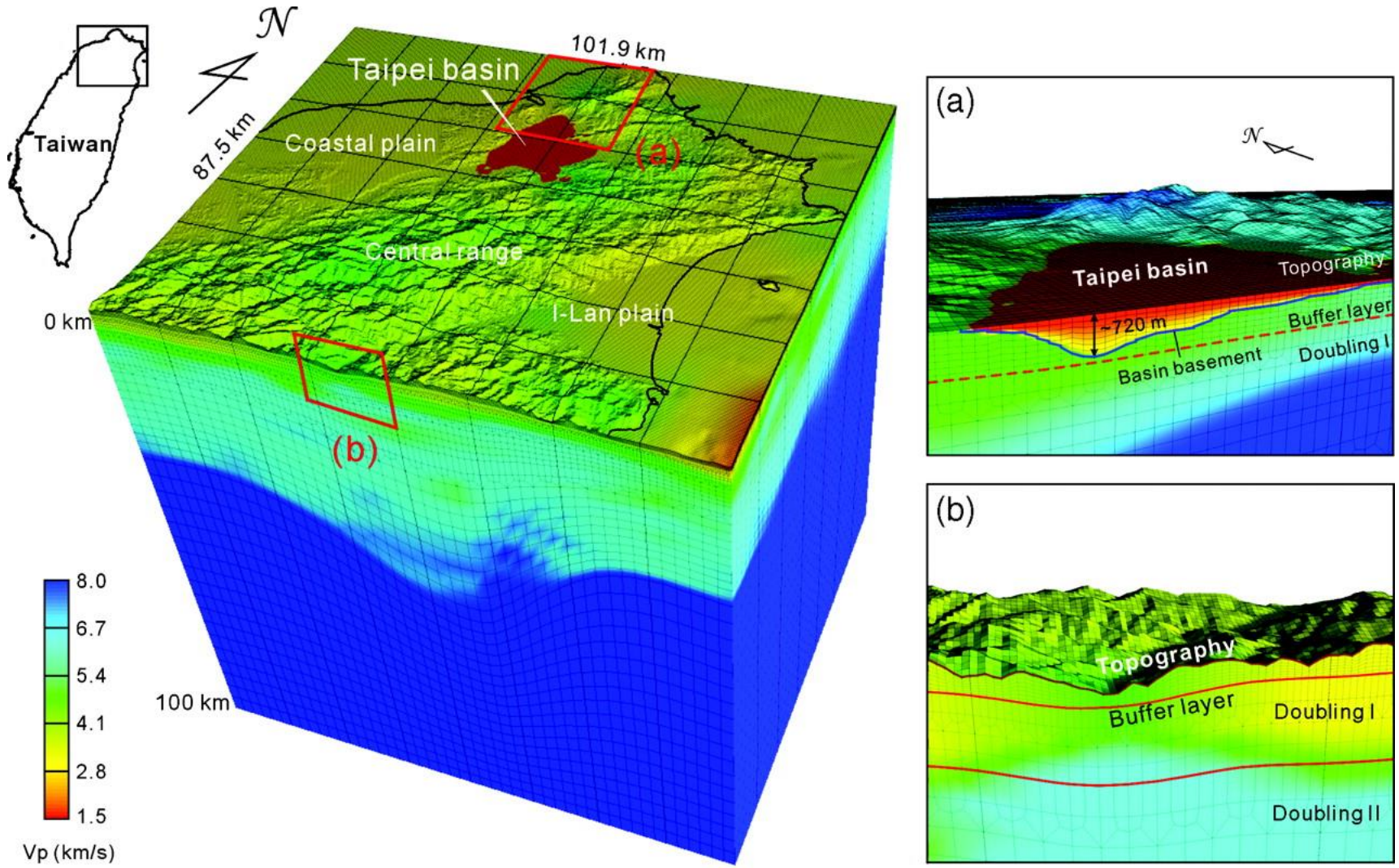
Taiwan
N
87.5 km
101.9 km
Taipei basin
Coastal plain
(a)
Central range
I-Lan plain
0 km
(b)
100 km
8.0
6.7
5.4
4.1
2.8
1.5
Vp (km/s)
(a)
N
Taipei basin
Topography
~720 m
Buffer layer
Basin basement
Doubling I
(b)
Topography
Buffer layer
Doubling I
Doubling II

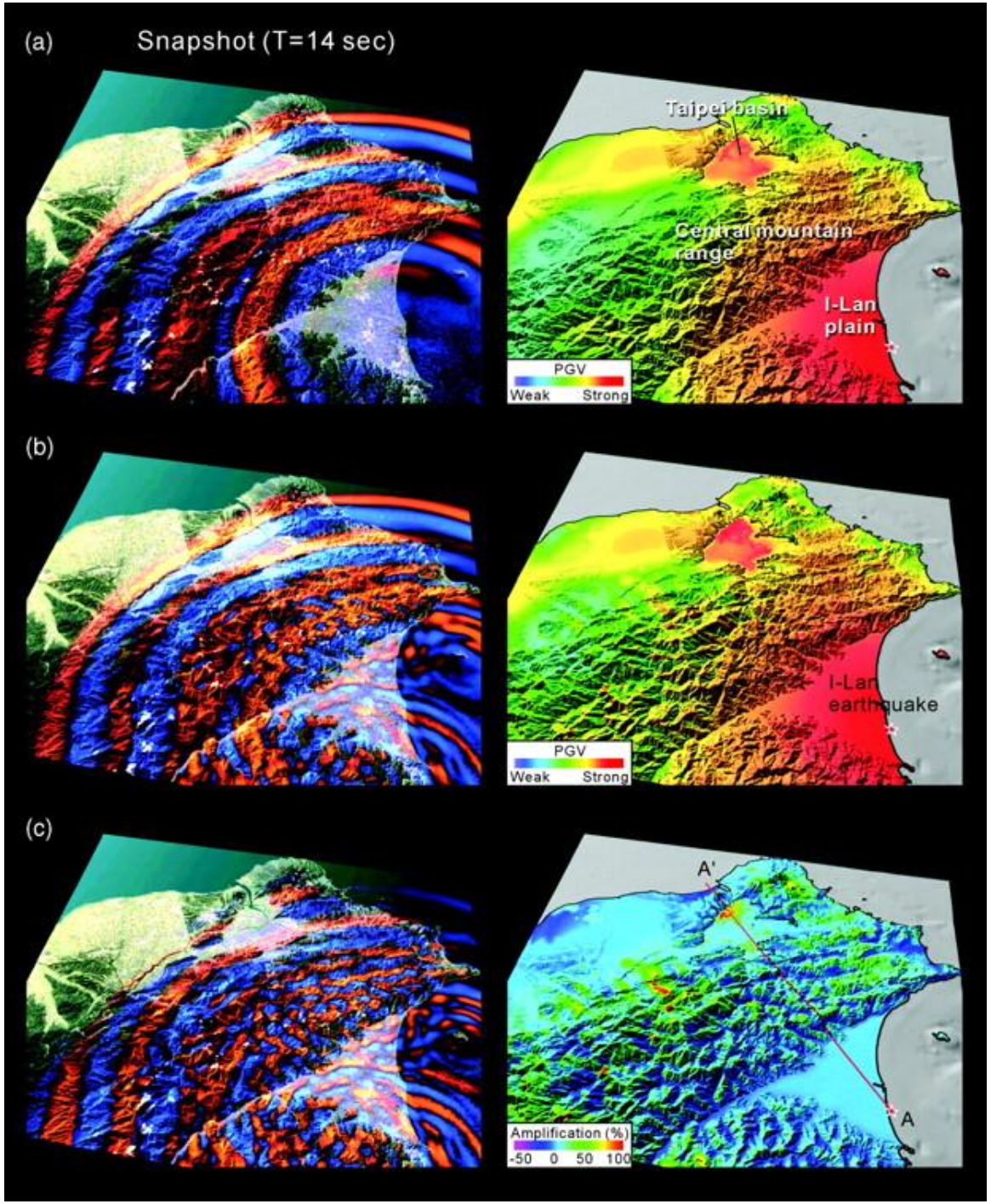
(a)
Snapshot (T=14 sec)
Taipei basin
Central mountain range
I-Lan plain
PGV
Weak
Strong
(b)
I-Lan earthquake
PGV
Weak
Strong
(c)
A'
A
Amplification (%)
-50 0 50 100

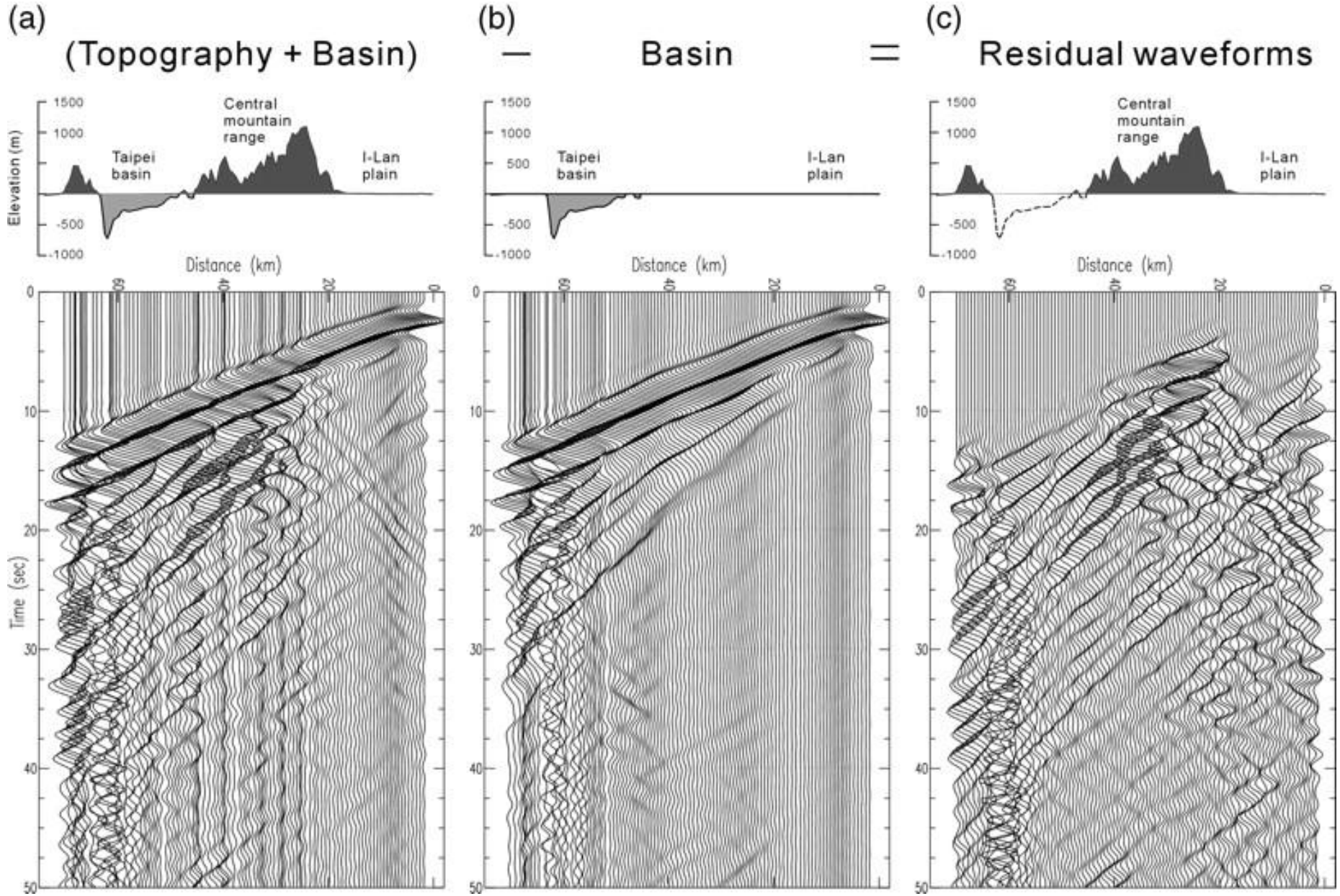
(a)
(Topography + Basin)
(b)
—
Basin
(c)
=
Residual waveforms
Elevation (m)
1500
1000
500
-500
-1000
Taipei basin
Central mountain range
I-Lan plain
Distance (km)
60
40
20
0
Time (sec)
0
10
20
30
40
50

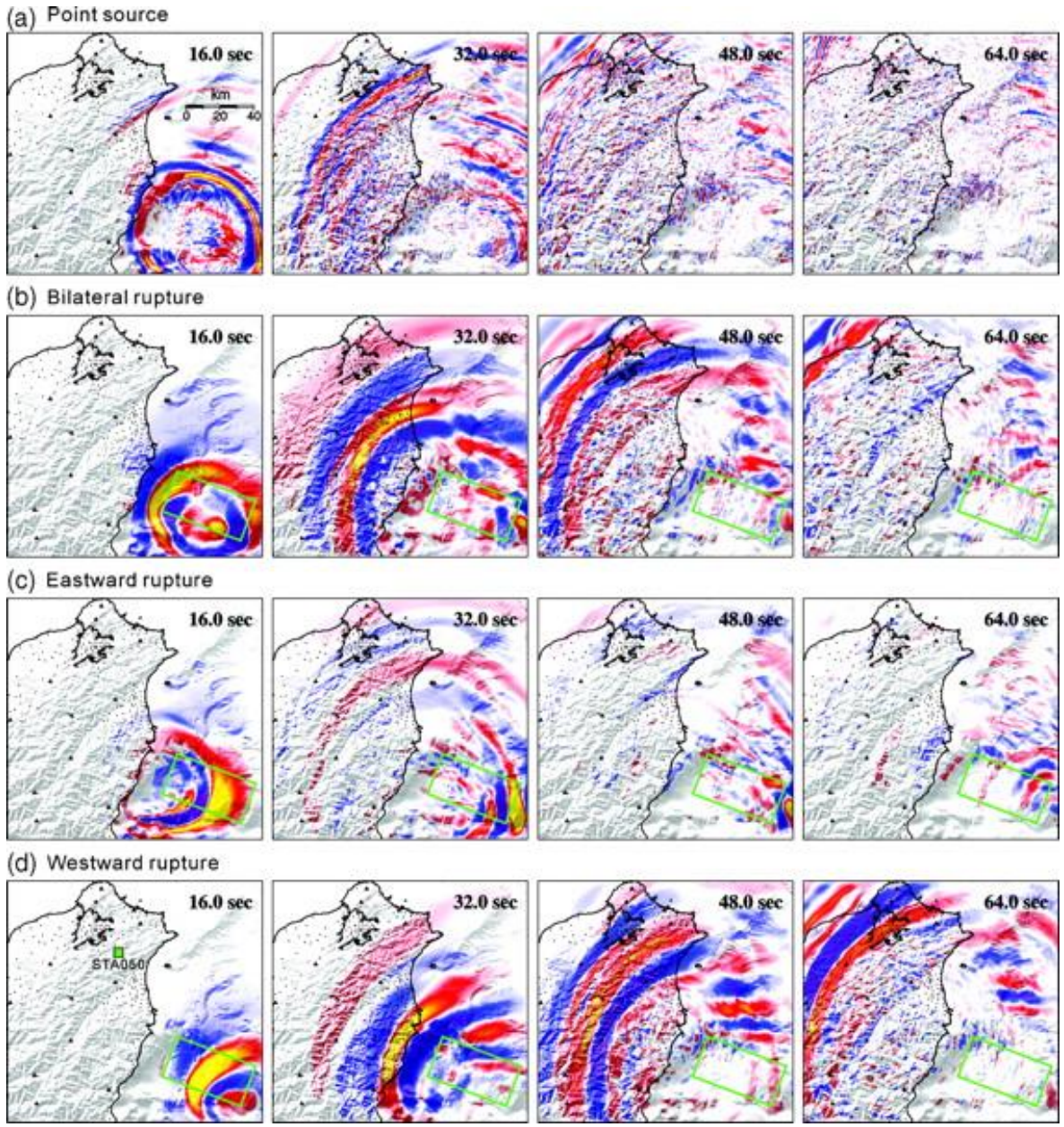
(a) Point source
16.0 sec
km
0 20 40
32.0 sec
48.0 sec
64.0 sec
(b) Bilateral rupture
16.0 sec
32.0 sec
48.0 sec
64.0 sec
(c) Eastward rupture
16.0 sec
32.0 sec
48.0 sec
64.0 sec
(d) Westward rupture
16.0 sec
STA050
32.0 sec
48.0 sec
64.0 sec

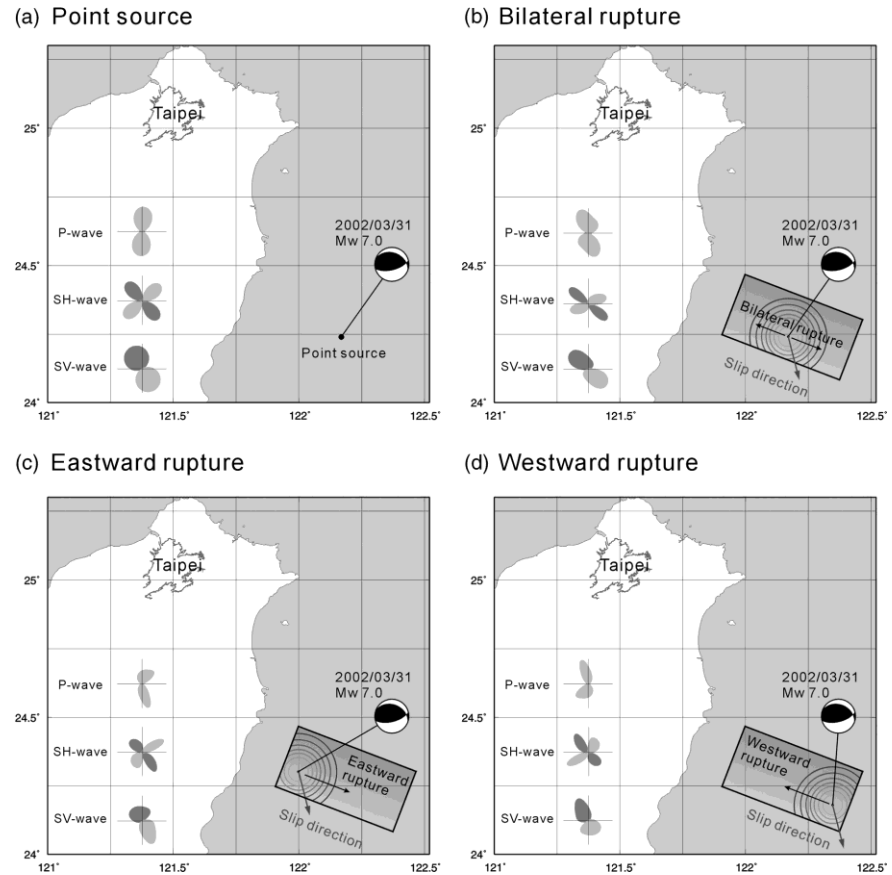
(a) Point source
(b) Bilateral rupture
(c) Eastward rupture
(d) Westward rupture
Taipei
25°
24.5°
24°
121°
121.5°
122°
122.5°
P-wave
SH-wave
SV-wave
2002/03/31
Mw 7.0
Point source
Bilateral rupture
Slip direction
Eastward rupture
Westward rupture

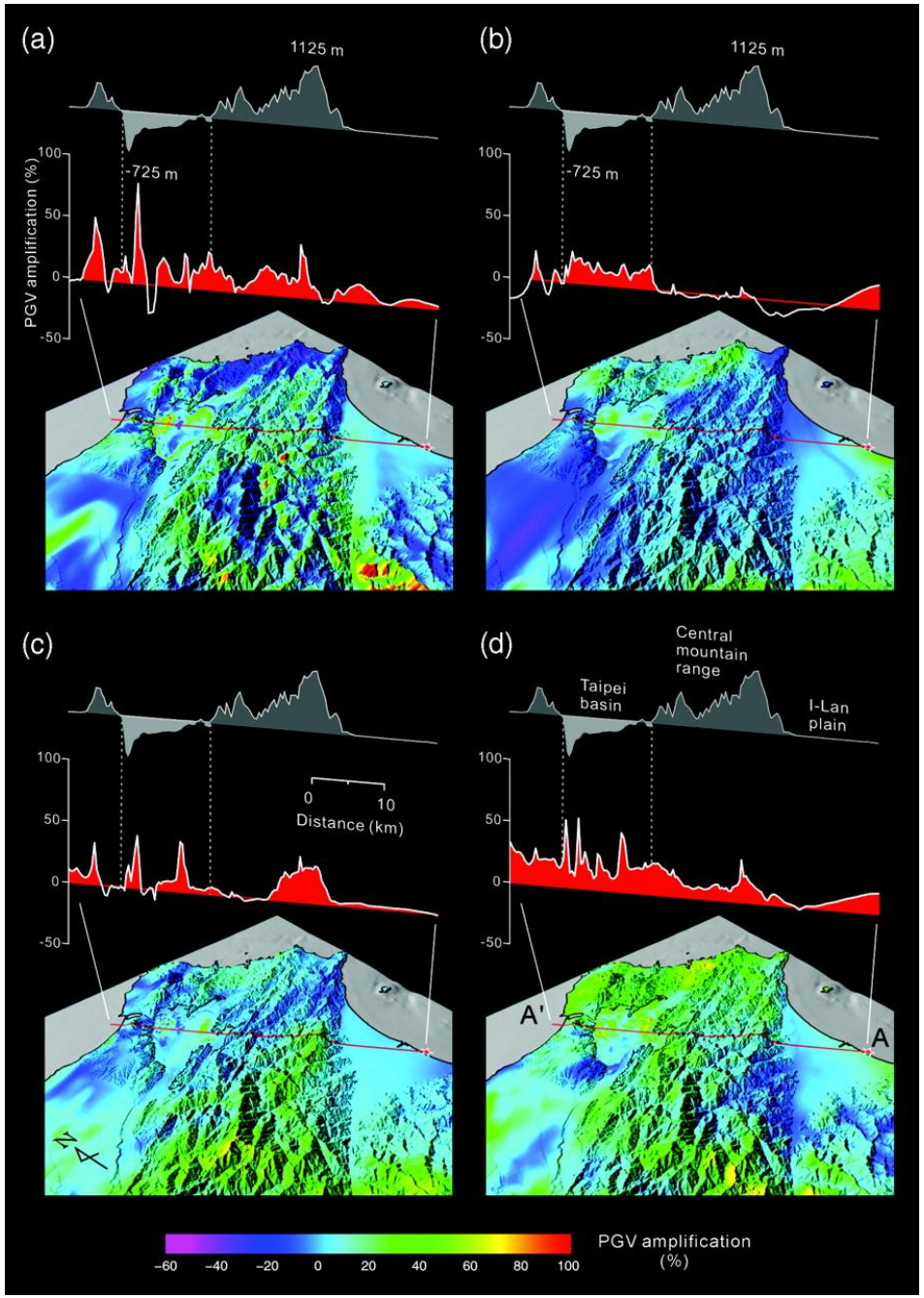
(a)
1125 m
725 m
PGV amplification (%)
100
50
0
-50
(b)
1125 m
725 m
(c)
0
10
Distance (km)
N
(d)
Central mountain range
Taipei basin
I-Lan plain
A'
A
−60 −40 −20 0 20 40 60 80 100
PGV amplification (%)

1999 集集地震破裂滑移分佈

Lee et al., 2006, JGR.

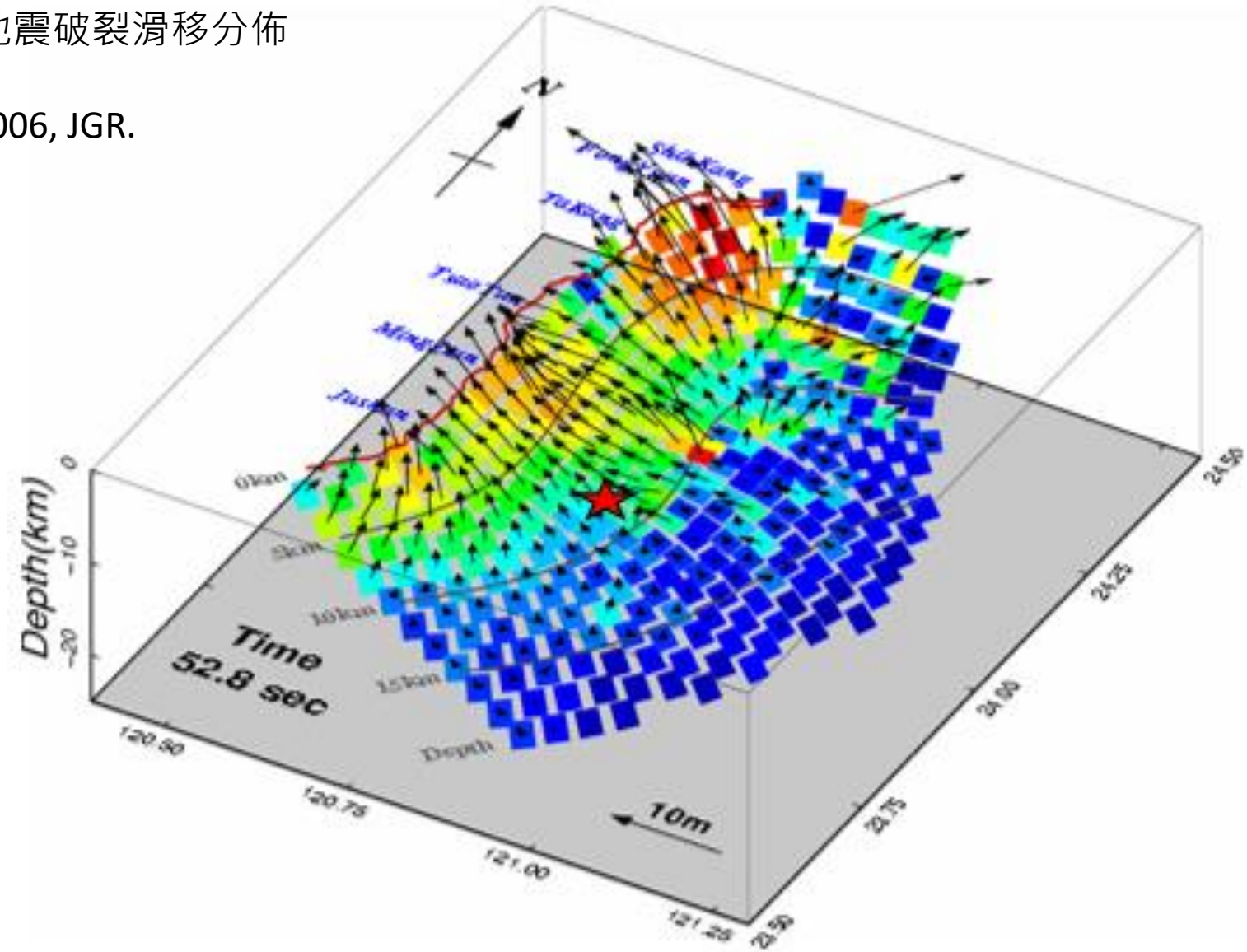

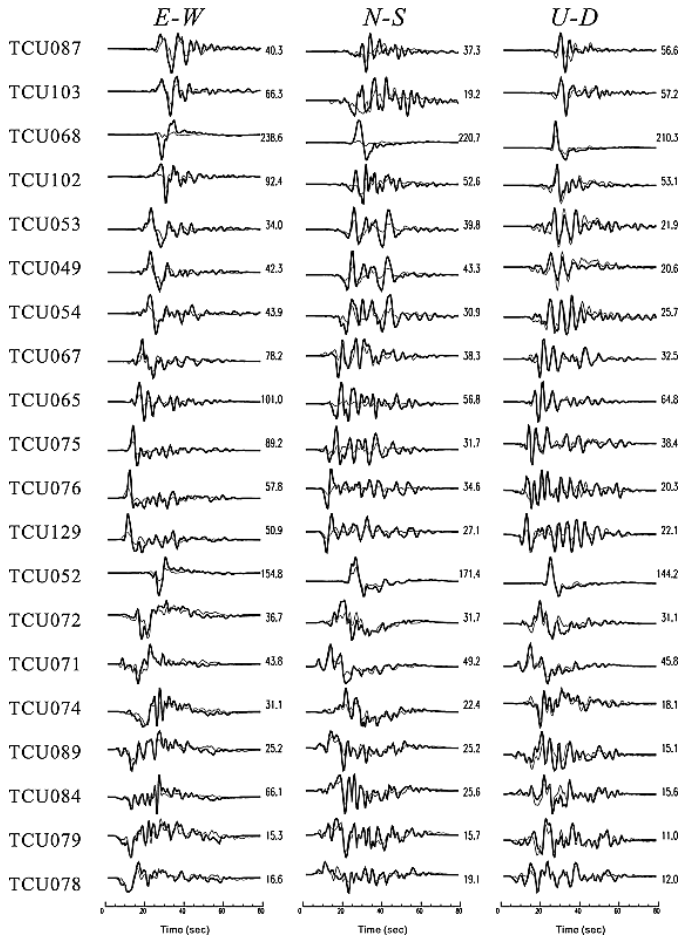
E-W
N-S
U-D
TCU087 40.3 37.3 56.6
TCU103 66.3 19.2 57.2
TCU068 238.6 220.7 210.3
TCU102 92.4 52.6 53.1
TCU053 34.0 39.8 21.9
TCU049 42.3 43.3 20.6
TCU054 43.9 30.9 25.7
TCU067 78.2 38.3 32.5
TCU065 101.0 56.8 64.8
TCU075 89.2 31.7 38.4
TCU076 57.8 34.6 20.3
TCU129 50.9 27.1 22.1
TCU052 154.8 171.4 144.2
TCU072 36.7 31.7 31.1
TCU071 43.8 49.2 45.8
TCU074 31.1 22.4 18.1
TCU089 25.2 25.2 15.1
TCU084 66.1 25.6 15.6
TCU079 15.3 15.7 11.0
TCU078 16.6 19.1 12.0
0 20 40 60 80
Time (sec)

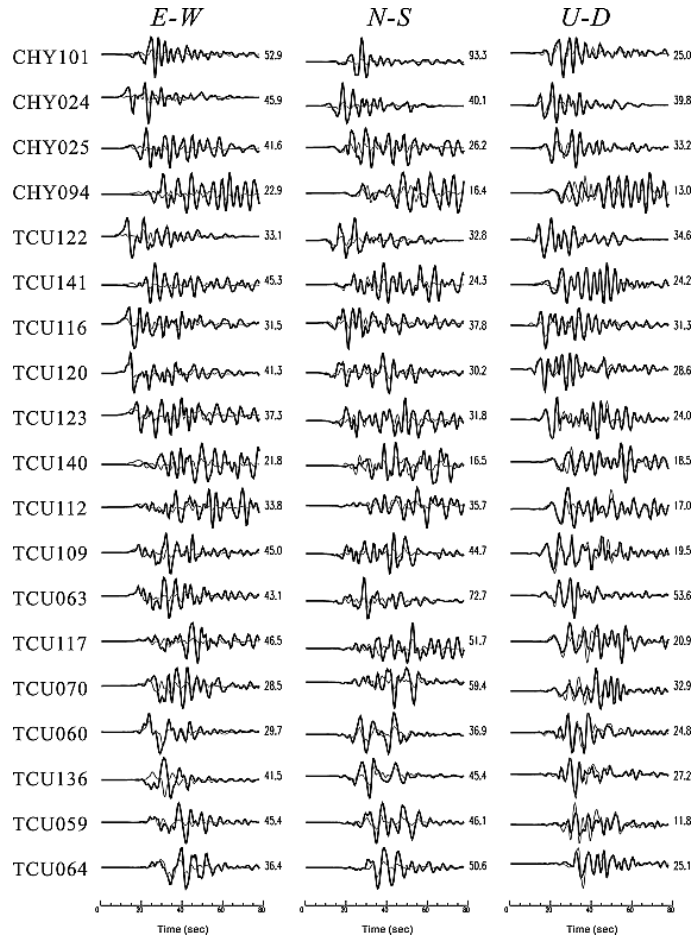
E-W
N-S
U-D
CHY101 52.9 93.3 25.0
CHY024 45.9 40.1 39.8
CHY025 41.6 26.2 33.2
CHY094 22.9 16.4 13.0
TCU122 33.1 32.8 34.6
TCU141 45.3 24.3 24.2
TCU116 31.5 37.8 31.3
TCU120 41.3 30.2 28.6
TCU123 37.3 31.8 24.0
TCU140 21.8 16.5 18.5
TCU112 33.8 35.7 17.0
TCU109 45.0 44.7 19.5
TCU063 43.1 72.7 53.6
TCU117 46.5 51.7 20.9
TCU070 28.5 59.4 32.9
TCU060 29.7 36.9 24.8
TCU136 41.5 45.4 27.2
TCU059 45.4 46.1 11.8
TCU064 36.4 50.6 25.1
0 20 40 60 80
Time (sec)

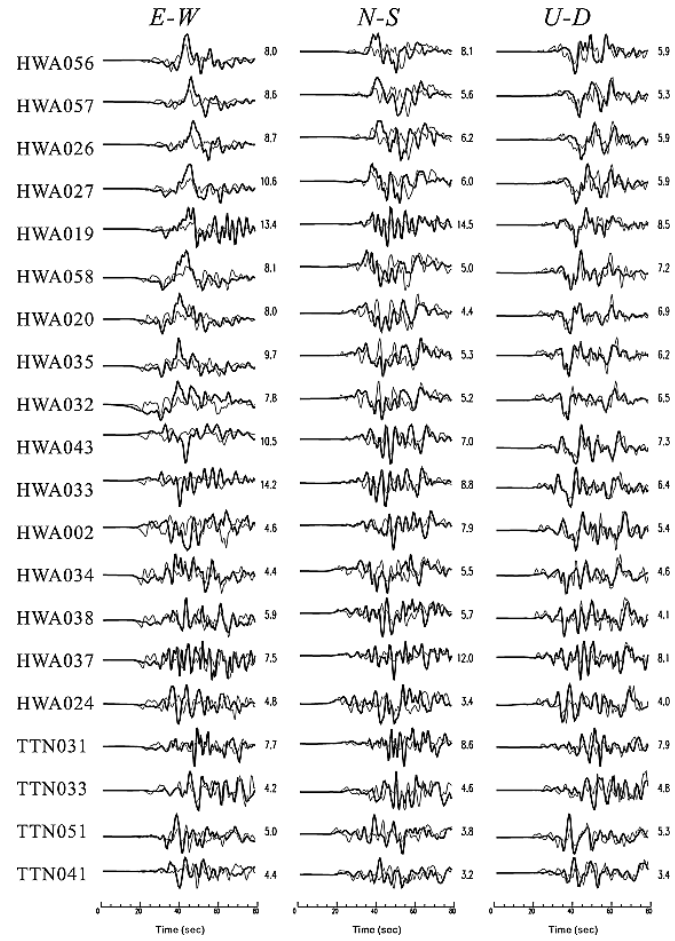
E-W
N-S
U-D
HWA056 8.0 8.1 5.9
HWA057 8.6 5.6 5.3
HWA026 8.7 6.2 5.9
HWA027 10.6 6.0 5.9
HWA019 13.4 14.5 8.5
HWA058 8.1 5.0 7.2
HWA020 8.0 4.4 6.9
HWA035 9.7 5.3 6.2
HWA032 7.8 5.2 6.5
HWA043 10.5 7.0 7.3
HWA033 14.2 8.8 6.4
HWA002 4.6 7.9 5.4
HWA034 4.4 5.5 4.6
HWA038 5.9 5.7 4.1
HWA037 7.5 12.0 8.1
HWA024 4.8 3.4 4.0
TTN031 7.7 8.6 7.9
TTN033 4.2 4.6 4.8
TTN051 5.0 3.8 5.3
TTN041 4.4 3.2 3.4
0 20 40 60 80
Time (sec)

Tohoku, Japan Earthquake: Finite Fault Model
U. California, Santa Barbara

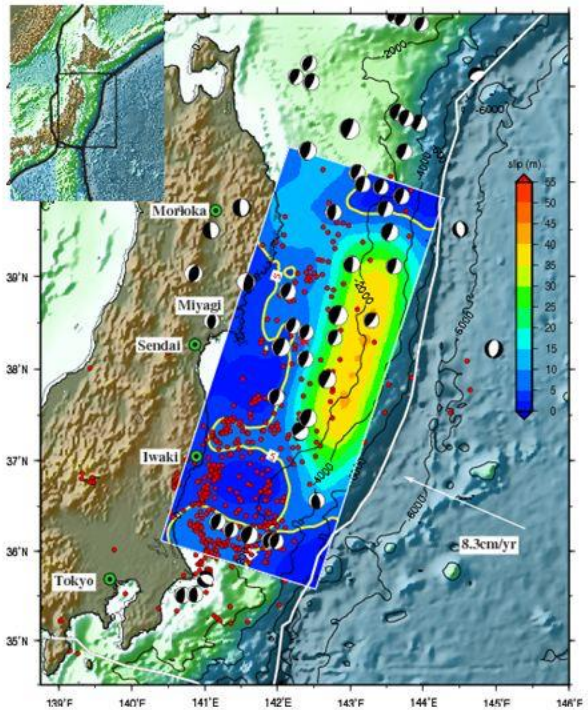

Version 1
NEIC Hypocenter

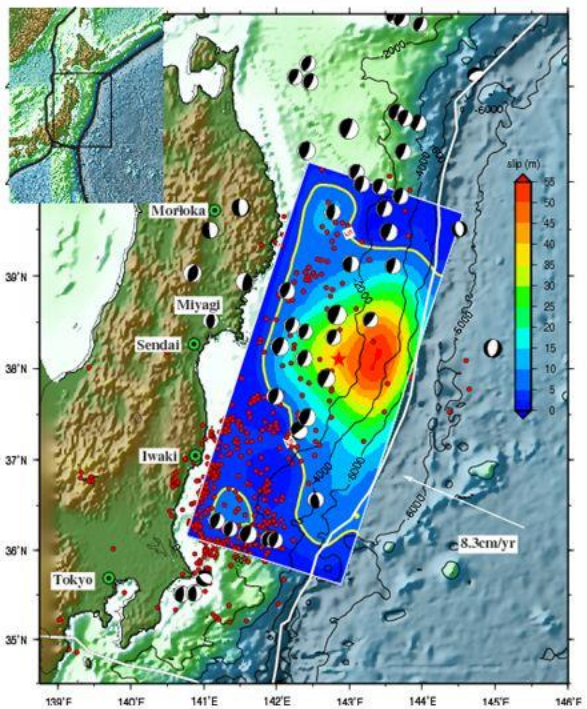

Version 2
JMA Hypocenter
(50 km ESE)

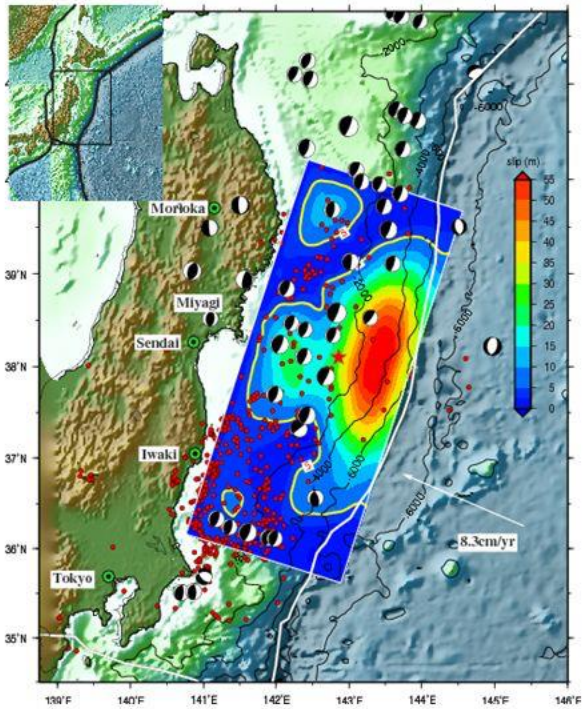

Version 3
Body & Surface Waves
realigned using the
03/09/2011 Mw 7.3
foreshock.

Figures courtesy of Guangfu Shao, U. California, Santa Barbara

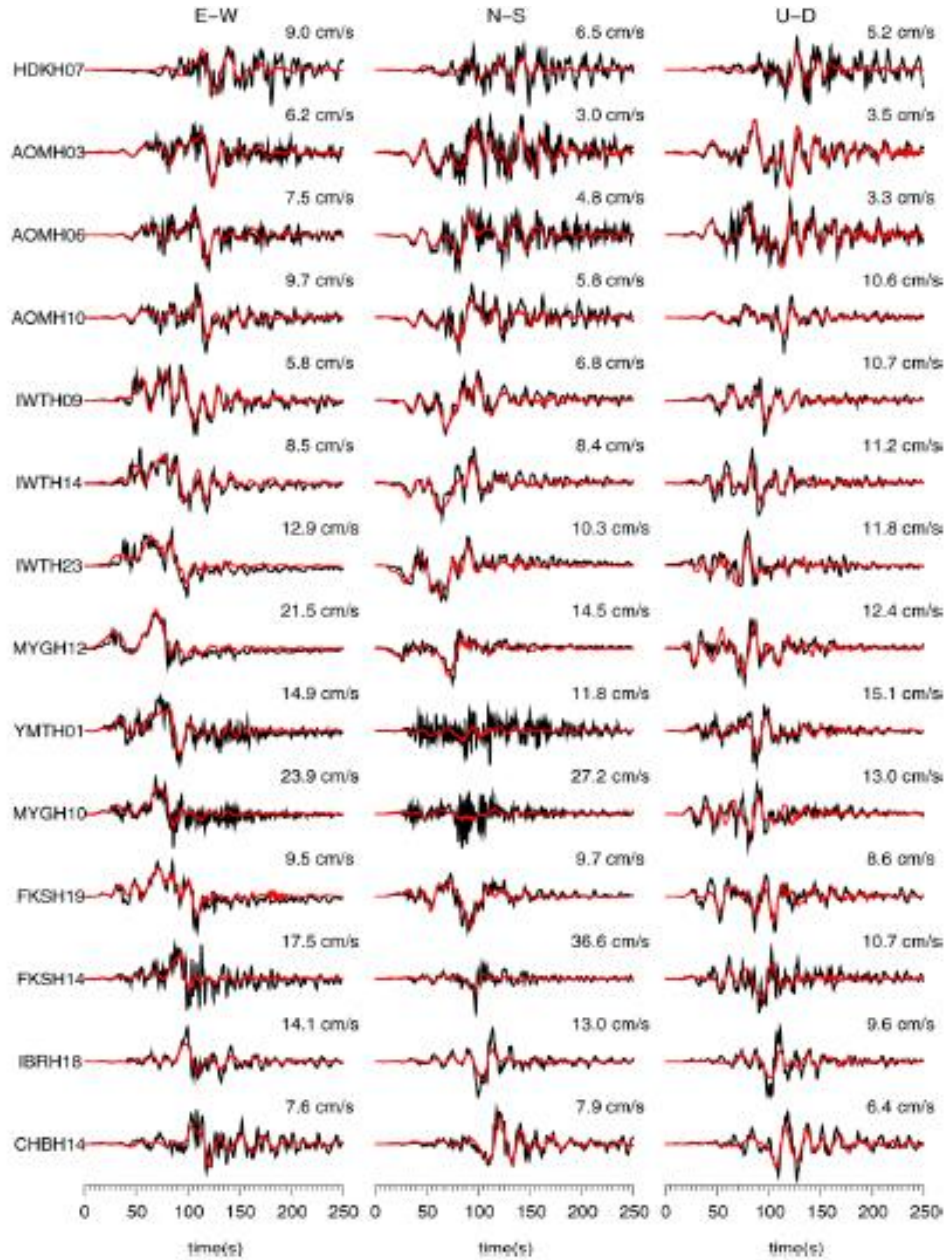
E–W
N–S
U–D
HDKH07
AOMH03
AOMH06
AOMH10
IWTH09
IWTH14
IWTH23
MYGH12
YMTH01
MYGH10
FKSH19
FKSH14
IBRH18
CHBH14
9.0 cm/s
6.5 cm/s
5.2 cm/s
6.2 cm/s
3.0 cm/s
3.5 cm/s
7.5 cm/s
4.8 cm/s
3.3 cm/s
9.7 cm/s
5.8 cm/s
10.6 cm/s
5.8 cm/s
6.8 cm/s
10.7 cm/s
8.5 cm/s
8.4 cm/s
11.2 cm/s
12.9 cm/s
10.3 cm/s
11.8 cm/s
21.5 cm/s
14.5 cm/s
12.4 cm/s
14.9 cm/s
11.8 cm/s
15.1 cm/s
23.9 cm/s
27.2 cm/s
13.0 cm/s
9.5 cm/s
9.7 cm/s
8.6 cm/s
17.5 cm/s
36.6 cm/s
10.7 cm/s
14.1 cm/s
13.0 cm/s
9.6 cm/s
7.6 cm/s
7.9 cm/s
6.4 cm/s
0 50 100 150 200 250
time(s)

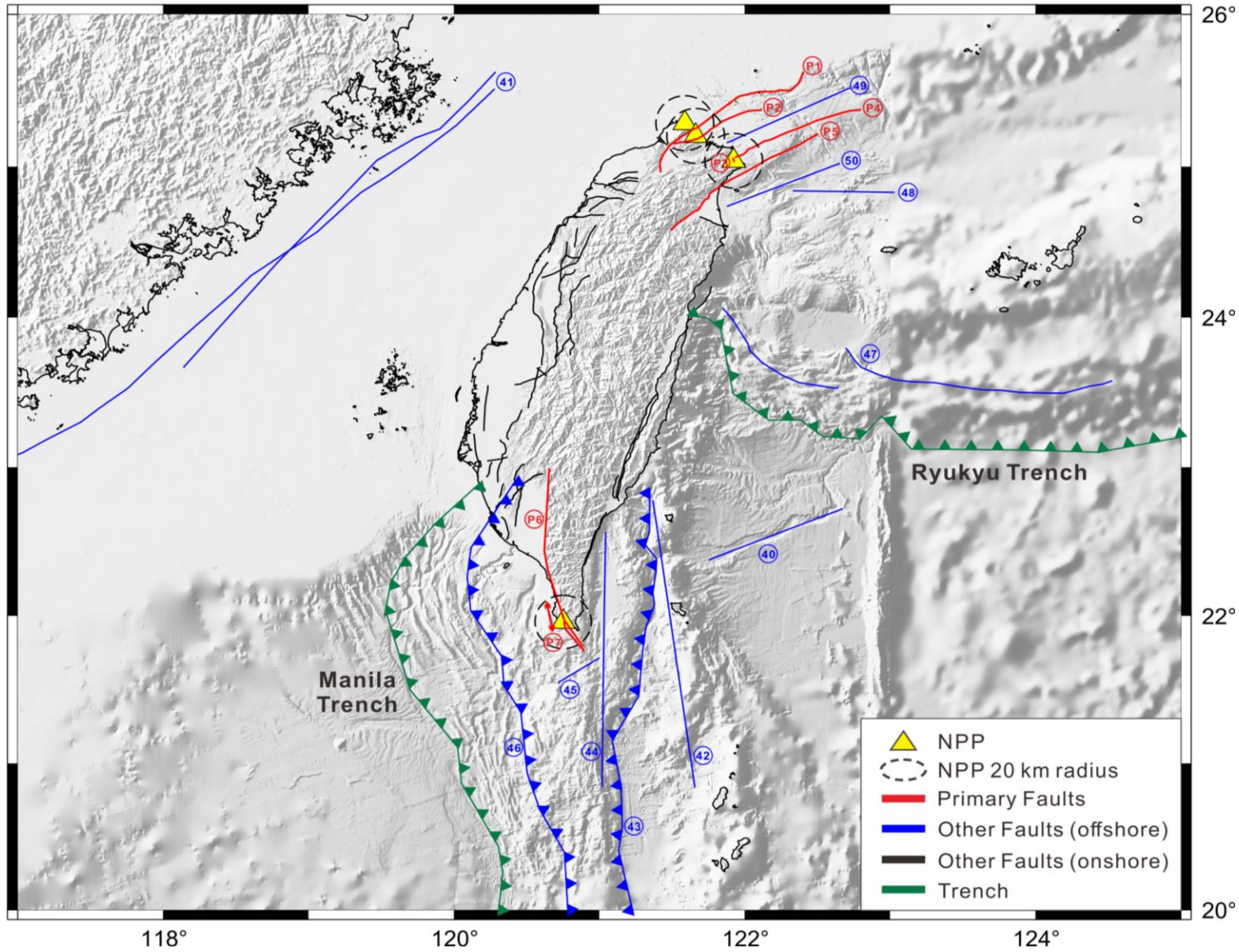
26°
24°
22°
20°
118°
120°
122°
124°
P1
P2
P3
P4
P5
P6
P7
41
49
50
48
47
40
45
46
44
42
43
Ryukyu Trench
Manila Trench
NPP
NPP 20 km radius
Primary Faults
Other Faults (offshore)
Other Faults (onshore)
Trench

高頻GPS的地動觀測及其應用

Review of GPS positioning

Dealing with errors

- Clock errors
- Ionosphere
- Troposphere
- Earth body deformations
- Orbit errors

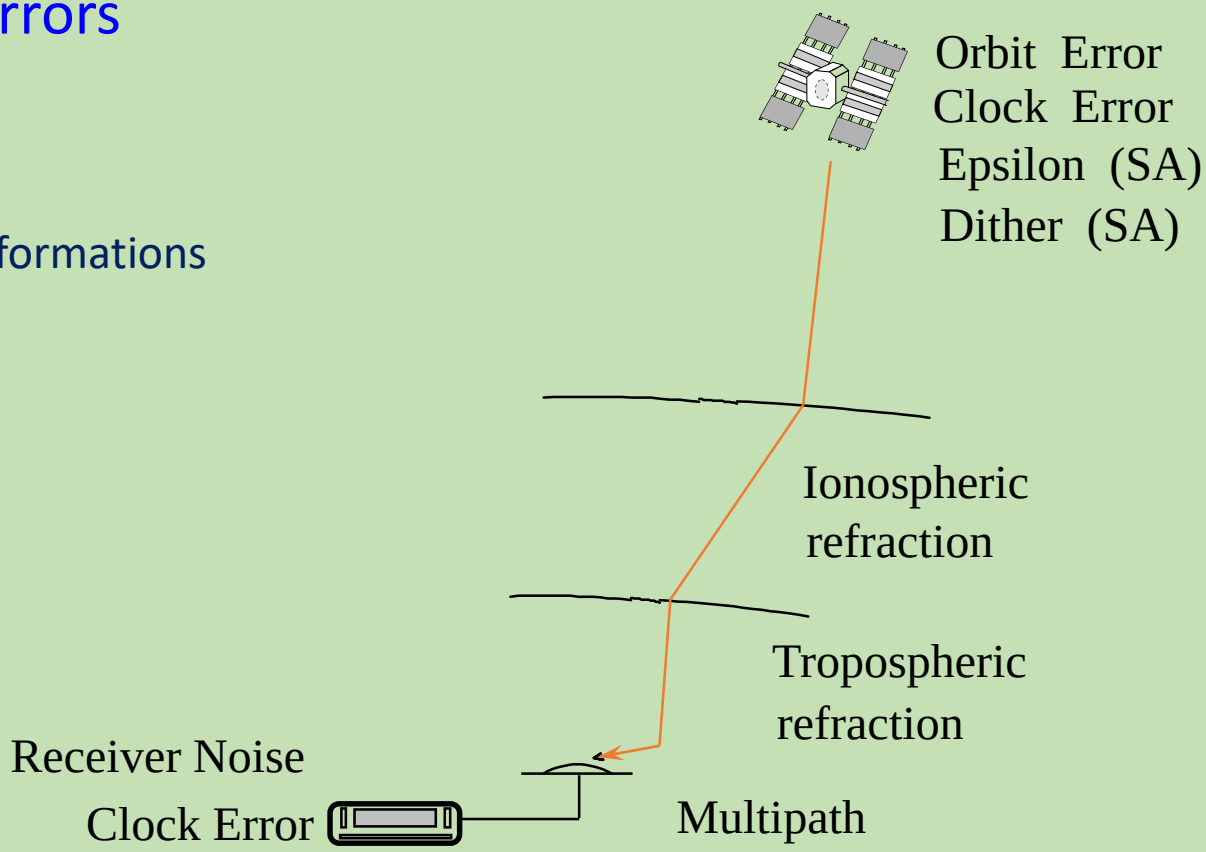

Tectonic plate movement observations from GPS

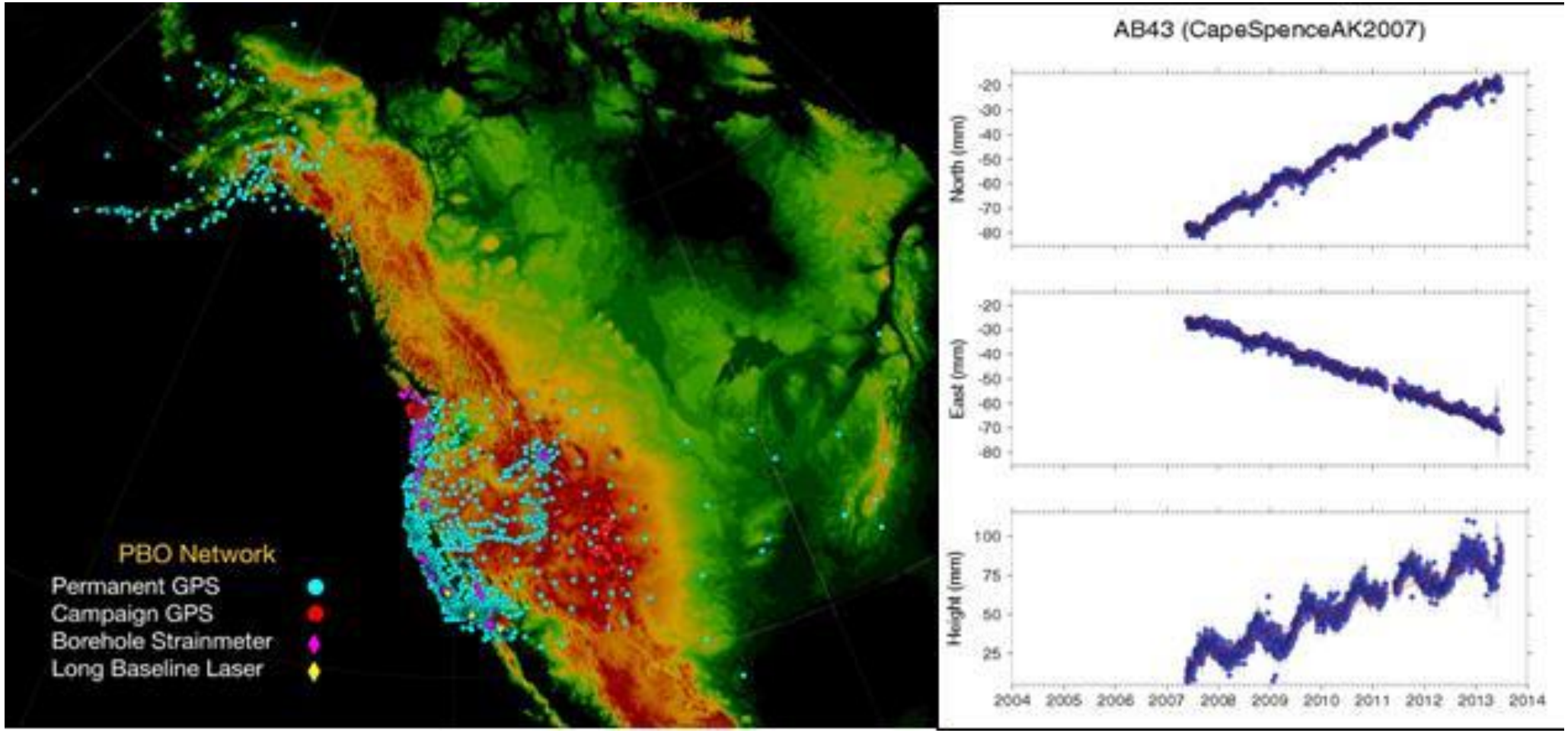


2011/03/19 13:38

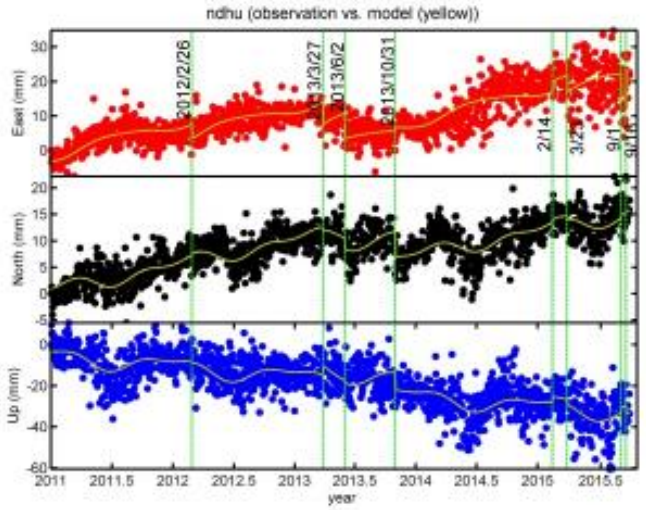
ndhu (observation vs. model (yellow))
East (mm)
North (mm)
Up (mm)
year
2012/2/26
2013/6/2
2013/10/31
2014
3/23
9/1

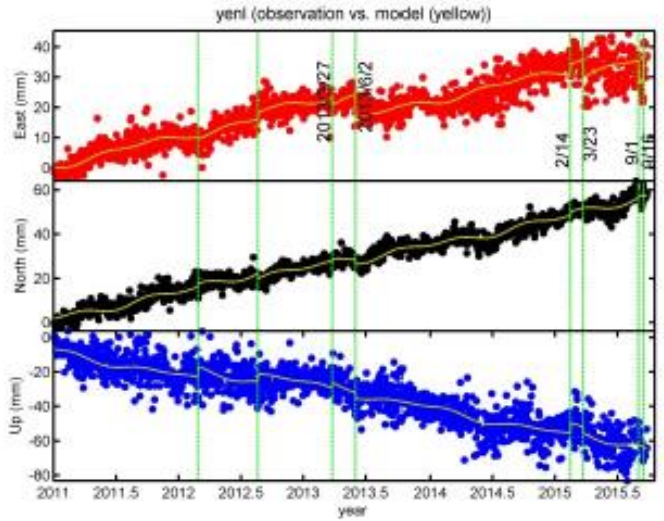
yenl (observation vs. model (yellow))
East (mm)
North (mm)
Up (mm)
year
2014
3/23
9/1

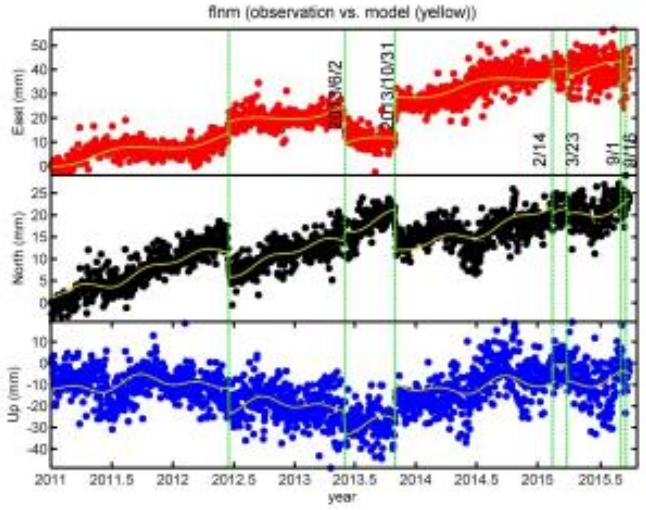
flnm (observation vs. model (yellow))
East (mm)
North (mm)
Up (mm)
year
2013/10/31
2014
3/23
9/1

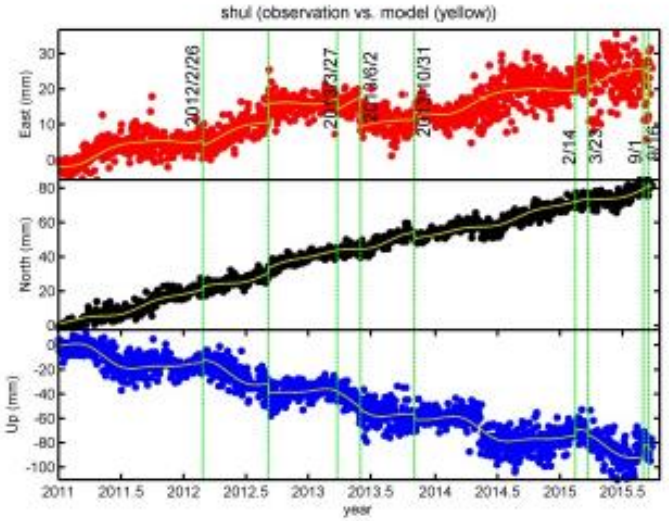
shul (observation vs. model (yellow))
East (mm)
North (mm)
Up (mm)
year
2012/2/26
2014
3/23
9/1

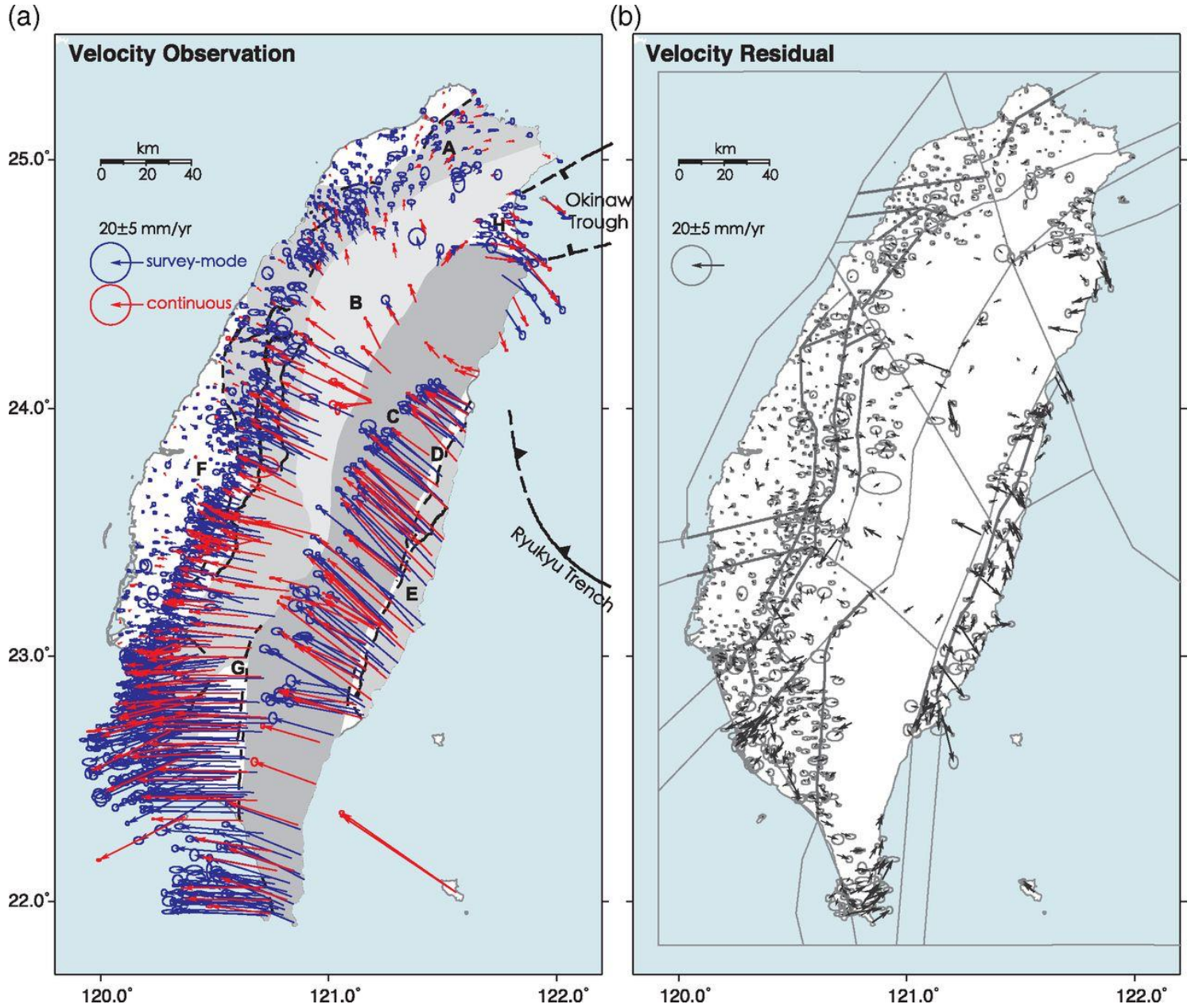
(a)
Velocity Observation
km
0 20 40
20±5 mm/yr
survey-mode
continuous
A
B
C
D
E
F
G
H
Okinawa Trough
Ryukyu Trench
25.0°
24.0°
23.0°
22.0°
120.0°
121.0°
122.0°
(b)
Velocity Residual
km
0 20 40
20±5 mm/yr
120.0°
121.0°
122.0°

Dealing with clock errors

- Undifferenced observable
  - Estimate both receiver and satellite clocks
  - Precise Point Positioning – Fix prior satellite clocks and estimate only receiver clocks
  - Parameter hungry

- Double-differenced observable
  - Undifferenced observations to two satellites at two stations
  - Form two between-station differences and then double-difference
  - Common clock terms difference

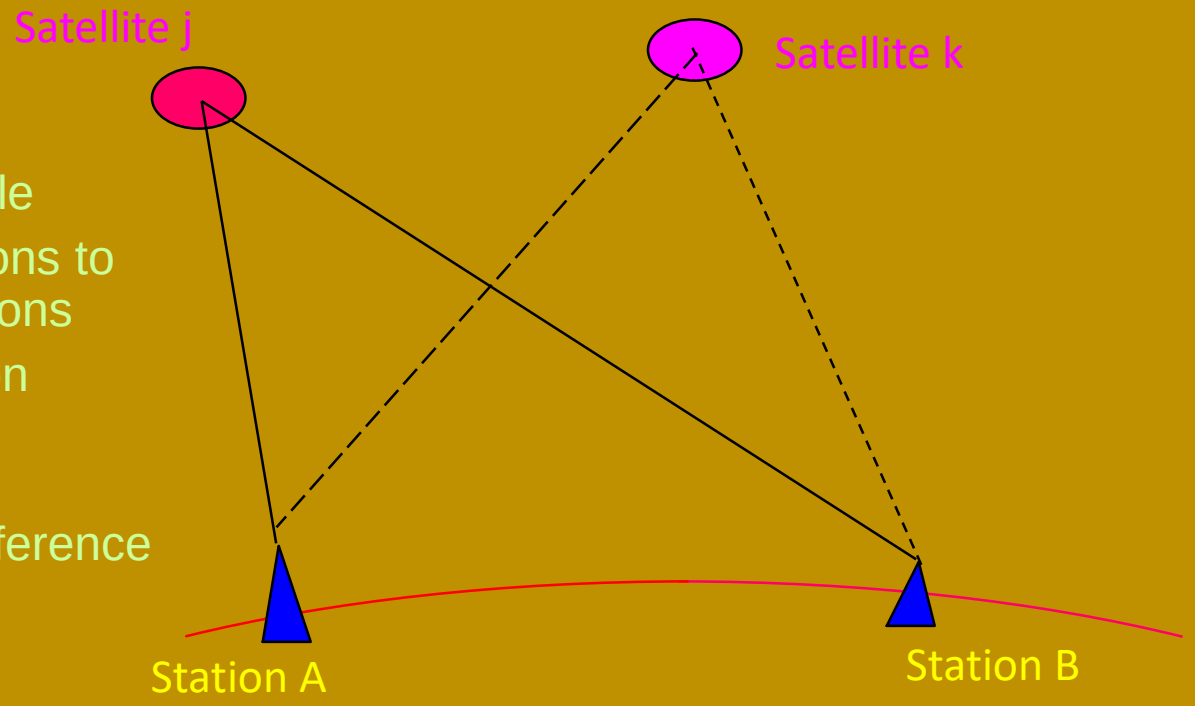

Double Difference vs PPP

Similar precision possible in 24 h solutions

- Software
  - Few software do geodetic PPP (GIPSY mainly)
  - GAMIT/Track are Double Difference

- PPP requires extra care
  - orbit/clock errors (some periodic) map 1:1 into positioning

- DD is more precise when short-baseline relative motion is all that is required, but depends on base station

GPS Seismology

GPS as a *strong motion* instrument

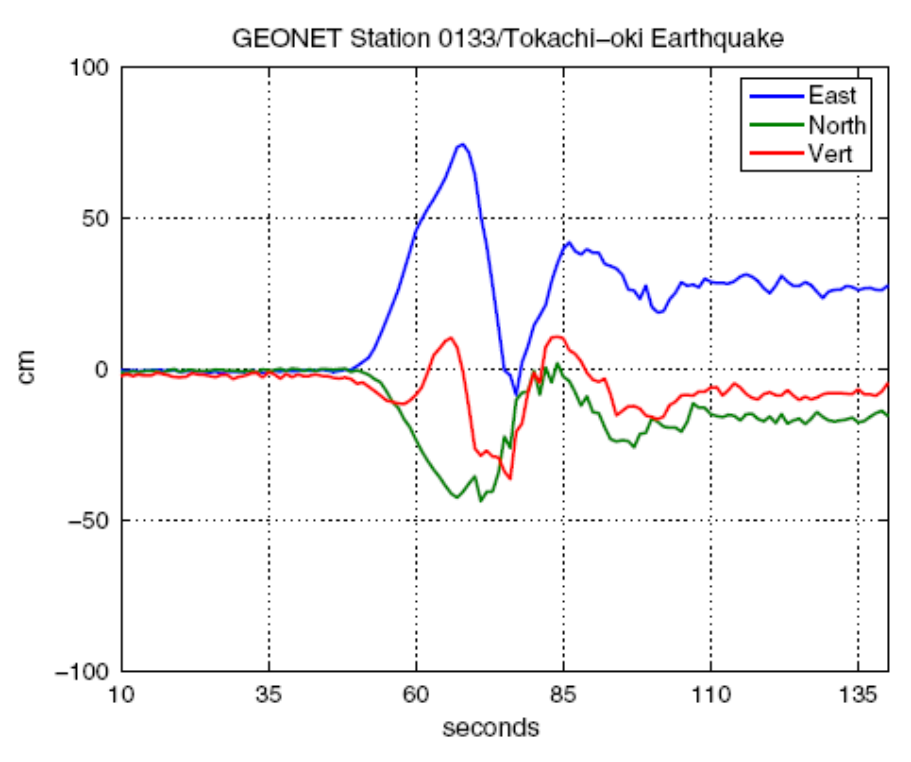

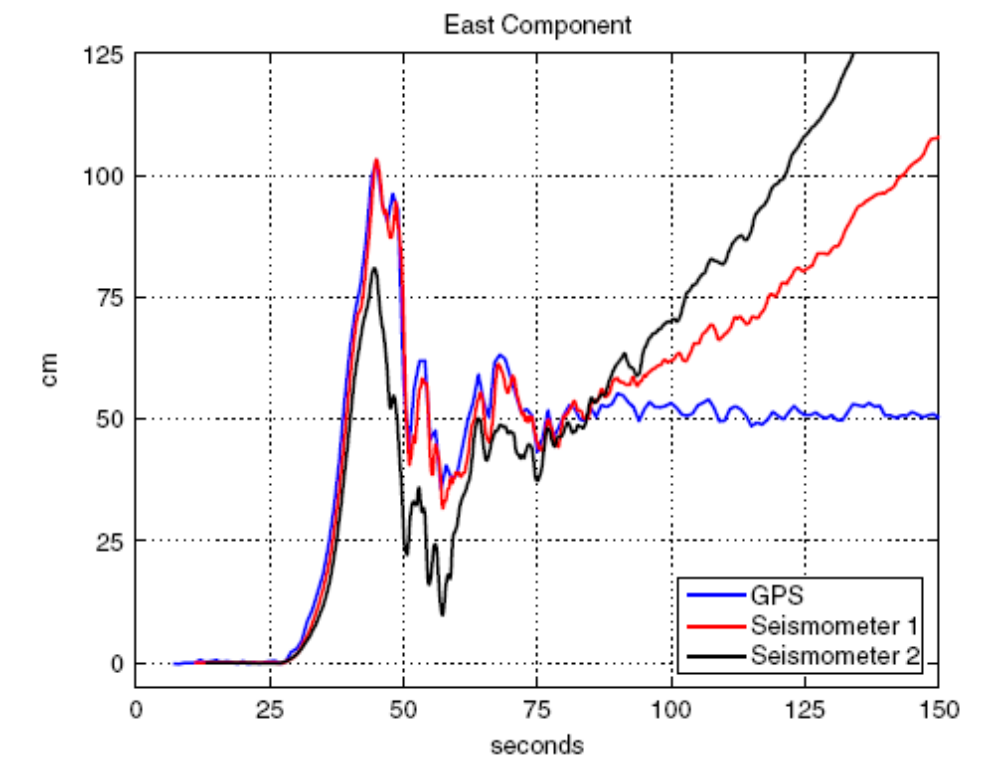

Miyazaki *et al*., 2004; Larson, 2009

GPS Seismology (位移量測)

GPS as a *strong motion* instrument

1. High rate GPS is an extra sensor
2. No clipping
3. Strong motion
4. No more double integrating acceleration
5. Static offset displacement
6. Direct link between coseismic and postseismic

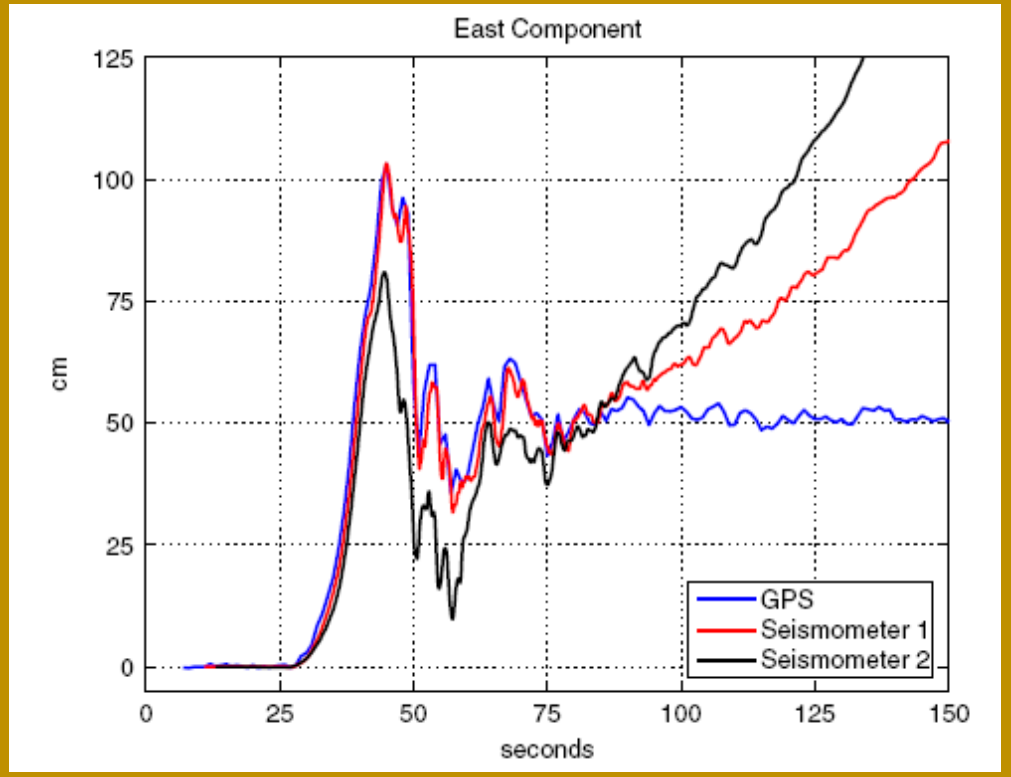

Miyazaki *et al*., 2004; Larson, 2009

Event: 1103110550 15.0 38.10N 142.86E 23 Mw=9.

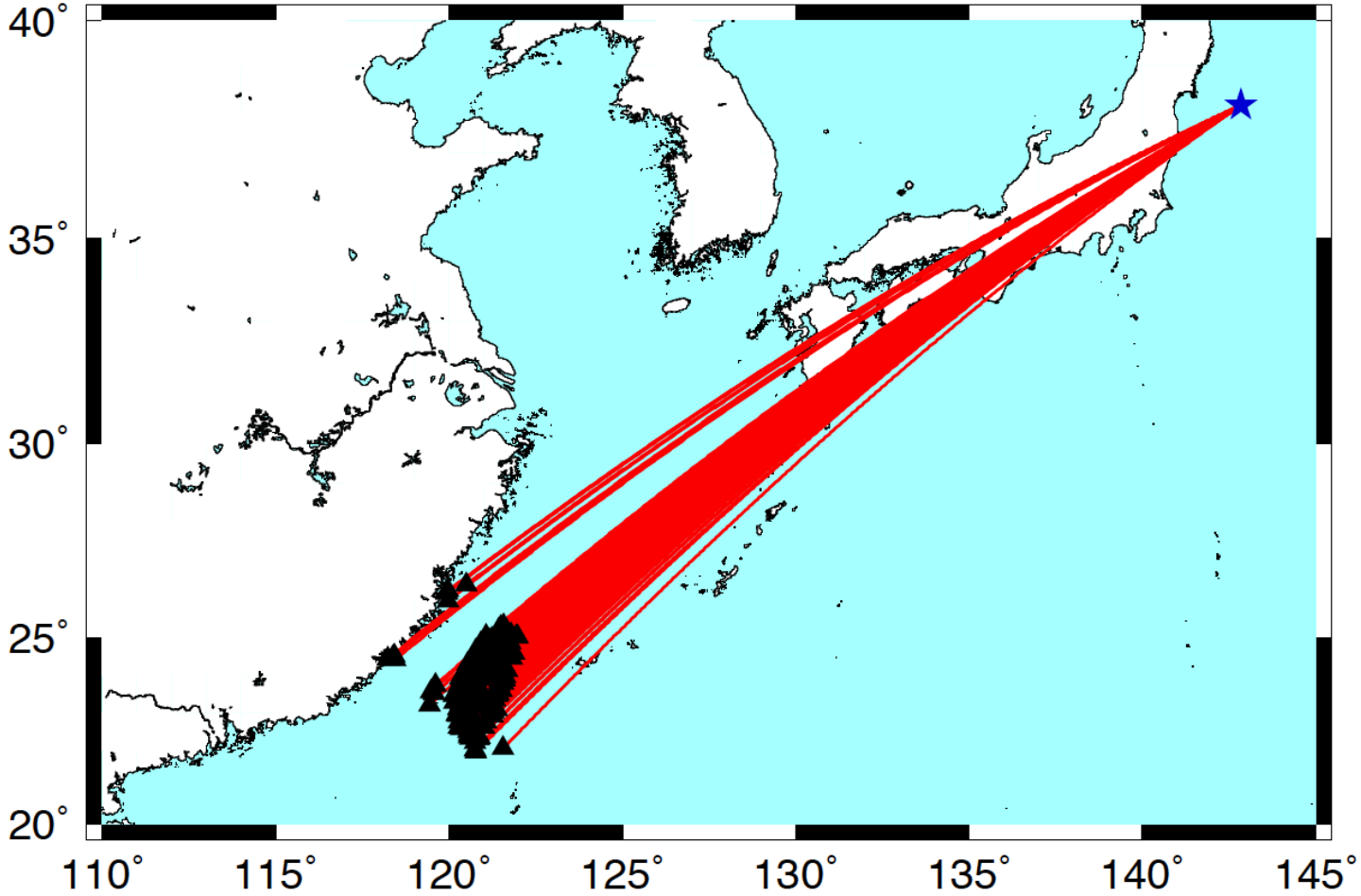

Near east coast of eastern Honshu, Japan

AV. DIST (KM) = 2636.9

Comparison between high-rate GPS and broadband data

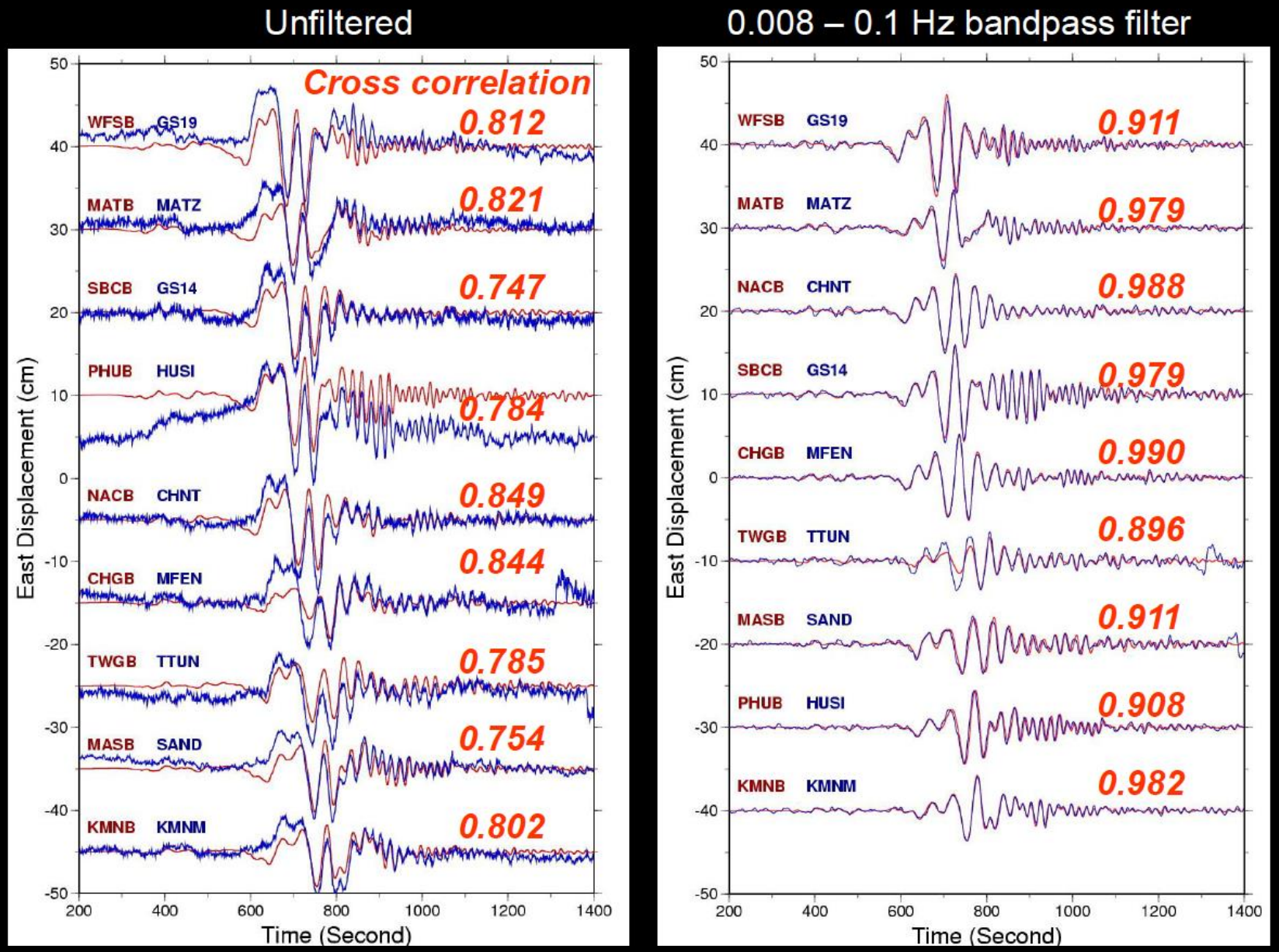

Hung and Rau (2011)

Event: 1103110546 23.0 38.10N 142.86E 23 0.0 9.0

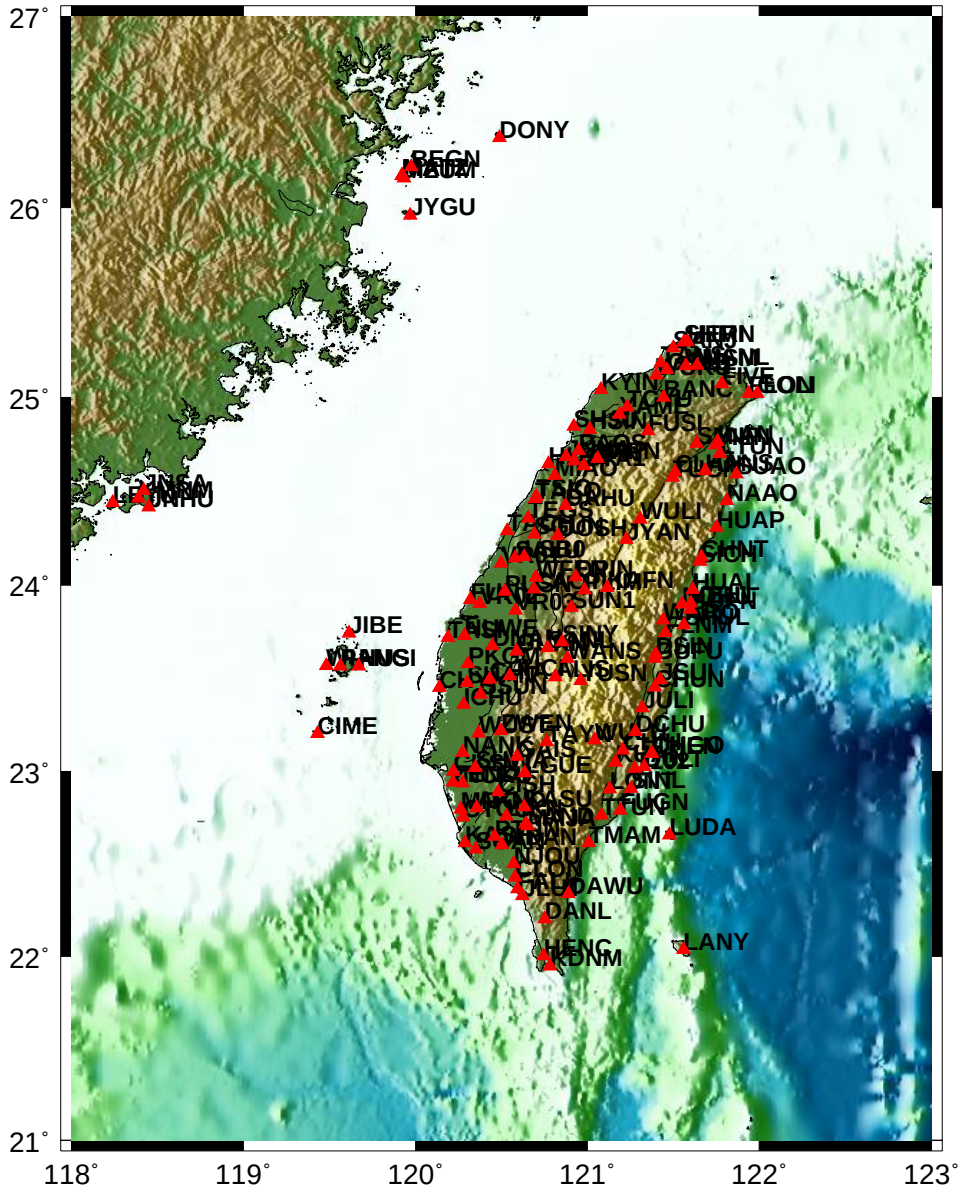

Near east coast of eastern Honshu, Japan

NUM (STA) = 149 *AV. DIST (KM) = 2642.6*

UD-COMP (1HZ GPS)

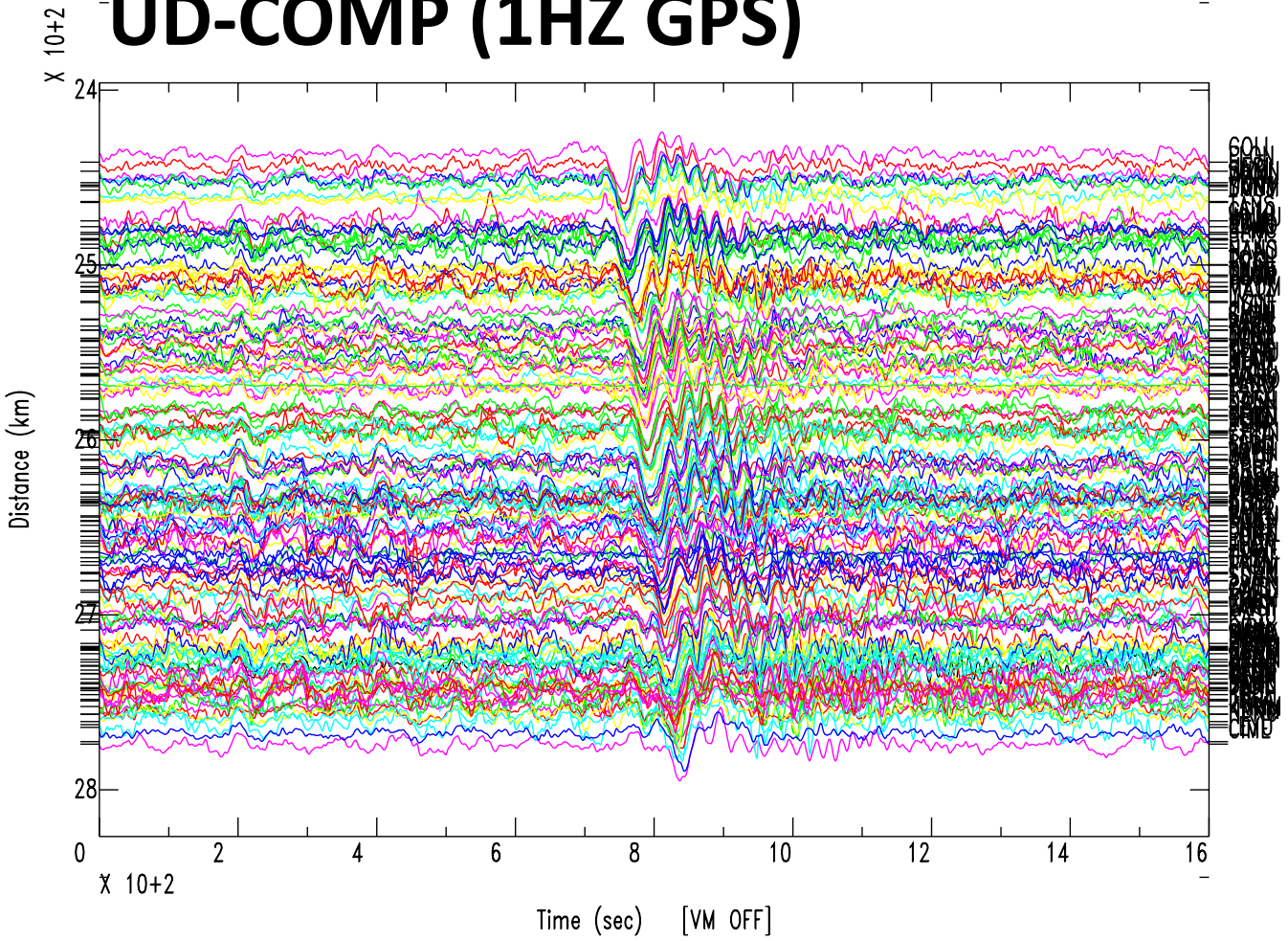

EW-COMP (1HZ GPS)

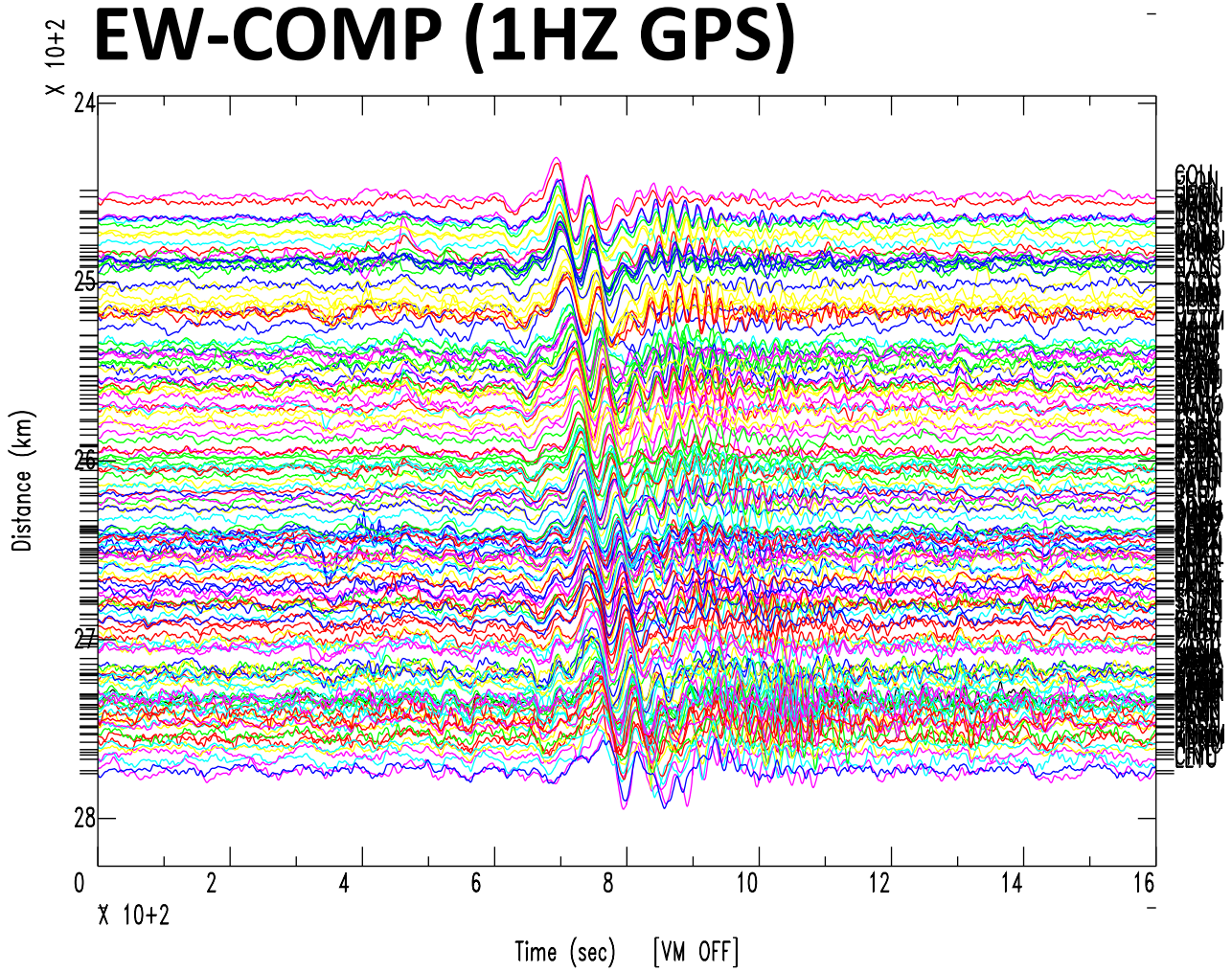

NS-COMP (1HZ GPS)

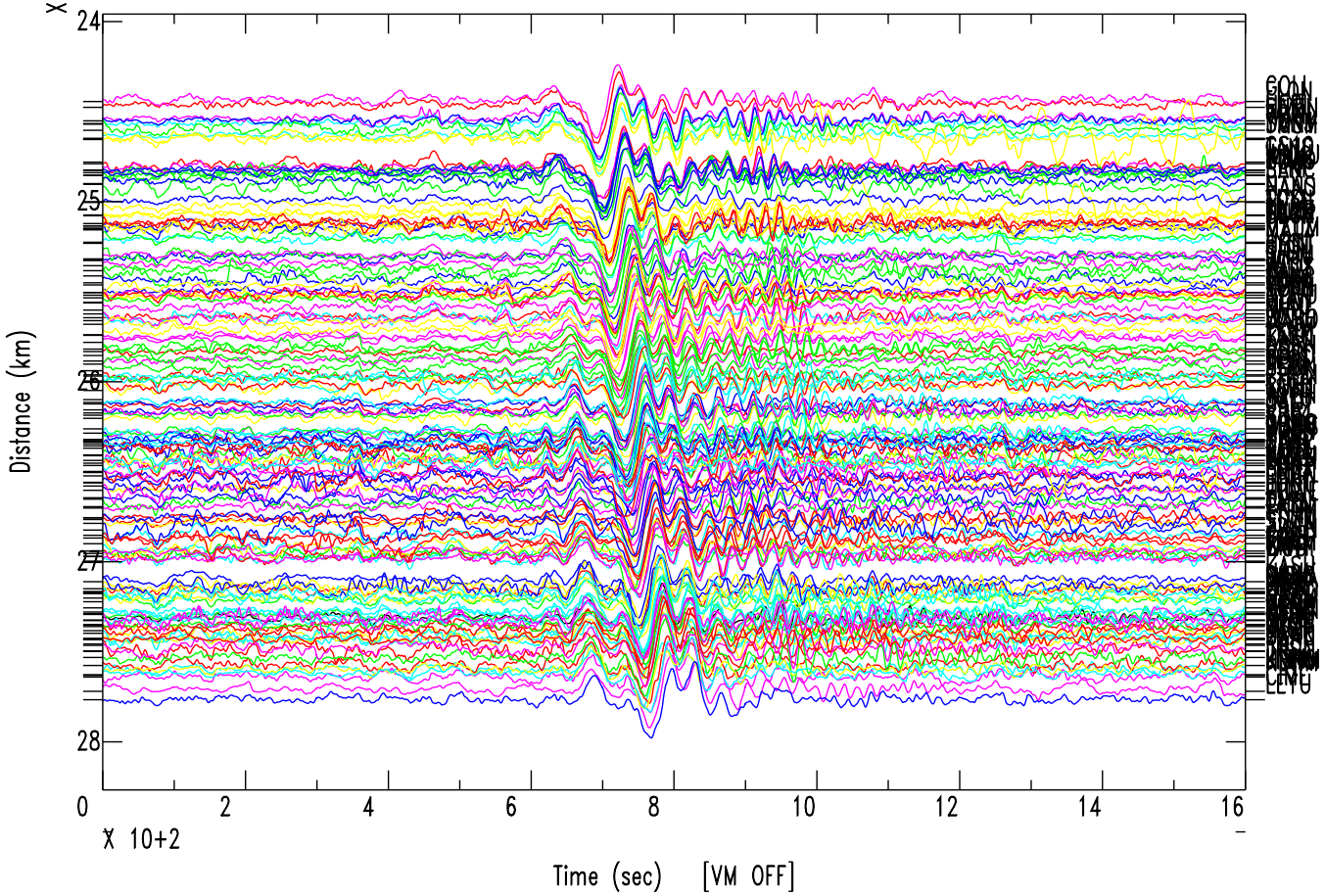

HWBS /Users/HWBS/Projects/EQ_STRAIN/GPS1Z_TW_2013/SAC_DATA Wed Aug 21 20:07:56 2013

Snapshots of Ground motions

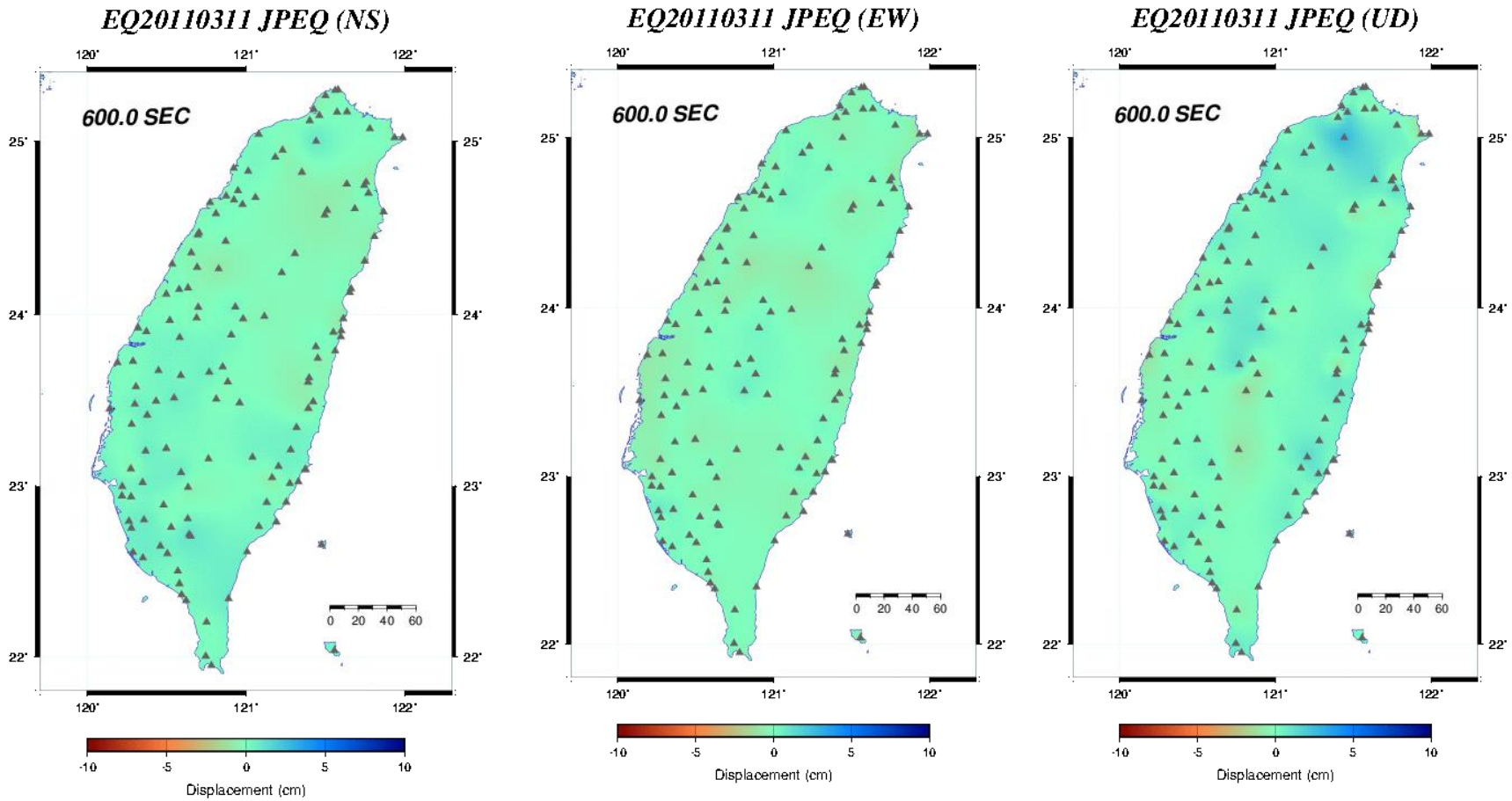

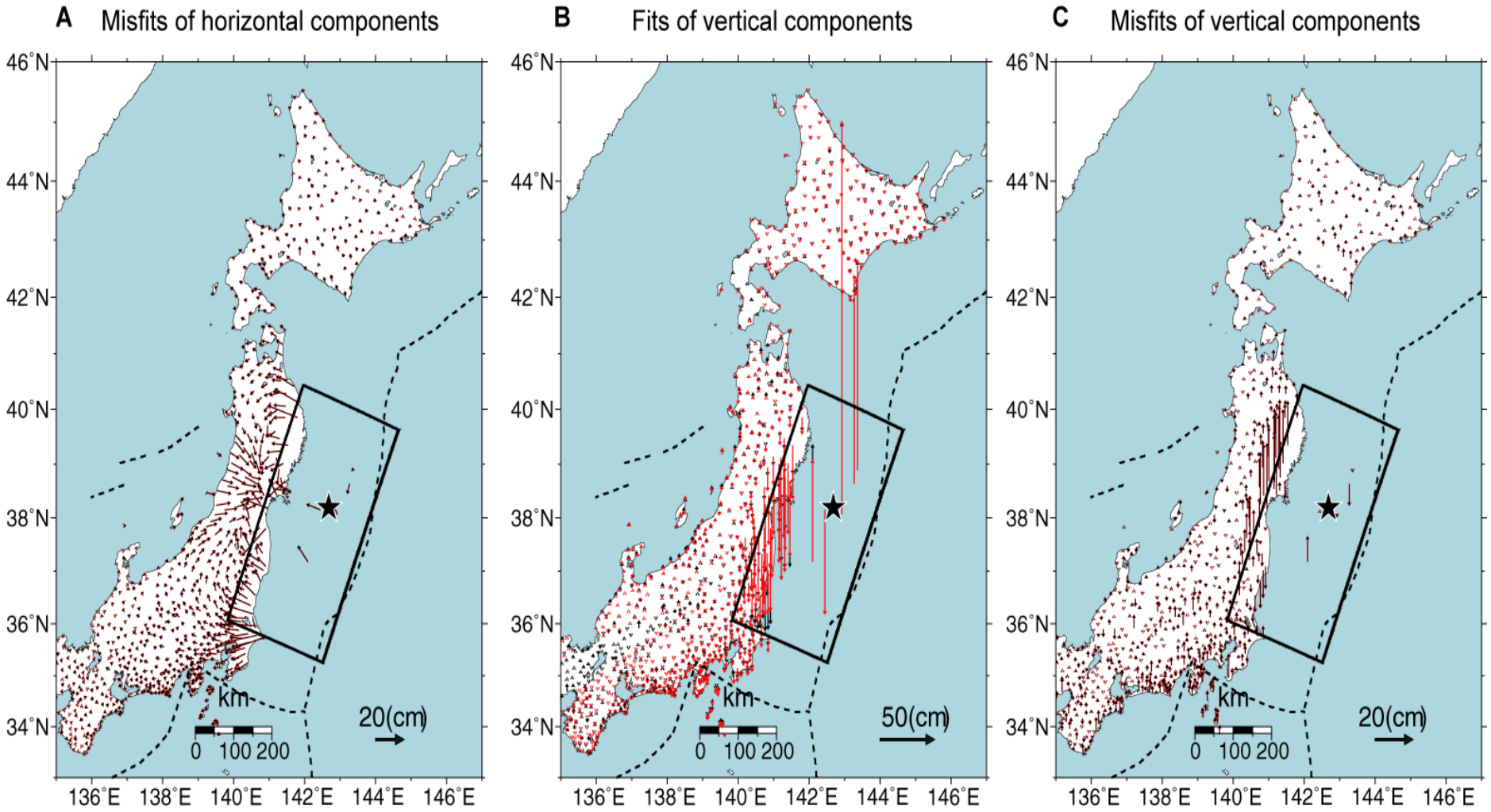
A
Misfits of horizontal components
B
Fits of vertical components
C
Misfits of vertical components
46°N
44°N
42°N
40°N
38°N
36°N
34°N
136°E
138°E
140°E
142°E
144°E
146°E
km
0 100 200
20(cm)
50(cm)

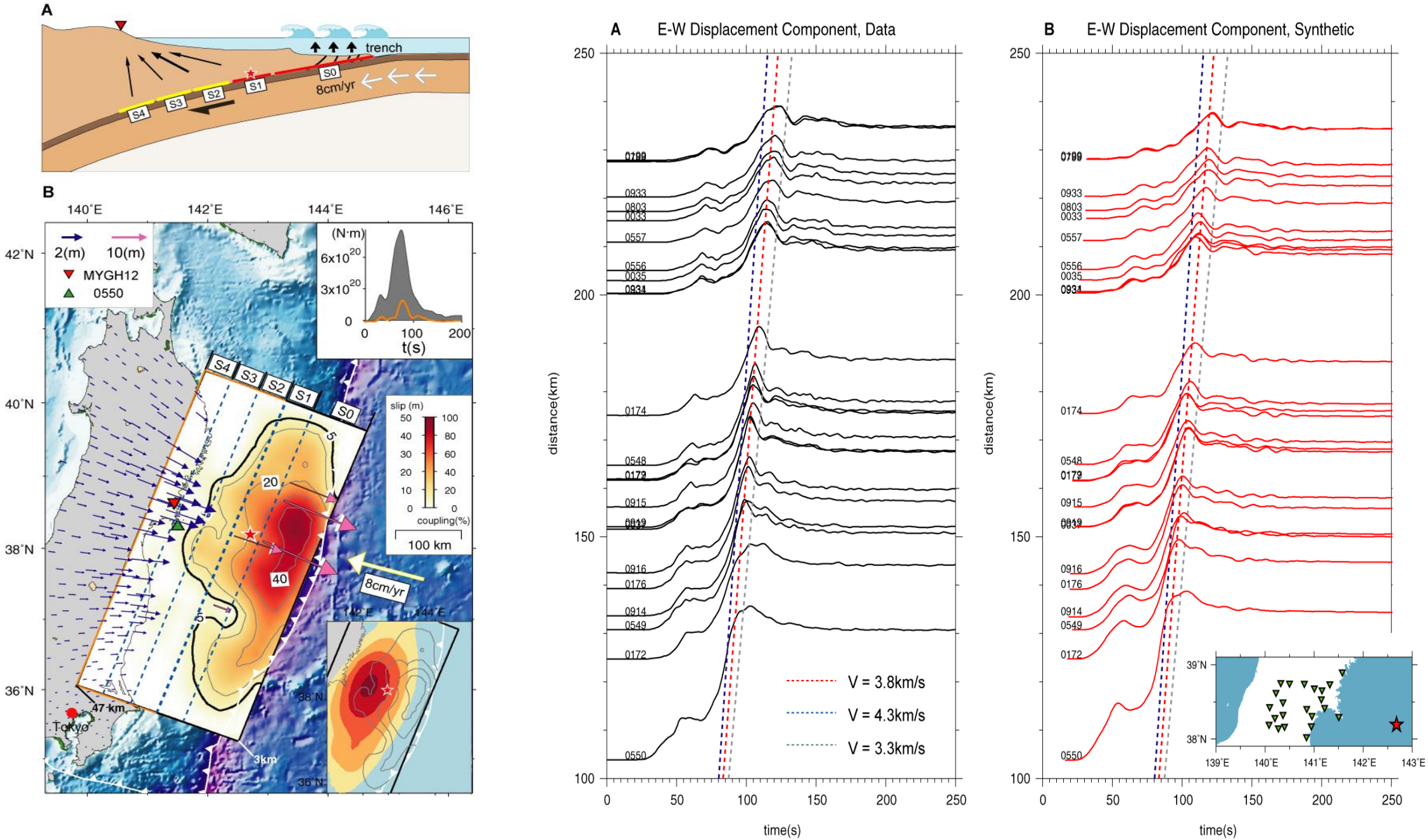
A
trench
S0
S1
S2
S3
S4
8cm/yr
B
140°E
142°E
144°E
146°E
42°N
40°N
38°N
36°N
2(m)
10(m)
MYGH12
0550
(N·m)
6x10^20
3x10^20
0
0
100
200
t(s)
slip (m)
50
40
30
20
10
0
100
80
60
40
20
0
coupling(%)
100 km
20
40
5
8cm/yr
47 km
Tokyo
3km
38°N
36°N
A
E-W Displacement Component, Data
B
E-W Displacement Component, Synthetic
distance(km)
time(s)
250
200
150
100
0
50
100
150
200
250
0799
0933
0803
0033
0557
0556
0035
0934
0174
0548
0172
0915
0916
0176
0914
0549
0550
V = 3.8km/s
V = 4.3km/s
V = 3.3km/s
39°N
38°N
139°E
140°E
141°E
142°E
143°E

簡介DAS觀測原理及其應用

Distributed Acoustic Sensing (DAS)

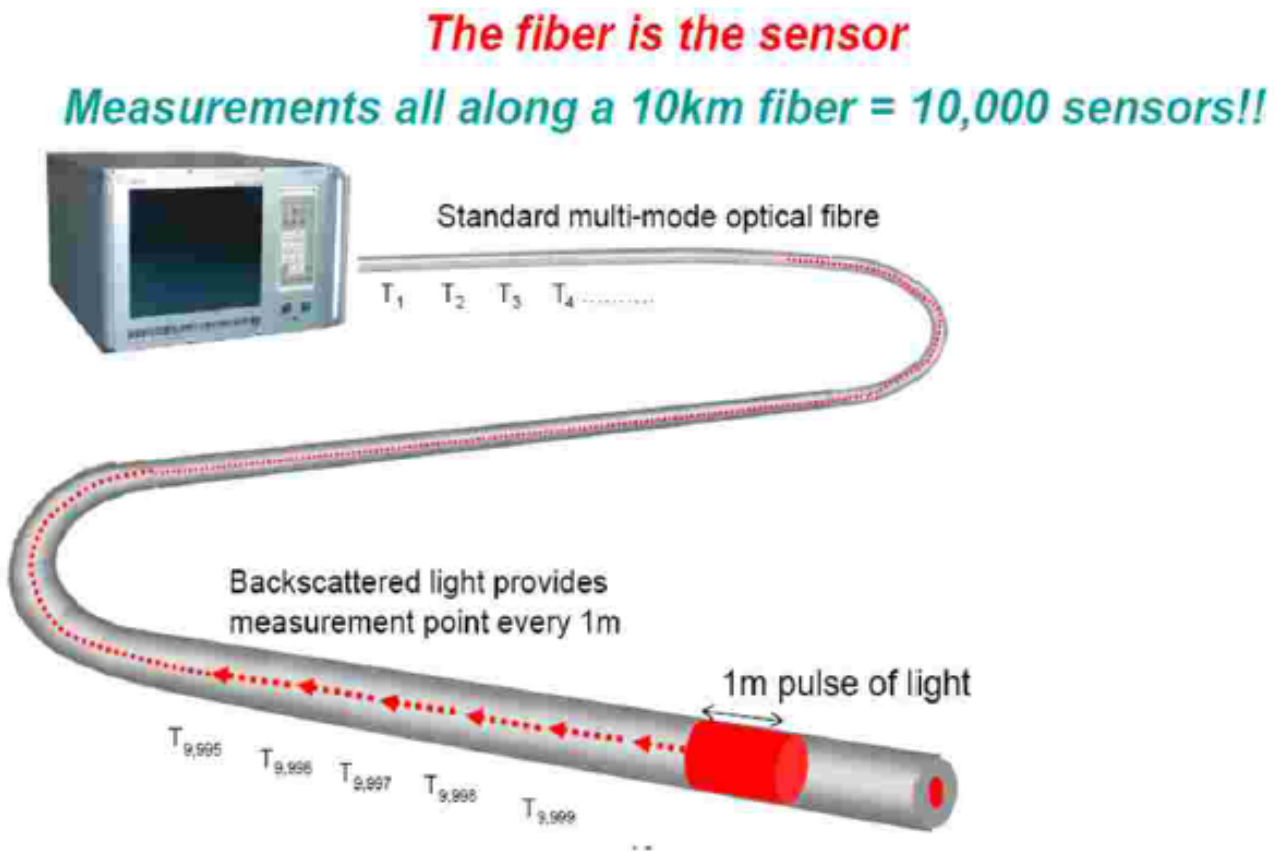

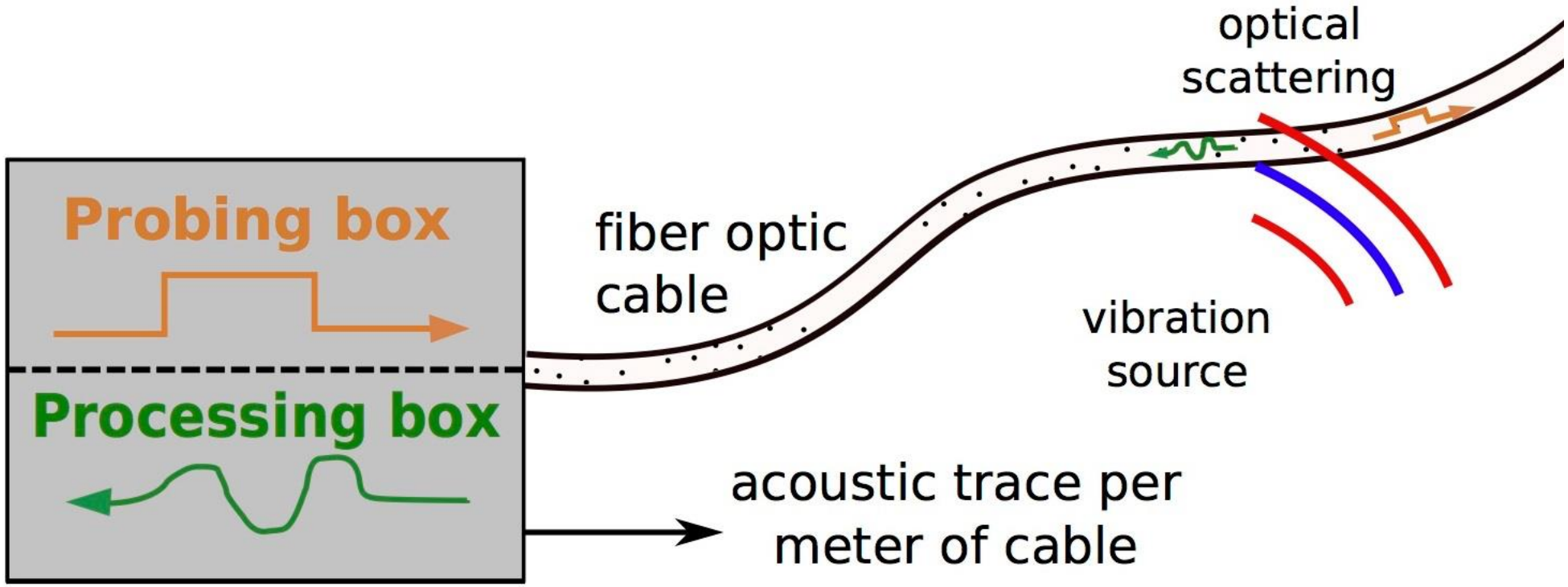
Probing box
Processing box
fiber optic
cable
optical
scattering
vibration
source
acoustic trace per
meter of cable

[redacted]

[redacted]

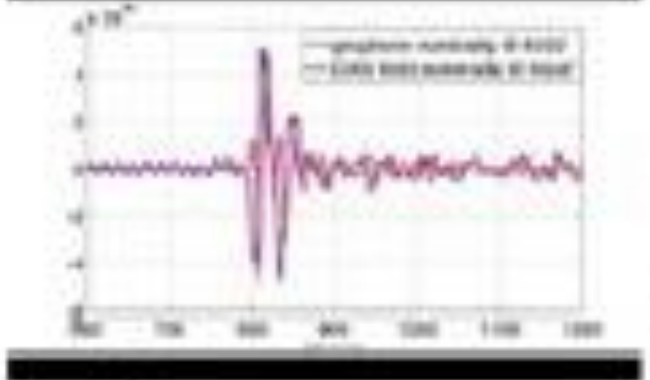

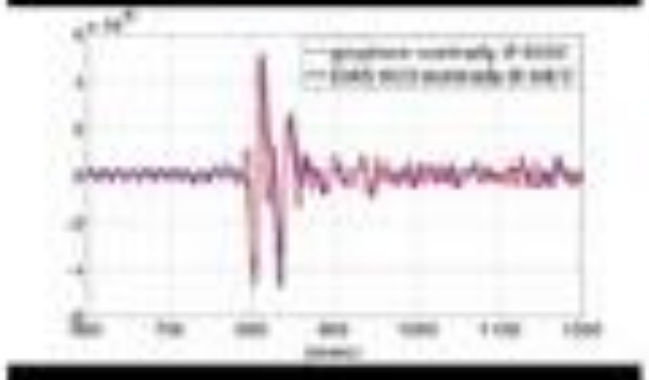

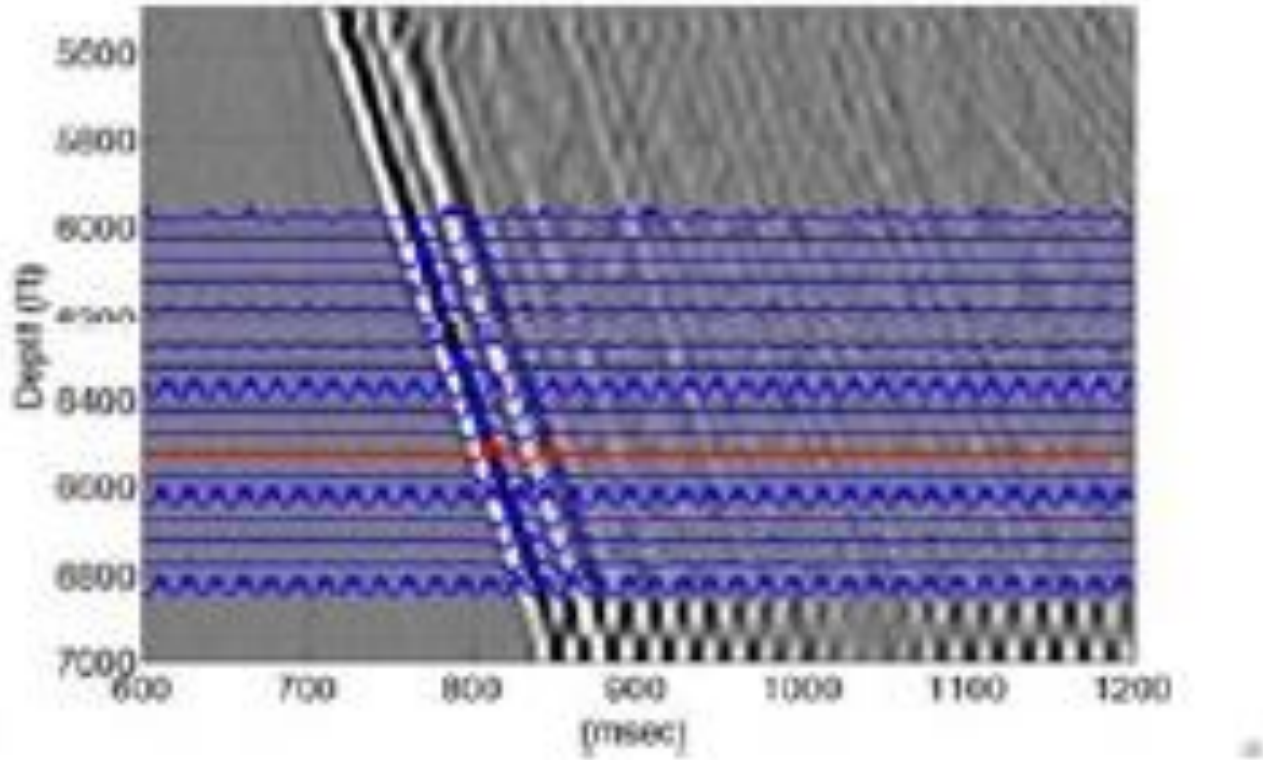

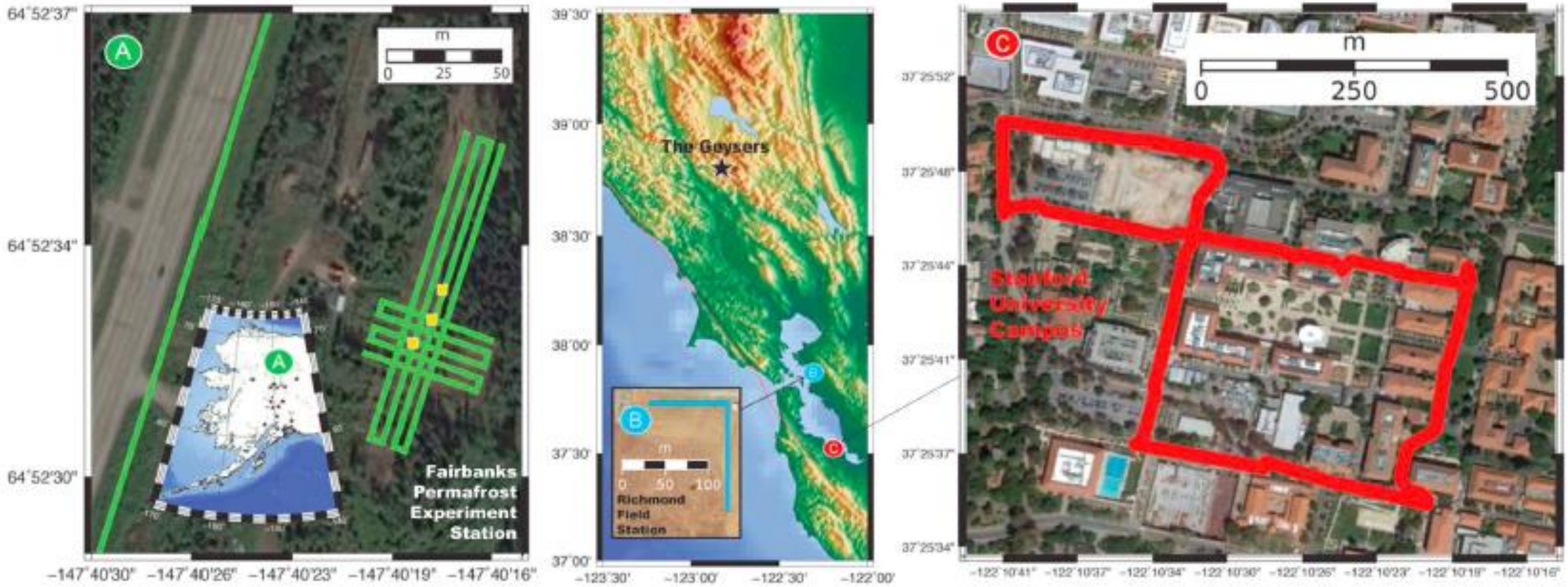
A
m
0 25 50
64°52'37"
64°52'34"
64°52'30"
Fairbanks
Permafrost
Experiment
Station
−147°40'30" −147°40'26" −147°40'23" −147°40'19" −147°40'16"
39°30'
39°00'
38°30'
38°00'
37°30'
37°00'
The Geysers
B
m
0 50 100
Richmond
Field
Station
C
−123°30' −123°00' −122°30' −122°00'
37°25'52"
37°25'48"
37°25'44"
37°25'41"
37°25'37"
37°25'34"
m
0 250 500
Stanford
University
Campus
−122°10'41" −122°10'37" −122°10'34" −122°10'30" −122°10'26" −122°10'23" −122°10'19" −122°10'16"

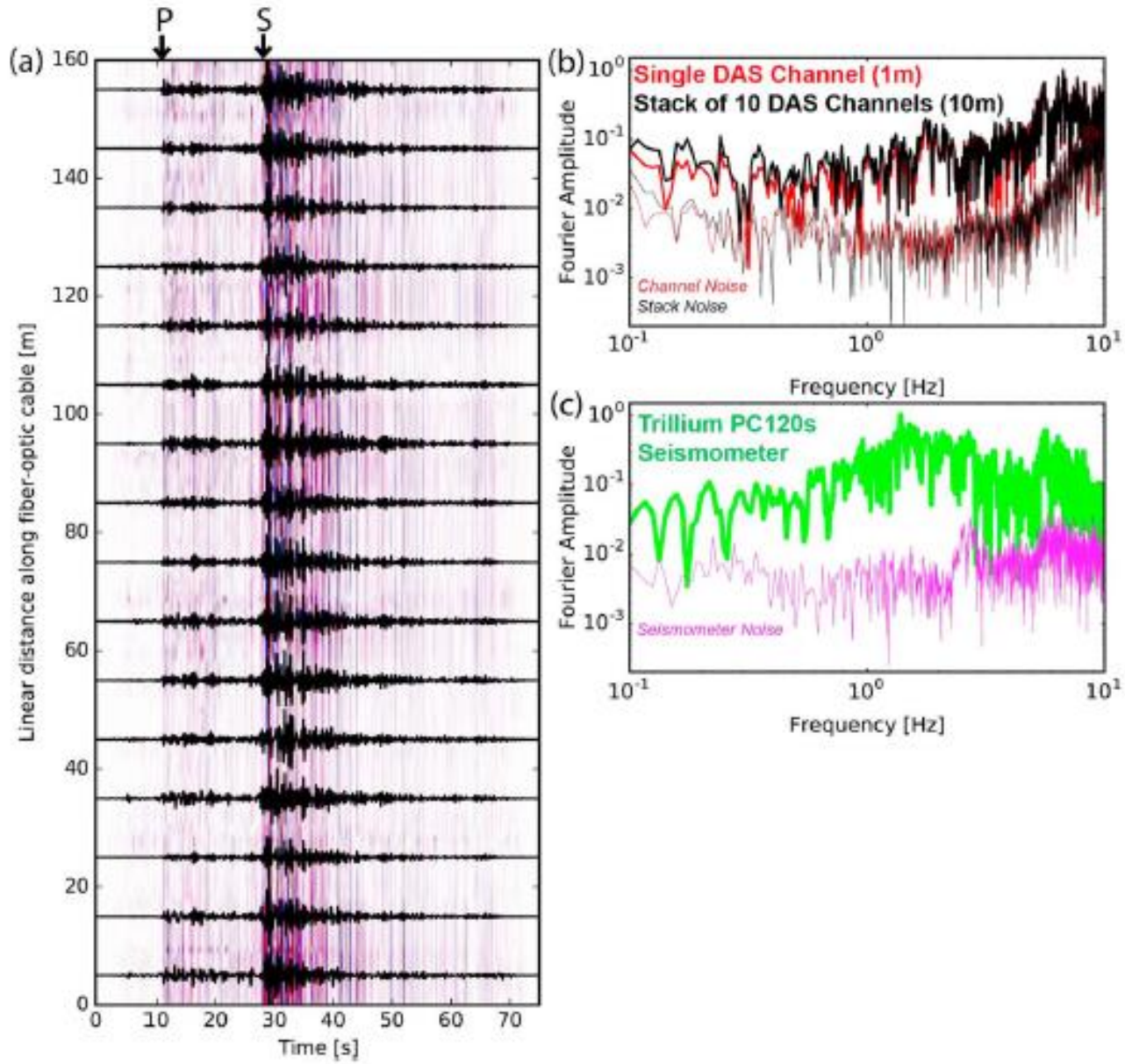
(a)
P
S
Linear distance along fiber-optic cable [m]
Time [s]
(b)
Single DAS Channel (1m)
Stack of 10 DAS Channels (10m)
Channel Noise
Stack Noise
Fourier Amplitude
Frequency [Hz]
(c)
Trillium PC120s
Seismometer
Seismometer Noise
Fourier Amplitude
Frequency [Hz]

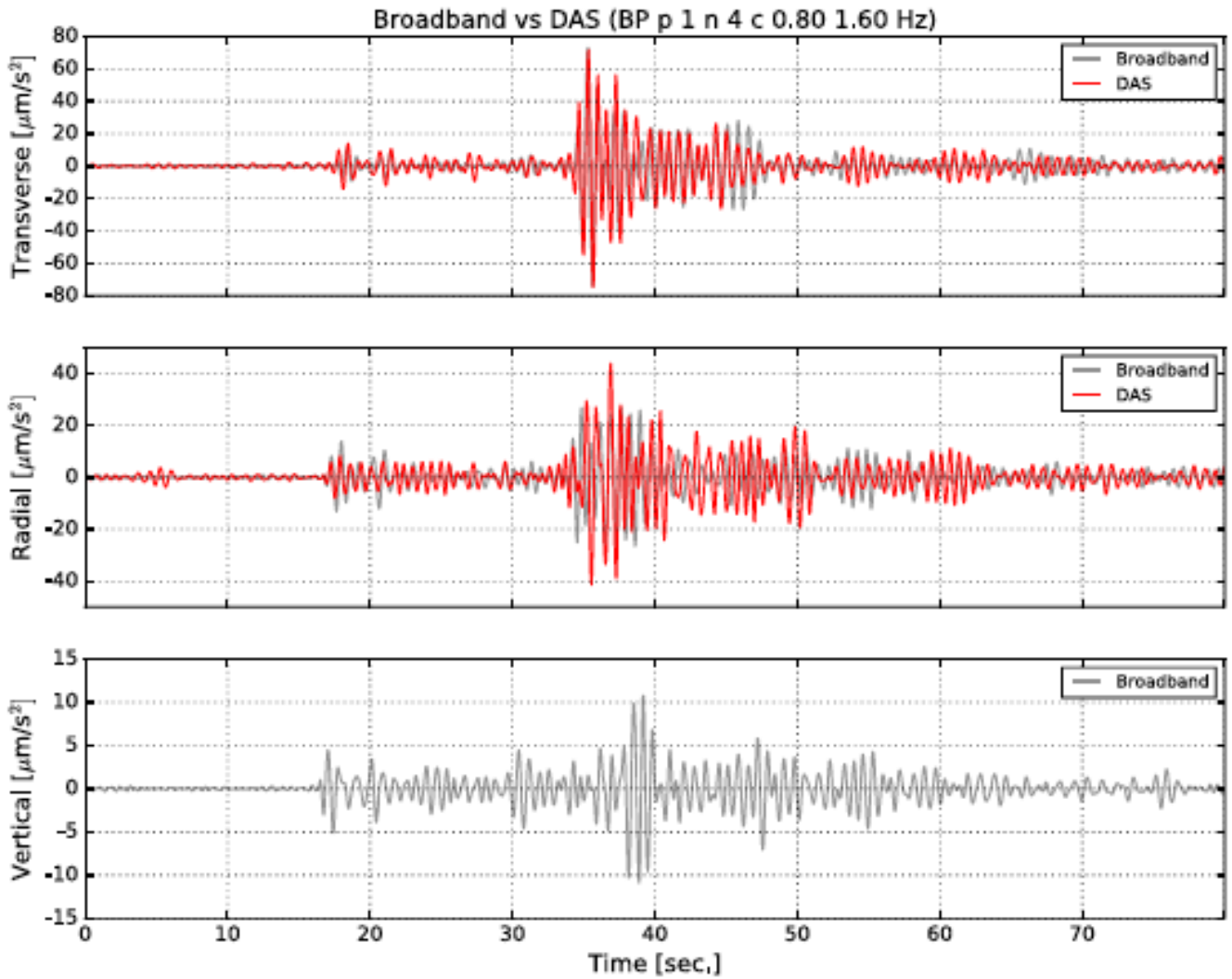
Broadband vs DAS (BP p 1 n 4 c 0.80 1.60 Hz)
Transverse [μm/s²]
Radial [μm/s²]
Vertical [μm/s²]
Broadband
DAS
Time [sec,]

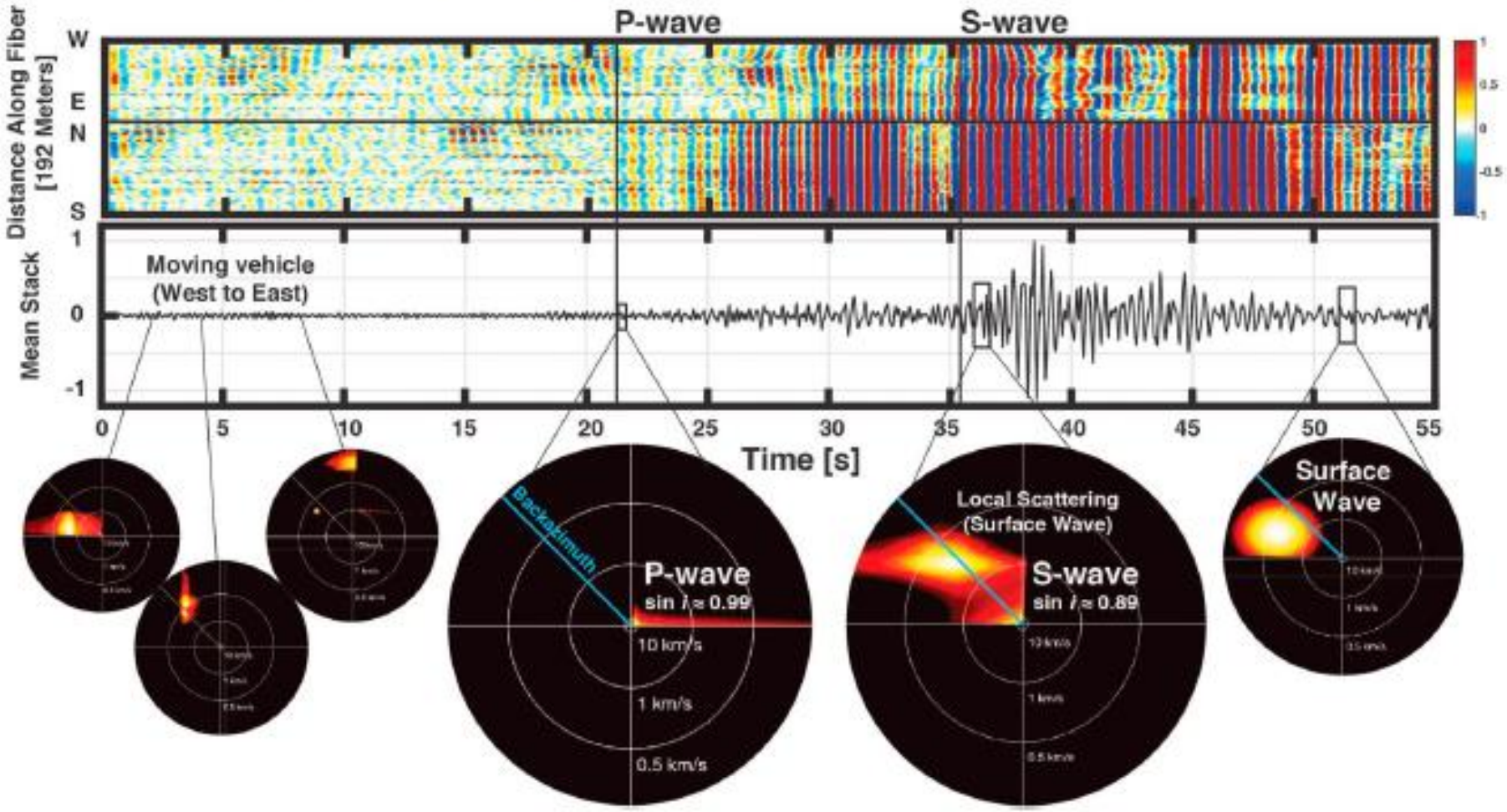
P-wave
S-wave
Distance Along Fiber [192 Meters]
W
E
N
S
Mean Stack
1
0
-1
Moving vehicle (West to East)
0
5
10
15
20
25
30
35
40
45
50
55
Time [s]
Backazimuth
P-wave
sin i ≈ 0.99
10 km/s
1 km/s
0.5 km/s
Local Scattering (Surface Wave)
S-wave
sin i ≈ 0.89
Surface Wave

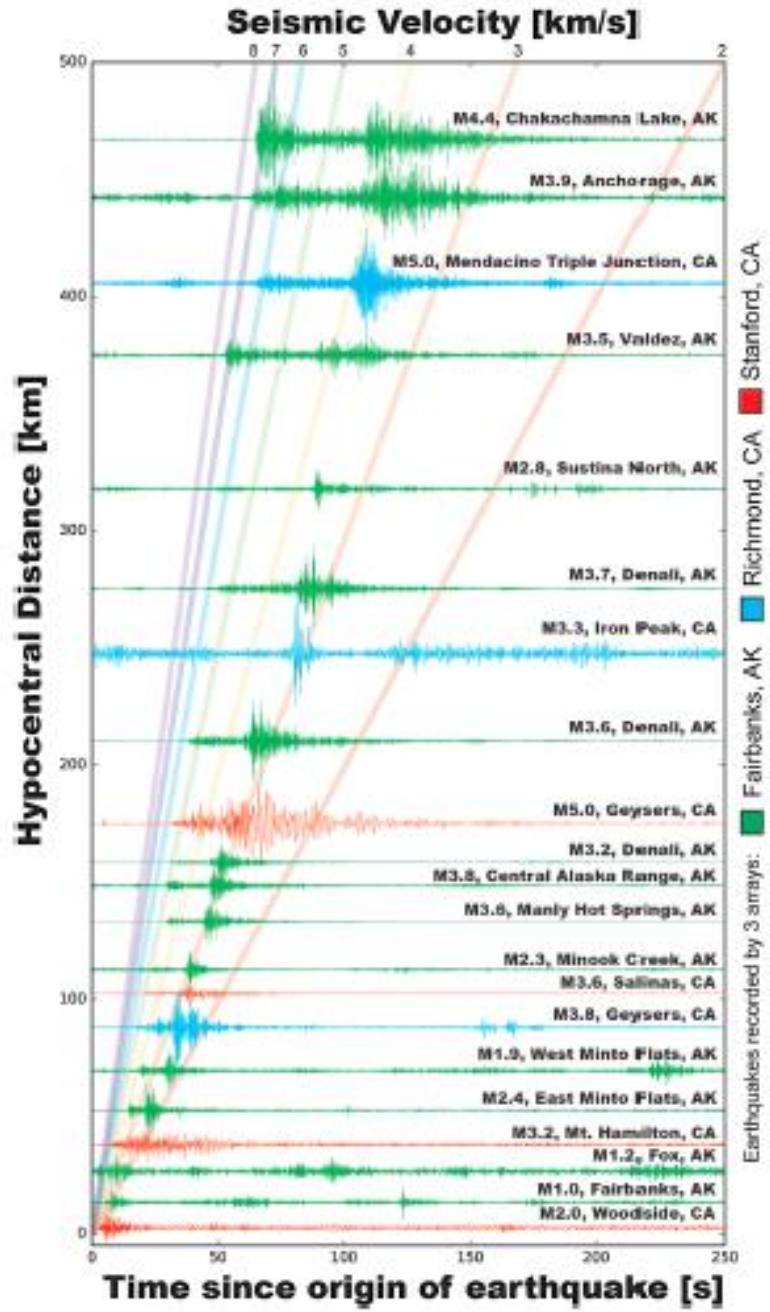
Seismic Velocity [km/s]
8 7 6 5 4 3 2
Hypocentral Distance [km]
0 100 200 300 400 500
M4.4, Chakachamna Lake, AK
M3.9, Anchorage, AK
M5.0, Mendacino Triple Junction, CA
M3.5, Valdez, AK
M2.8, Sustina North, AK
M3.7, Denali, AK
M3.3, Iron Peak, CA
M3.6, Denali, AK
M5.0, Geysers, CA
M3.2, Denali, AK
M3.8, Central Alaska Range, AK
M3.6, Manly Hot Springs, AK
M2.3, Minook Creek, AK
M3.6, Salinas, CA
M3.8, Geysers, CA
M1.9, West Minto Flats, AK
M2.4, East Minto Flats, AK
M3.2, Mt. Hamilton, CA
M1.2, Fox, AK
M1.0, Fairbanks, AK
M2.0, Woodside, CA
0 50 100 150 200 250
Time since origin of earthquake [s]
Earthquakes recorded by 3 arrays: Fairbanks, AK Richmond, CA Stanford, CA

討論:

- 地動旋轉量(Rotation)的觀測與應用
- 地震源與波傳的數值模擬
- 高頻GPS的地動觀測及其應用
- 簡介DAS觀測原理及其應用

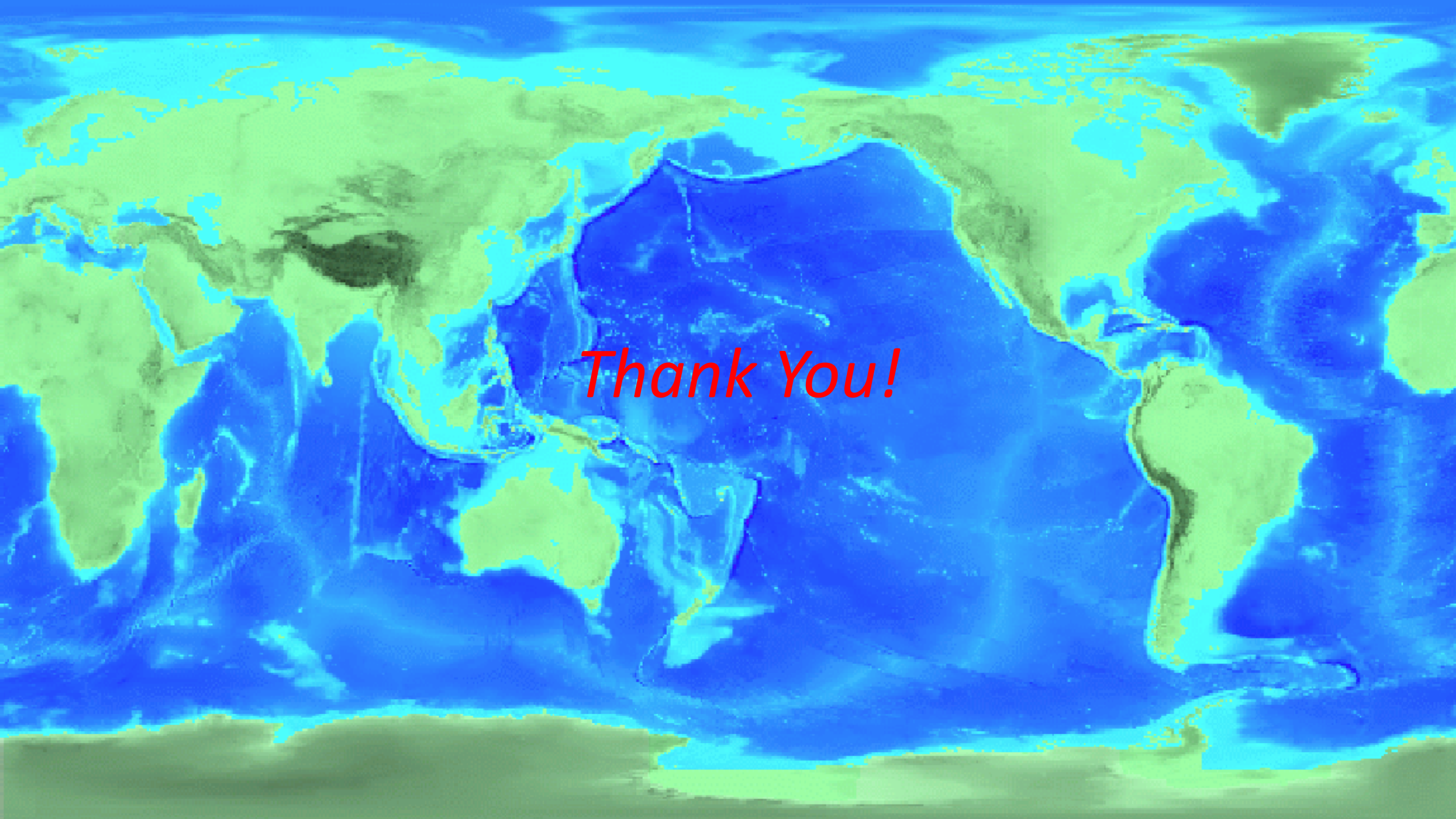
Thank You!